MOTOR SYSTEMS OF FRONTAL LOBE IN PROSIMIAN GALAGOS: AREAS,

NUCLEI, AND CONNECTIONS

By

Pei-chun Fang

Dissertation

Submitted to the Faculty of the

Graduate School of Vanderbilt University

in partial fulfillment of the requirements

for the degree of

DOCTOR OF PHILOSOPHY

in

Psychology

May, 2005

Nashville, Tennessee

Approved: Date

Dr. Jon H. Kaas   February 22, 2005

Dr. Jo-Anne Bachorowski   February 22, 2005

Dr. Vivien A. Casagrande   February 22, 2005

Dr. Ford F. Ebner   February 22, 2005

Dr. Kenneth C. Catania   February 22, 2005

ACKNOWLEDGEMENTS

TABLE OF CONTENTS

Page

Chapter

LIST OF TABLES

LIST OF FIGURES

LIST OF ABBREVIATIONS

Abbreviation

3.1   Abbreviations of tracers, cortical areas and thalamic nuclei

Tracers:

FB   Fast blue

DY   Diamidino yellow

FR   Fluororuby

FE   Flurescein-dextran

WGA-HRP   Wheat-germ agglutinin conjugated to horseradish-peroxidase

BDA Biotinylated dextran amine

CTB   Cholera toxin B subunit

Cortical Areas:

M1   Primary motor area

PMD   Dorsal premotor area

PMV   Ventral premotor area

SMA   Supplementary motor area

FEF   Frontal eye field

PFC   Prefrontal cortex

FSa   Frontal sulcus, anterior

FSp   Frontal sulcus, posterior

Tk/HL Trunk and hindlimb movements

FL   Forelimb movements

OF   Orofacial movements

EM   Eye movements

Mix   Shoulder, trunk, neck, ear, eye lid and eye movements

Thalamic nucleus:

VA   Ventral anterior

VAl   Ventral anterior, lateral subdivision

VAm   Ventral anterior, medial subdivision

VL   Ventral lateral

VLa   Ventral lateral, anterior subdivision

VLp   Ventral lateral, posterior subdivision

VM   Ventral medial

MDmf   Medial dorsal, multiform subdivision

IL   Intralaminar

CL   Central lateral

CM   Central median

Pc   Paracentral

Pf   Parafascicular

ANT   Anterior nucleus

LP   Lateral posterior

VP   Ventral posterior

4.1   Abbreviations of sulci, cortical areas and body movements

Sulci:

FSa   Frontal sulcus, anterior

FSp   Frontal sulcus, posterior

IPS   Intraparietal sulcus

LS   Lateral sulcus

OS   Orbit sulcus

CgS   Cingulate sulcus

Cortical subdivisions:

M1   Primary motor area

PMD   Premotor area, dorsal subdivision

PMV   Premotor area, ventral subdivision

SMA   Supplementary motor area

FEF   Frontal eye field

CSMA Cingulate sensory motor area

sPPC   Posterior parietal cortex, superior subdivision

iPPC   Posterior parietal cortex, inferior subdivision

Intracortical microstimulation (ICMS) mapping body movements:

Hindlimb (HL) and trunk (tr)

   ak   ankle

   kn   knee

   hp   hip

   l.tr lower trunk

   to   toe

   u.tr upper trunk

   i.   ipsilateral

   b.   bilateral

Forelimb (FL)

am arm

el elbow

fa forearm

dg digit

sh shoulder

wr wrist

Orofacial (OF)

ck cheek

fc face

jw jaw

l.l lower lip

mo mouth

nk neck

no nose

tg tongue

th throat

u.l upper lip

Eye and ear

eb eye blink

ed eye lid

em eye movement

er ear

CHAPTER I

GENERAL INTRODUCTION: BACKGROUND AND SIGNIFICANCE

<u>**Organization of Premotor Cortex in Simian Primates (Macaque Monkey)**</u>

The motor system in simian primates, especially macaque monkeys, has been extensively

studied. The research on the motor cortical areas includes studies of the cytoarchitecture,

connections, and physiology (single cell recording and intracortical microstimulation).

Based on these results, motor cortex has been divided into a primary motor area (M1 or

area 4) and several non-primary motor areas. The primary motor area is located rostral to

the central sulcus and the primary somatosensory area (S1), and extends medio-laterally.

The non-primary motor areas include area 6 (premotor cortex and supplementary motor

area) and the areas related to the motor movement in the cingulate cortex. The premotor

cortex (PM) is located rostral to M1 extending medio-laterally; whereas the

supplementary motor area (SMA) extending rostro-caudally in the mesial wall is rostral

to M1 and medial to PM (Brodmann, 1909; Vogt and Vogt, 1919; Von Bonin and Bailey,

1947; Barbas and Pandya, 1987; Matelli et al., 1985). Some of the relevant architectonic

subdivisions of cortex have been related to physiologically identified subdivisions of

cortex (see Wu et al for galagos). As less is known about the organization of the motor

thalamus in galagos, it will be necessary to characterize the architecture of the motor

thalamus. The results will allow an extensive and detailed comparison of the motor

system of prosimian galagos with those of more fully studied anthropoid primates.

Both the primary motor area (M1) and non-primary motor areas contain body movement

representations: hindlimb/trunk, forelimb and orofacial representations (Woolsey et al.,

1951; Rizzolatti et al., 1981b & c; Godschalk et al., 1995; Tanne-Gariepy et al., 2002).

The primary motor area is basically involved in the movement execution, and the non-

primary motor areas are involved in motor planning and programming, and preparation of

the movement in response to sensory cues (Weinrich and Wise, 1982; Godschalk et al.,

1985).

Among the non-primary motor areas, the premotor cortex (PM) is thought to integrate a

variety of sensory information from the posterior parietal cortex and prefrontal cortex,

and guide movements at higher-order cognitive levels (Wise, 1985; Wise et al., 1997;

Geyer et al., 2000; Luppino and Rizzolatti, 2000; Rizzolatti and Luppino, 2001).

However, PM is not architectonically or functionally uniform. Multiple subdivisions

have been delineated based on the architectonic appearance and functions (or

connections). Basically, PM can be divided into two main regions: dorsal (PMD) and

ventral (PMV). There are also rostral-caudal differences within PMD, and the two rostral

(PMDr) and caudal (PMDc) PMD regions have been described (Geyer et al. review,

2000).

Cytoarchitecture of Premotor Cortex in Monkeys

The PMDc, as well as M1, lacks a granular layer IV (agranular cortex), but unlike M1,

PMDc contains only few large pyramidal cells (Betz cells) and lots of medium pyramidal

cells in layer V. In contrast, PMDr contains a thin granular layer IV (dysgranular cortex)

and small-sized pyramidal cells in layer V. The ventral region, PMV has a thin granular

layer IV and a scattered population of large pyramidal cells (Brodmann, 1909; Barbas and Pandya, 1987; Matelli et al., 1985).

Corticocortical Connections of Premotor Cortex in Monkeys

The connections of PM cortex with other cortical areas are topographically organized. The PMD receives projections mainly from the dorsal regions of cortex, and PMV from the ventral regions. Within PMD, the caudal region (PMDc) receives projections mainly from the posterior parietal cortex, and the rostral (PMDr) from the prefrontal cortex. Topographic connections are also seen between somatotopic representations and PM cortex, so the same body movement representations of PM areas and other cortical areas are connected with each other (Strick 1985; Lu et al., 1994; Hatanaka et al., 2001). PMDc is strongly connected with M1, SMA, the dorsal part of the dorsolateral prefrontal cortex (DLPFd), cingulate motor area (CMA), and superior parietal cortex (area 5). PMDc is also weakly connected with PMDr and PMV (Arikuni et al., 1980; Petrides and Pandya, 1984; Barbas and Pandya, 1987; Cavada and Goldman-Rakic, 1989; Kurata, 1991; Lu et al., 1994; Ghosh and Gattera, 1995; Marconi et al., 2001; Tanne-Gariepy et al., 2002).

Similar to PMDc, PMDr connects with the cortical areas located in the dorsal part of the brain (Barbas and Pandya, 1987). The PMDr is strongly connected with the dorsal part of the dorsolateral prefrontal cortex (DLPFd), supplementary eye field (SEF), frontal eye field (FEF), CMA, and caudal part of the posterior parietal cortex. Interestingly, the PMDr only receives very weak projections from the PMDc and PMV, and not from M1

(Cavada and Goldman-Rakic, 1989; Petrides and Pandya, 1984 & 1999; Matelli et al, 1998; Shipp et al., 1998; Leichnetz, 2001; Marconi et al., 2001; Luppino et al., 2003). Unlike PMD, PMV is connected mainly with both prefrontal and parietal cortex located in the ventral part of the brain. The PMV receives strong connections from the DLPF, FEF, M1, pre-SMA, SMA, and somatosensory areas in the parietal cortex (S2, area 5, and area 7). Additional weak projections are from CMA and PMDc (Muakkassa and Strick, 1979; Arikuni et al., 1980; Godschalk et al., 1984; Matelli et al., 1986; Barbas and Pandya, 1987; Cavada and Goldman-Rakic, 1989; Kurata, 1991; Lu et al., 1994; Ghosh and Gattera, 1995; Tanne-Gariepy et al., 2002).

Thalamocortical Connections with Premotor Cortex in Monkeys

The motor thalamus that sends prominent projections to the cortical motor areas can be divided into ventroanterior (VA), and ventrolateral (VL) regions based on Nissl staining. The VA can be furthered divided into magnocellular (VAmc) and parvocellular (VApc) subdivisions. The VL can be divided into ventral lateral nucleus, pars caudalis (VLc), ventroposterior lateral nucleus, pars oralis (VPLo), area X, ventral lateral nucleus, pars oralis (VLo), and ventral lateral nucleus, medial division (VLm) (Olszewski, 1952). There is a point-to-point topographic organization of thalamocortical connections to PM. The most posterior cortical motor area, M1, receives dominant projections from the posterior part of the motor thalamus, and the most anterior cortical motor areas, PMDr, receive projections from the anterior motor thalamus. The dorsal cortical motor area receives inputs from the dorsal motor thalamus, and the ventral motor cortical area receives inputs from the ventral motor thalamus (Kievit and Kuypers, 1977; Miyata and

Sasaki, 1983; Schell and Strick, 1984; Wiesendanger and Wiesendanger, 1985; Matelli et al., 1989; Darian-Smith et al., 1990; Matelli and Luppino, 1996). The somatotopic topography is also observed. The somatotopic representations in the motor cortex from medial to lateral: hindlimb/ trunk, forelimb, and face, receive the strongest connections from the motor thalamus from lateral to medial that include hindlimb/trunk, forelimb, and face representations respectively (Strick, 1976b; Jones et al., 1979; Kunzle, 1978; Ghosh et al., 1987).

While M1 receives dominant connections from VPLo, PMDc receives projections from the VLo, and the PMDr from area X and VAmc. Additional projections from VPLo, VLm and VLc go to PMDc, and VLa and VLo to PMDr (Kievit and Kuypers, 1977; Schell and Strick, 1984; Darian-Smith et al., 1990; Matelli and Luppino, 1996; Rouiller et al., 1998 & 1999; McFarland and Haber, 2002). The PMV receives strongest inputs from area X and VLo, and additionally from VPLo, VLc, and VLm (Schell and Strick, 1984; Matelli et al., 1989;.Rizzolatti et al., 1989; McFarland and Haber, 2000).

Motor research in macaque monkeys and humans has led to an extensive understanding of how the motor systems of these primates are organized. Especially after functional image and transcranial magnetic stimulation (TMS) techniques have been introduced, knowledge about the human motor system has been advanced. However, little is known about the motor system in prosimian primates. Prosimian primates, diverged from anthropoids perhaps as early as 50 million years ago (Goodael and Mittermeier, 1996). Prosimian galagos have smaller brains with fewer sulci than most simian primates, and it is assumed that prosimian galagos preserve more of the ancestral ("primitive") brain organization of early primates. Although sensory regions of cortex in galagos have been

studied (Xu et al, 2004; Lyon and Kaas, 2002; Collins et al, 2001), little is known about the connections of the motor system. There is one major study of motor cortex in prosimian galagos (Wu et al., 2000), which focuses on the organization of the primary motor area (M1) that suggests that the organization of M1 is similar to that in simian primates.

The goal of my thesis research was to study the connections of PM areas with other cortical areas and with motor thalamic subdivisions in prosimian galagos. In order to describe the thalamocortical connections in the motor thalamus, the subdivisions of motor thalamus have to be defined and specified, as there is not much information about the motor thalamus in prosimian galagos. There is only one architectonic study of the motor thalamus in galagos. Simmons (1980) divided the motor thalamus into three main regions, ventroanterior (VA), ventrolateral (VL), and ventromedial (VM) according to Nissl and myelin staining techniques. However, the subdivisions and the locations described by Simmons (1980) are not obvious and totally convincing. Since currently there are more advanced histological preparations available, additional new techniques will be used to differentiate the subdivisions of motor thalamus.

Results from prosimian galagos will be compared with simian primates (mostly Old World macaque monkeys that are well studied and New World owl monkeys). The results of my projects suggest that the organization of PM, including corticocortical and thalamocortical connections, and the architectonic subdivisions of motor thalamus is similar in prosimian and simian primates.

References

Arikuni T, Sakai M, Hamada I, Kubota K. 1980. Topographical projections from the prefrontal cortex to the post-arcuate area in the rhesus monkey, studied by retrograde axonal transport of horseradish peroxidase. Neuroscience Letters 19: 155-160.

Barbas H, Pandya DN. 1987. Architecture and frontal cortical connections of the premotor cortex (area 6) in the rhesus monkey. Journal of Comparative Neurology 256: 211-228.

Brodmann K. 1909. Vergleichende Lokalisationslehre der Groshirnride, In: Brodmann, K. Leipzig: Barth (reprinted 1925). p 324.

Campbell, MJ, Morrison JH. 1989. Monoclonal antibody to neurofilament protein (SMI-32) labels a subpopulation of pyramidal neurons in the human and monkey neocortex. J Comp Neurol 282: 191-205.

Cavada C, Goldman-Rakic PS. 1989. Posterior parietal cortex in rhesus monkey: I. Parcellation of areas based on distinctive limbic and sensory corticocortical connections. Journal of Comparative Neurology 287: 393-421.

Celio MR. 1990. Calbindin D-28k and parvalbumin in the rat nervous system. Neuroscience 35: 375-475.

Darian-Smith I, Cheema SS, Darian-Smith C. 1990. Thalamic projections to sensorimotor cortex in the newborn macaque. Journal of Comparative Neurology 299: 17-46.

Gallyas F. 1979. Silver staining of myelin by means of physical development. Neurol Res 1: 203-209.

Geneser-Jensen FA, Blackstad TW. 1971. Distribution of acetyl cholinesterase in the hippocampal region of the guinea pig. I. Entorhinal area, parasubiculum, and presubiculum. Z Zellforsch Mikrosk Anat 114: 460-481.

Geyer S, Zilles K, Luppino G, Matelli M. 2000. Neurofilament protein distribution in the macaque monkey dorsolateral premotor cortex. European Journal of Neuroscience 12: 1554-1566.

Ghosh S, Brinkman C, Porter R. 1987. A quantitative study of the distribution of neurons projecting to the precentral motor cortex in the monkey (M. fascicularis). Journal of Comparative Neurology 259: 424-444.

Ghosh S, Gattera R. 1995. A comparison of the ipsilateral cortical projections to the dorsal and ventral subdivisions of the macaque premotor cortex. Somatosensory and Motor Research 12: 359-378.

Gibson AR, Hansma DI, Houk JC, Robinson FR. 1984. A sensitive low artifact TMB procedure for the demonstration of WGA-HRP in the CNS. Brain Res 298: 235-241.

Godschalk M, Lemon RN, Kuypers HG, van der Steen J. 1985. The involvement of monkey premotor cortex neurones in preparation of visually cued arm movements. Behavioural Brain Research 18: 143-157.

Godschalk M, Mitz AR, van Duin B, van der Burg H. 1995. Somatotopy of monkey premotor cortex examined with microstimulation. Neuroscience Research - Supplement 23: 269-279.

Goodael J, Mittermeier R. 1996. The pictorial guide to the living primates pogonias. East Hampton Press. New York.

Hatanaka N, Nambu A, Yamashita A, Takada M, Tokuno H. 2001. Somatotopic arrangement and corticocortical inputs of the hindlimb region of the primary motor cortex in the macaque monkey. Neuroscience Research - Supplement 40: 9-22.

Hendry SH, Jones EG, Hockfield S, McKay RD. 1988. Neuronal populations stained with the monoclonal antibody Cat-301 in the mammalian cerebral cortex and thalamus. J Neurosci 8: 518-542.

Hockfield S, McKay RD, Hendry SH, Jones EG. 1983. A surface antigen that identifies ocular dominance columns in the visual cortex and laminar features of the lateral geniculate nucleus. Cold Spring Harb Symp Quant Biol 48: 877-889.

Jones EG, Coulter JD, Wise SP. 1979. Commissural columns in the sensory-motor cortex of monkeys: Differential thalamic relationships of sensory-motor and parietal cortical fields in monkeys. Journal of Comparative Neurology 188: 113-135.

Kievit J, Kuypers HG. 1977. Organization of the thalamo-cortical connexions to the frontal lobe in the rhesus monkey. Experimental Brain Research 29: 299-322.

Kunzle H. 1978. An autoradiographic analysis of the efferent connections from premotor and adjacent prefrontal regions (areas 6 and 9) in macaca fascicularis. Brain, Behavior & Evolution 15: 185-234.

Kurata K. 1991. Corticocortical inputs to the dorsal and ventral aspects of the premotor cortex of macaque monkeys. Neuroscience Research - Supplement 12: 263-280.

Leichnetz GR. 2001. Connections of the medial posterior parietal cortex (area 7m) in the monkey. Anatomical Record 263: 215-236.

Lu MT, Preston JB, Strick PL, Strickland D. 1994. Interconnections between the prefrontal cortex and the premotor areas in the frontal lobe

Luppino G, Rizzolatti G. 2000. The organization of the frontal motor cortex. News Physiological Science 15: 219-224.

Luppino G, Rozzi S, Calzavara R, Matelli M. 2003. Prefrontal and agranular cingulate projections to the dorsal premotor areas F2 and F7 in the macaque monkey. The Journal of European Neuroscience 17: 559-578.

Marconi B, Genovesio A, Battaglia-Mayer A, Ferraina S, Squatrito S, Molinari M, Lacquaniti F, Caminiti R. 2001. Eye-hand coordination during reaching. I. Anatomical relationships between parietal and frontal cortex. Cerebral Cortex 11: 513-527.

Matelli M, Luppino G, Rizzolatti G. 1985. Patterns of cytochrome oxidase activity in the frontal agranular cortex of the macaque monkey. Behavioural Brain Research 18: 125-136.

Matelli M, Luppino G. 1996. Thalamic input to mesial and superior area 6 in the macaque monkey. Journal of Comparative Neurology 372: 59-87.

Matelli M, Govoni P, Galletti C, Kutz DF, Luppino G. 1998. Superior area 6 afferents from the superior parietal lobule in the macaque monkey. Journal of Comparative Neurology 402: 327-352.

McFarland NR, Haber SN. 2002. Thalamic relay nuclei of the basal ganglia form both reciprocal and nonreciprocal cortical connections, linking multiple frontal cortical areas. Journal of Neuroscience 22: 8117-8132.

Miyata M, Sasaki K, Darian-Smith C. 1983. HRP studies on thalamocortical neurons related to the cerebellocerebral projection in the monkey thalamic projections to sensorimotor cortex in the macaque monkey: use of multiple retrograde fluorescent tracers. Brain Research 274: 213-224.

Muakkassa KF, Strick PL. 1979. Frontal lobe inputs to primate motor cortex: evidence for four somatotopically organized 'premotor' areas. Brain Research 177: 176-182.

Olszewski J. 1952. The Thalamus of Macaca Mulatta, In: Olszewski, J. Basel: Karger. p 93.

Petrides M, Pandya DN. 1984. Projections to the frontal cortex from the posterior parietal region in the rhesus monkey. Journal of Comparative Neurology 228: 105-116.

Petrides M, Pandya DN, Morris R. 1999. Dorsolateral prefrontal cortex: comparative cytoarchitectonic analysis in the human and the macaque brain and corticocortical connection patterns. 11: 1011-1036.

Petrides M, Pandya DN. 1999. Dorsolateral prefrontal cortex: comparative cytoarchitectonic analysis in the human and the macaque brain and corticocortical connection patterns. European Journal of Neuroscience 11: 1011-1036.

Preuss TM, Goldman-Rakic PS. 1991. Myelo- and cytoarchitecture of the granular frontal cortex and surrounding regions in the strepsirhine primate Galago and the anthropoid primate Macaca. Journal of Comparative Neurology 310: 429-474.

Rizzolatti G, Scandolara C, Gentilucci M, Camarda R. 1981. Response properties and behavioral modulation of "mouth" neurons of the postarcuate cortex (area 6) in macaque monkeys. Brain Research 225: 421-424.

Rizzolatti G, Luppino G. 2001. The cortical motor system. Neuron 31: 889-901.

Rouiller EM, Tanne J, Moret V, Kermadi I, Boussaoud D, Welker E. 1998. Dual morphology and topography of the corticothalamic terminals originating from the primary, supplementary motor, and dorsal premotor cortical areas in macaque monkeys. Journal of Comparative Neurology 396: 169-185.

Rouiller EM, Tanne J, Moret V, Boussaoud D. 1999. Origin of thalamic inputs to the primary, premotor, and suppleentary motor cortical areas and to area 46 in macaque monkeys: A multiple retrograde tracing study. Journal of Comparative Neurology 409: 131-152.

Schell GR, Strick PL. 1984. The origin of thalamic inputs to the arcuate premotor and supplementary motor areas. Journal of Neuroscience 4: 539-560.

Shipp S, Blanton M, Zeki S. 1998. A visuo-somatomotor pathway through superior parietal cortex in the macaque monkey: cortical connections of areas V6 and V6A. European Journal of Neuroscience 10: 3171-3193.

Simmons RMT. 1980. The morphology of the diencephalon in the Prosimii. II. The Lemuroidea and Lorisoidea. Part I. Thalamus and Metathalamus. Journal fur Hirnforschung 21: 449-491.

Strick PL. 1985. Anatomical analysis of ventrolateral thalamic input to primate motor cortex. Journal of Neurophysiology 39: 1020-1031.

Strick PL. 1976. Activity of ventrolateral thalamic neurons during arm movement :Anatomical analysis of ventrolateral thalamic input to primate motor cortex. Journal of Neurophysiology 39: 1032-1044.

Tanne-Gariepy J, Bello A, Fadiga L, Rizzolatti G. 2002. Parietal inputs to dorsal versus ventral premotor areas in the macaque monkey: evidence for largely segregated visuomotor pathways. Neuropsychologia 40: 492-502.

Vogt O, Vogts C. 1919. Ergebnisse unserer Hirnforschung. J Psychol Neurol (Leipzig) 25: 277-462.

von Bonin G, P. B. 1947. The Neocortex of Macaca Mulatta, In: von Bonin, G,P., B. Urbana: University of Illinois. p 136.

Weinrich M, Wise SP. 1982. The premotor cortex of the monkey. Journal of Neuroscience 2: 1329-1345.

Wiesendanger R, Wiesendanger M, Weynants P. 1985. The thalamic connections with medial area 6 (supplementary motor cortex) in the monkey (macaca fascicularis). Experimental Brain Research 59: 91-104.

Wise SP. 1985. The primate premotor cortex: past, present, and preparatory. Annual Review of Neuroscience 8: 1-19.

Wise SP, Boussaoud D, Johnson PB, Caminiti R. 1997. Premotor and parietal cortex: corticocortical connectivity and combinatorial computations. Annual Review of Neuroscience 20: 25-42.

Wong-Riley M. 1979. Changes in the visual system of monocularly sutured or enucleated cats demonstrable with cytochrome oxidase histochemistry. Brain Res 171: 11-28

Woolsy CN, Settlage PH, Meyer DR, Sencer W, Pinto Hamuy T, Travis AM. 1952. Patterns of localization in precentral and "supplementary" motor areas and their relation to the concept of a premotor area. Res Publ Assoc Res Nerv Ment Dis 30: 238-264.

Wu CW, Bichot NP, Kaas JH. 2000. Converging evidence from microstimulation, architecture, and connections for multiple motor areas in the frontal and cingulate cortex of prosimian primates. Journal of Comparative Neurology 423: 140-177.

.

CHAPTER II

ARCHITECTONIC SUBDIVISIONS OF MOTOR THALAMUS AND ADDITIONAL MOTOR NUCLEI IN PROSIMIAN GALAGOS

<u>**Introduction**</u>

An early, important architectonic study of the human motor thalamus of Hassler (1959)

divided the motor thalamus into more than 15 subdivisions, based on differences in their

appearances in cytoarchitecture and myeloarchitecture (Macchi and Jones, 1997 review).

Early studies of motor thalamus of Old World monkeys include Walker's (1938)

microelectronic mapping study. Walker divided monkey motor thalamus into several

subdivisions, based on the movement responses initiated by microstimulation of the

thalamic neurons (Macchi and Jones, 1997 review). Later, Olszewski (1952) divided the

motor thalamus of Old World monkeys into more subdivisions based on

cytoarchitectonic results. Olszewski concluded that the motor thalamus of macaque

monkeys includes ventroanterior (VA), ventrolateral (VL), and ventroposterior (VP)

divisions. The VA could be further divided into magnocellular (VAmc) and

parvocellular (VApc) subnuclei, while the VL could be divided into anterior and

posterior. The anterior VL nuclei include nucleus pars oralis (VLo), nucleus pars

caudalis (VLc), and nucleus anterior medial (area X). The medial VL nucleus is called

VLm, and the posterior VL nuclei include nucleus pars postrema (VLps), nucleus oral

ventral posterior lateral (VPLo) and nucleus caudal ventral posterior lateral (VPLc)

(Olszewski, 1952). Olszewski's work on non-human primates set the foundation for the

following architectonic studies on motor thalamus.

In New World monkeys, Stepniewska and colleagues (1994) showed that owl monkeys
share the similar subdivisions of the motor thalamus with the Old World macaque
monkeys. The motor thalamus of owl monkeys includes ventral anterior (VA), ventral
medial (VM), and ventral lateral (VL) nuclei. The VL nuclei could be divided into
anterior (VLa) and posterior subdivisions. The posterior VL is further divided into
principal nucleus (VLp), medial nucleus (VLx), and dorsal nucleus (VLd). These
subdivisions were defined based on the results of cytoarchitecture, histochemistry, and
myeloarchitecture (Stepniewska et al, 1994). Divisions of the motor thalamus of the Old
World monkeys by Olszewski and of New World monkeys by Stepniewska reveal that,
both species share similar subdivisions. Both have ventral anterior (VA), ventral lateral
(VL), and ventral medial (VM) major subdivisions. The nucleus VM in Stepniewska
corresponds to VLm in Olszewski's study. Moreover, ventral lateral subdivisions of both
species could be divided into three subnuclei: the VLp, VLx, and VLd. The VLp, VLx,
and VLd in Stepniewska correspond to the VPLo, area X, and VLc (and VLps) in
Olszewski, respectively (Stepniewska et al, 1994).

The research on humans and macaque monkeys also show that the motor thalamus can be
differentiated into several subdivisions via immunochemical techniques. Based on the
Parvalbumin (PV) and Calbindin (Cb) results, the human motor thalamus is mainly
divided into ventral lateral (VL), ventral anterior (VA), and ventral medial (VM) three
nuclei (Morel et al., 1997). The VL is then divided into anterior (VLa) and posterior
(VLp) subnuclei. The VLp is even further divided into ventral, dorsal and medial
paralamellar parts. The VA separated into paracellular (VApc) and magnocellular
(VAmc) parts. Basically, the population of PV cells gradually decreases as moving

toward VLa from VLp. The most anterior part of the motor thalamus, VA, contains no or very sparse PV cells. On the contrary, the nuclei, VA, VLa, and VM, which are poor in PV staining, contain rich positive Cb cells (Morel et al., 1997). Similarly, the distributions of the PV and Cb cells in motor thalamus of the macaque monkeys are very close to those in the humans. The positive PV cell population in VLp is much higher than in other motor subnuclei; on the other hand, there are no or few Cb cells in VLp. The VLa contains almost equal amounts of PV and Cb positive cells in macaque monkeys (Jones, 2001 review).

Macaque and owl monkeys belong to Old World and New World monkeys, respectively. Both primates are included in simian primate category. Thus, it is not so surprising that simian primates share a similar architecture in the motor thalamus. According to the evolutionary time scale, the prosimian primates appeared much earlier than the simian primates in the world. The most recent study on the thalamus architecture in prosimian primates, galagos, was conducted by Simmons in 1980. He delineated motor thalamus into three main structures: nucleus ventralis anterior (VA), lateral (VL) and medialis (VM). The VL is further divided into lateral and medial parts (Simons, 1980). The lateral VL (VLl) contains small cells that are distributed irregularly among the fibers, and the medial VL (VLm) contains even smaller oval-shaped cells that are lightly stained. The results he got were based on coronally-cut brain sections processed with myelin and Nissl stainings. There are three questions raised by his study. The first is that the VA and VM nuclei were located really medial-ventrally, and they appeared to be too separated and far away from VL nucleus. The second is that VA in his study was located very posteriorly and was co-extensive with ventroposterior nucleus (VP). The third

question is that the delineation of VL complex into lateral and medial subdivisions was

not obvious or convincing. Thus, the purpose of our study was to reconsider the

architectonic differentiation of the motor thalamus of prosimian galagos. In order to

reveal the subdivisions of the motor thalamus of the galagos, different planes of

sectioning and various staining methods were applied. The brains were sectioned not

only coronally, but also horizontally and sagittally. The multiple staining techniques

included Nissl stain for cytoarchitecture, and histochemical procedures for cytocrome

oxidase (CO), AChE, fiber stain for myeloarchitecture, and immunochemical procedures

for Cat 301, Cb and Pv. Among these cutting planes and staining methods, the thalamus

that was cut horizontally and stained with AChE showed the clearest and most consistent

pictures across cases. The results show that the prosimian primate, *Galago garnitti*

(Otolemur garnetti), shares similarities in architectonic organization of the motor

thalamus with the simian primates. However, the motor thalamus of galagos is not as

clearly differentiated and does not have as many subdivisions as the motor thalamus in

simians.

Methods

A total of 22 adult prosimian galagos, *Galago garnetti*, was used in this study. Ten of

them were from the cortical and thalamic connectional studies and 12 of them were from

other studies. For the animals from the connectional studies, motor cortex or posterior

parietal cortex was microstimulated and injected with multiple neuroanatomical tracers.

After a suitable survival period, the animals were given a lethal dose of barbiturate and

were perfused with saline, followed by 2% paraformaldehyde, and 2% paraformaldehyde

with 10% sucrose. The brains were removed and thalami were separated and stored in

30% sucrose overnight. The thalami of an additional 12 adult galagos from other studies

were used for describing thalamic architecture. These thalami were processed for

histology only. All experimental procedures followed the guidelines of the National

Institutes of Health and Vanderbilt University for the care and use of animals in research.

The thalami of all animals were sectioned at either 40 or 50 μm thickness in either

coronal, sagittal, or horizontal planes. Series of thalamic sections were processed with

various staining techniques to reveal the architecture of the thalamus. The techniques

included a Nissl preparation, histochemical stainings for acetylcholinestrase (AChE,

Geneser-Jensen and Blackstad, 1971), myelin (Gallyas, 1979), or CO (Wong-Riley,

1979), and immunocytochemical procedures for parvalbumin (Pv) (Celio, 1990),

Calbindin D-28K (Cb) (Celio, 1990), and Cat-301 (Hockfield et al., 1983; Hendry et al.,

1988). These thalamic sections were analyzed on a bright-field microscope or

microprojector. The adjacent sections with the architectonic features were superimposed

based on the blood vessel patterns. The architectonic borders of the nuclei were marked

and compared from the various stainings.

Results

The Motor Thalamus

In this chapter, we describe the architecture of thalamic nuclei that we found to be

connected to the motor cortical regions (primary motor, supplementary motor and

premotor areas) of the prosimian primate, galago. The results of the thalamocortical

connection study are described in a subsequent chapter. The motor thalamus in galago is

separated anteriorly from the anterior nuclei (Ant) and posteriorly from the lateral

posterior nucleus (LP) at dorsal thalamic levels. Ventrally, it is adjacent to the

ventroposterior nucleus (VP). Laterally, the motor thalamus is surrounded by the

reticular nucleus (Ret), and medially, it borders intralaminar nucleus (IL) and

mediodorsal nucleus (MD) (Fig. 2-1). The motor thalamus is not architectonically

homogeneous. Based on the architectonic features, we suggest that the motor thalamus

consists of three main regions: ventral anterior (VA), ventral lateral (VL), and ventral

medial (VM). There are two subdivisions within VA: lateral (VAl) and medial (VAm),

and the VL consists of anterior (VLa) and posterior (VLp) two nuclei (Fig. 2-1). Our

descriptions of these motor nuclei most rely on the horizontally cut thalamic sections,

which provide the clearest and most consistent picture of the motor thalamic subdivisions,

although the coronal and sagittal sections are also illustrated. The sagittal plane clearly

revealed VLa and its borders with VA and VLp in AChE staining; however, the borders

of VLa with VM, and the borders of VAl with VAm were not as clear. The coronal plane

was not very useful in revealing the motor thalamus subdivisions, and only VLp and VM

were reliably delineated from the neighboring structures.
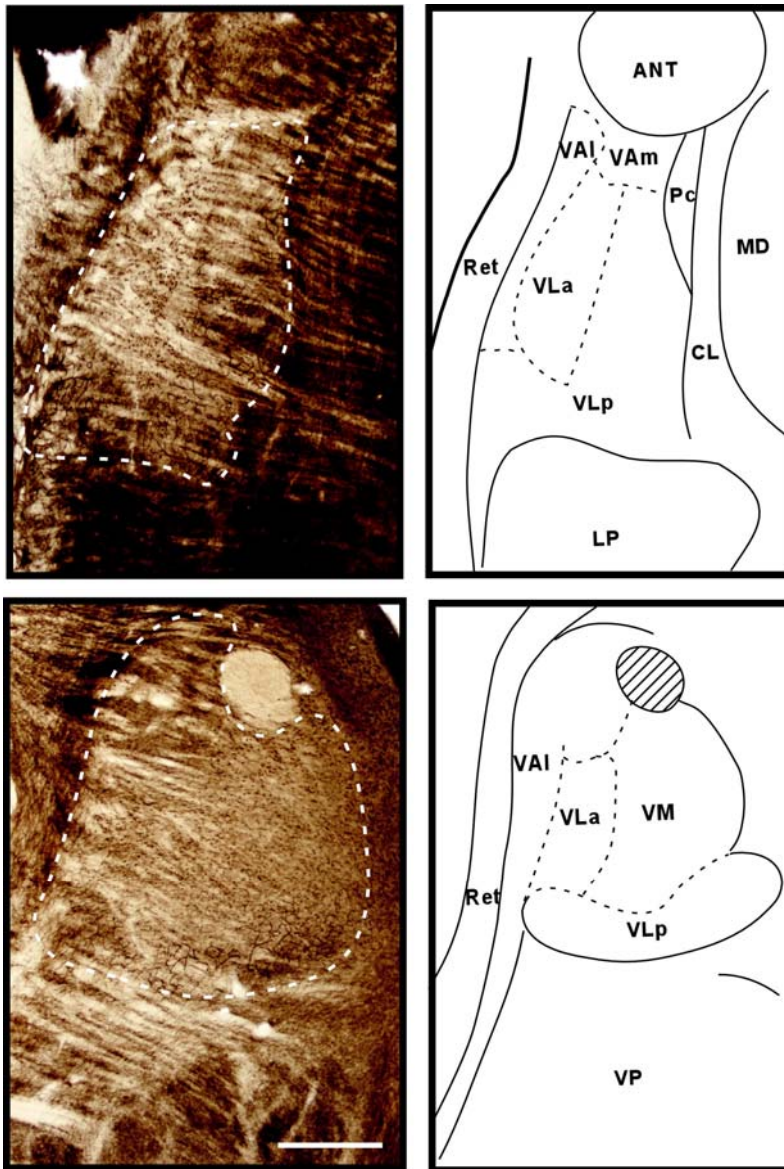
Fig. 2-1. Photomicrographs of the motor thalamus of a galago (#03-74) illustrated in AChE staining (left panel), and the symbolic drawings according to the stainings showing on the right panel. Thalamus was sectioned horizontally from dorsal (top) to ventral (bottom). The motor thalamus sits medially to the reticular nucleus (Ret), posteriorly to the anterior nucleus (Ant), and anteriorly to the lateral posterior nucleus (LP) at dorsal levels or to the ventral posterior nucleus (VP) at ventral levels. AChE staining displayed the motor thalamus as a nonuniform-structure with some parts that are lightly stained and some parts were darkly stained. The motor thalamus can be divided into three main regions, ventral anterior (VA), ventral lateral (VL) and ventral medial (VM). VA has two small subdivisions, lateral (VAl) and medial (VAm), and the VL complex is further divided into anterior (VLa) and posterior (VLp) subdivisions. VLp is shown with the most striking landmark of the motor thalamus that had darkly stained reticular network. The drawings on the right correspond to the photos on the left. The solid lines are the boundaries of the motor thalamus, and the dash lines are the borders of the motor thalamic subdivisions. Top = anterior; Left = lateral; Scale bar = 1mm.

18

Among the staining techniques we used, AChE staining was one of the most useful, and it provides the clearest and most consistent pictures. The CO and Pv preparations revealed similar architectonic results because both of these preparations stain the same population of the cells. However, Pv preparation revealed a better picture of the motor thalamic subdivisions such as VLp than CO preparation. While Cat 301 immunocytochemistry clearly shows VLa and VLp in macaque monkeys, it failed to reveal subdivisions of the motor thalamus in galagos. The Cb staining only distinguished moderately dark VA from the pale neighboring structures in galagos.

In simian primates and galagos, the ventral lateral (VL) region is also known as the part of the motor thalamus that contributes the most connections to the motor cortex. Its anterior part (VLa) sends strong projections to the premotor areas (PM) and supplementary motor area (SMA), and the posterior part (VLp) to the primary motor cortex (M1). The ventral anterior region (VA), unlike VL, only sends moderate inputs to the motor cortical areas. The lateral VA (VAl) sends some inputs to PM and SMA, but not to M1. The VM region also sends projections to the motor cortical areas (including primary and non-primary motor areas). Here we give the most detailed descriptions to ventral lateral (VL), ventral anterior (VA), and ventral medial (VM) thalamic regions that are strongly related to the motor cortical regions, although we describe other nuclei as well.

Ventral Lateral Region

The ventral lateral region, VL, occupies a very large territory, about two-third of the motor thalamus. The VL sits anteriorly to the LP (at dorsal levels) and VP (at ventral

levels), and the VL is between the reticular nucleus and IL. The VL complex is not a

uniform structure that can be further divided into posterior (VLp) and anterior (VLa)

subdivisions. Based on the connectional and architectonic results, the VLp and VLa have

very dense connections with different cortical motor areas. In the architectonic study, it

shows that the VLp and VLa can be easily distinguished in either horizontal or sagittal

sections.

Ventral lateral nucleus, posterior subdivision (VLp)

The territory of the semi-circular-shaped VLp is bigger than the rostrally adjacent VLa.

VLp is posteriorly adjacent to the LP at the dorsal and to the VP at the ventral levels.

VLp sits between the Reticular nucleus and IL, and the anterior nucleus is anteriorly

adjacent to VLp. In all planes, VLp has a distinctive appearance that allows us to

recognize it easily from the neighboring nuclei. In most of the staining techniques such

as AChE, CO, and Pv, VLp could be seen easily as a darkly stained, distinctive structure.

In Nissl preparation, VLp could be further divided medio-laterally into smaller

subdivisions based on the slight differences in cytoarchitectonic appearance.

In all planes, AChE staining reveal VLp with dense and dark reticular pattern that

probably reflects the presence of AChE enzyme in the endothelial cells of the capillary

walls. This pattern makes it the most distinctive landmark of the VL region (Fig. 2-2, 2-6,

2-7). Moreover, the densely packed and non-uniformly stained neuropil results in patchy

appearance of VLp. There are few AChE-stained cell bodies distributed among these

darkly stained capillaries in VLp. The neuropil patches and the AChE dark
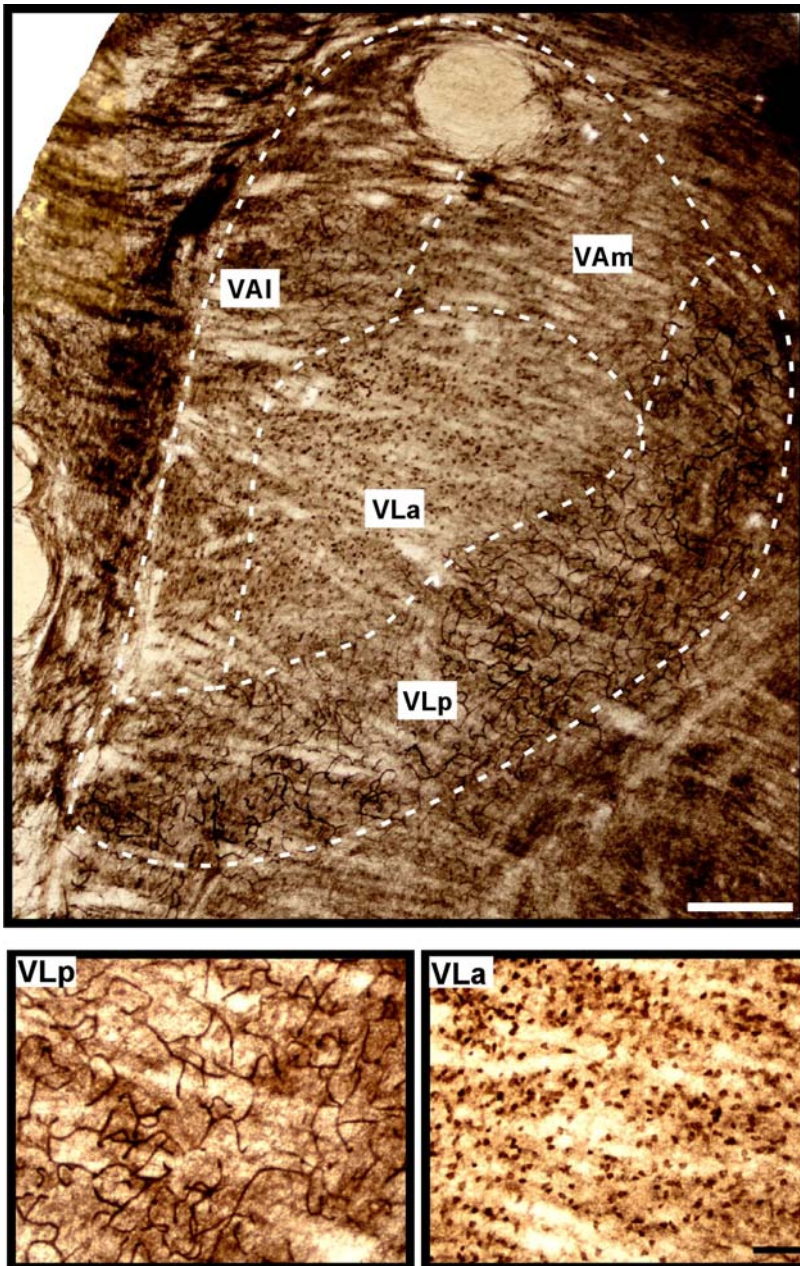
Fig. 2-2. Photomicrographs of a AChE-stained section with high magnification. (Top) VA is not a uniform structure that the lateral VA (VAl) has darkly stained neuropli and capillary network on the medial sector, which is adjacent to VAm. The medial VA (VAm), on the other hand, was seen with light neuropil and some cell bodies located on the lateral sector that is adjacent to VAl. The anterior (VLa) and posterior (VLp) subdivisions of VL complex also presents absolutely different architectonic features. VLa consists of densely-packed and darkly-stained cell bodies that are much more prominent than VAm, and VLp consists of densely-packed and darkly-stained capillary network that is much more prominent than VAl. It seems that AChE preparations reveal only cell bodies in VLa and only capillary network in VLp. (Bottom) Photomicrographs of AChE-stained sections with much higher magnification showing the detailed features of VLp and VLa. The dash lines are the boundaries between the subdivisions. top = anterior; left = lateral; scale bar = 0.5 mm (top), 250 µm (bottom).
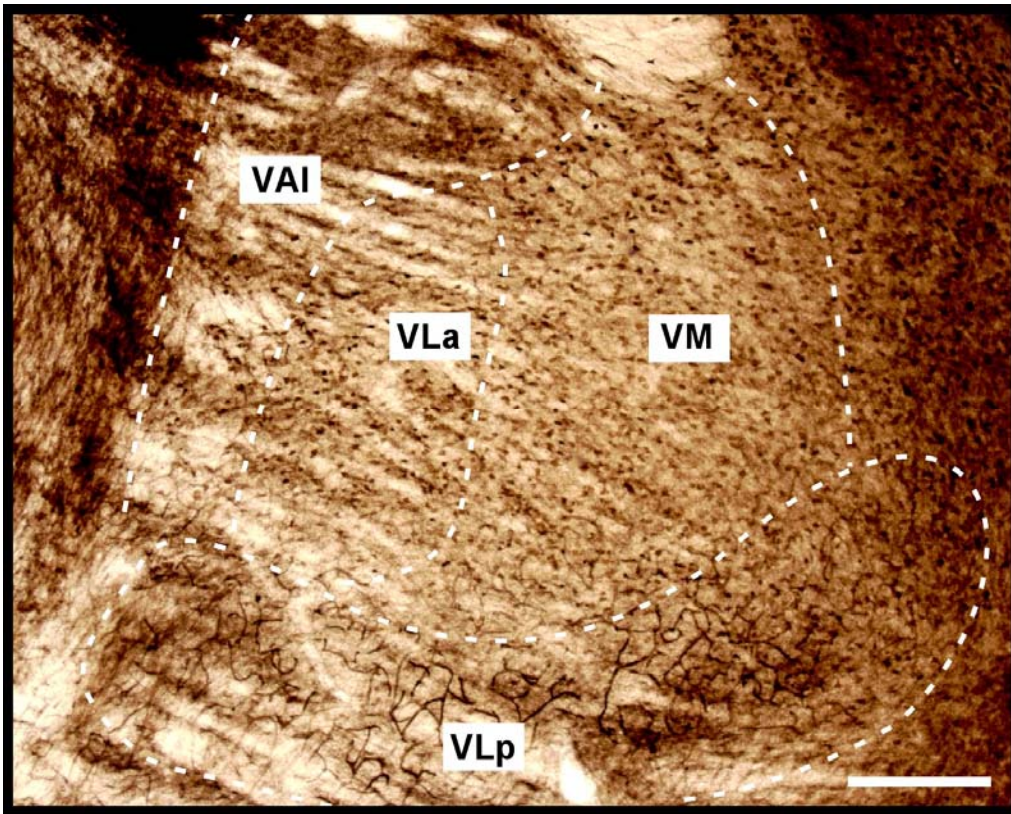
Fig. 2-3. A horizontal section with AChE stains showing the architectonic features of the motor thalamic nuclei. At ventral thalamic levels, VM starts to appear and replace VLa. The appearance of VLa and VM is very similar in AChE sections, except that the cell bodies revealed in VM are much more lightly-stained than the cell bodies in VLa. Moreover, the density of the cell body in VM seems to be higher than in VLa. Scale bar = 0.5 mm.

capillaries in the medial part of the VLp are a little darker and denser than in the remaining VLp (Fig. 2-2). Moreover, density of the reticular network decreases at the ventral levels (Fig. 2-3).

In Nissl sections, VLp is characterized densely packed cells of different sizes and shapes that are not uniformly distributed throughout this region. There are medio-lateral and dorso-ventral differentiations across VLp. In the medial sector of VLp adjacent to the intralaminar nuclei (IL), the cells are slightly larger than those in the central sector of

VLp. The cells in the medial VLp are round in shape, and are evenly distributed due to

densely packed thin fibers (Fig. 2-3). The central VLp subdivision contained medium-

sized cells that are slightly larger than those in the lateral sector of VLp. The cells in the

central VLp are in multipolar and round in shape. The lateral VLp adjacent to the

reticular nuclei (Ret), however, contains small-sized cells and most of these cells are

elongated and oval in shape. These cells are aggregated into small clusters among the

thick fiber bundles (Fig. 2-3). Thus, from medial to lateral VLp, the cells become not

only smaller but also less uniformly distributed. In addition, the cells in the dorsal VLp

are larger, and more densely packed than the cells in the ventral VLp that contains small,

irregular-shaped and loosely-packed cells (Fig. 2-4). Thus, according to the Nissl

sections, there are likely several subdivisions within the dorsal VLp. Lateral, central and

medial subdivisions can be seen in the horizontal and coronal sections.

It is difficult to distinguish VLp from LP in Nissl staining in the horizontal plane due to

the similarity of the cytoarchitecture of the dorsal VLp and posteriorly adjacent LP, as

both nuclei contain densely packed cells. However, the loosely-packed cells of ventral

VLp contrast with the densely-packed cells in VP (Fig. 2-5). So it is easy to distinguish

VLp and VP at ventral thalamic levels. In general, the cells in the VL are much smaller

than those in the ventral anterior region (VA). However, the AChE staining reveals clear

borders of VLp with LP and VP, because the unique capillary stained in VLp contrasts

with the lack of this kind of reticular pattern in LP and VP.
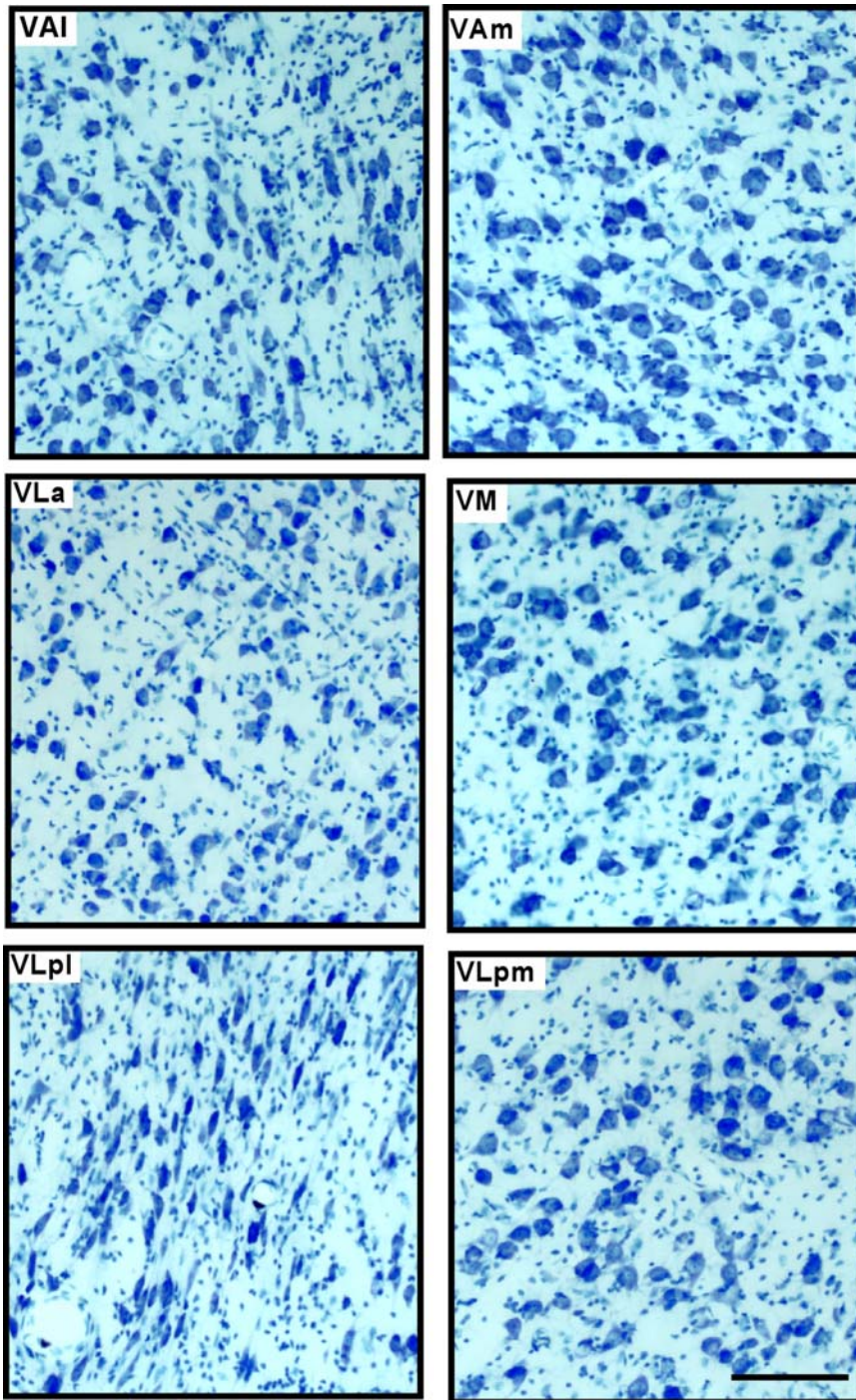
Fig. 2-4. Photomicrographs of Nissl-stained sections from case 03-19 showing the distribution and size of the neurons in the motor thalamus. The medial VM (VAm) contains more densely-packed and larger-sized cells than the lateral VM (VAl). The cells in VLa are small and clustered in groups, unlike the cells in VM that are larger. The medial sector of VLp (VLpm) contains the cells that are larger than the cells in the lateral sector (VLpl). The cells in VLpl are elongated in shape, which are very different from the cells in VLpm that are round in shape. Scale bar = 250 μm.

The myelin staining shows that the fibers in VLp are thin and densely packed. Within

VLp, the fibers in the lateral part are thicker and sparser than the fibers in the medial part.

The myelin pattern of VLp was not so different from VLa. However, the fibers in VLp

are slightly thinner and denser than in VLa (Fig. 2-5, 2-6, 2-7), as the fibers enter from

the reticular nucleus and traveled posteriorly. These fibers travel from anterior to

posterior motor thalamus. While these fibers travel posteriorly, they split into thinner and

more densely packed fibers. Besides, because of the similar myeloarchitecture between

VLp and LP, it is hard to distinguish these two nuclei. Thus, the borders of VLp with

adjacent nuclei are delineated based on AChE sections. On the other hand, the border of

VLp with VP is clearly marked because the ventral VLp contains denser and darker fibers

than VP since VP contains lightly stained thin fibers (Fig 2-5).

In Pv and CO sections with three cutting planes, the whole VLp contains darkly to

moderately stained neuropil with some darkly stained cell bodies that are well visible.

These two stainings revealed the whole VLp as a homogeneous structure (Fig. 2-5, 2-6,

2-7), which make VLp easily distinguished from the rostrally adjacent lighter structures

such as VLa and VA. Besides, the posteriorly adjacent LP looks pale in CO and Pv

preparations, and this contrasts with the darkly stained VLp. However, at the ventral

levels, the VP nucleus is stained just slightly darker than VLp. So, it is not easy to

delineate the border between VLp and VP at ventral levels.
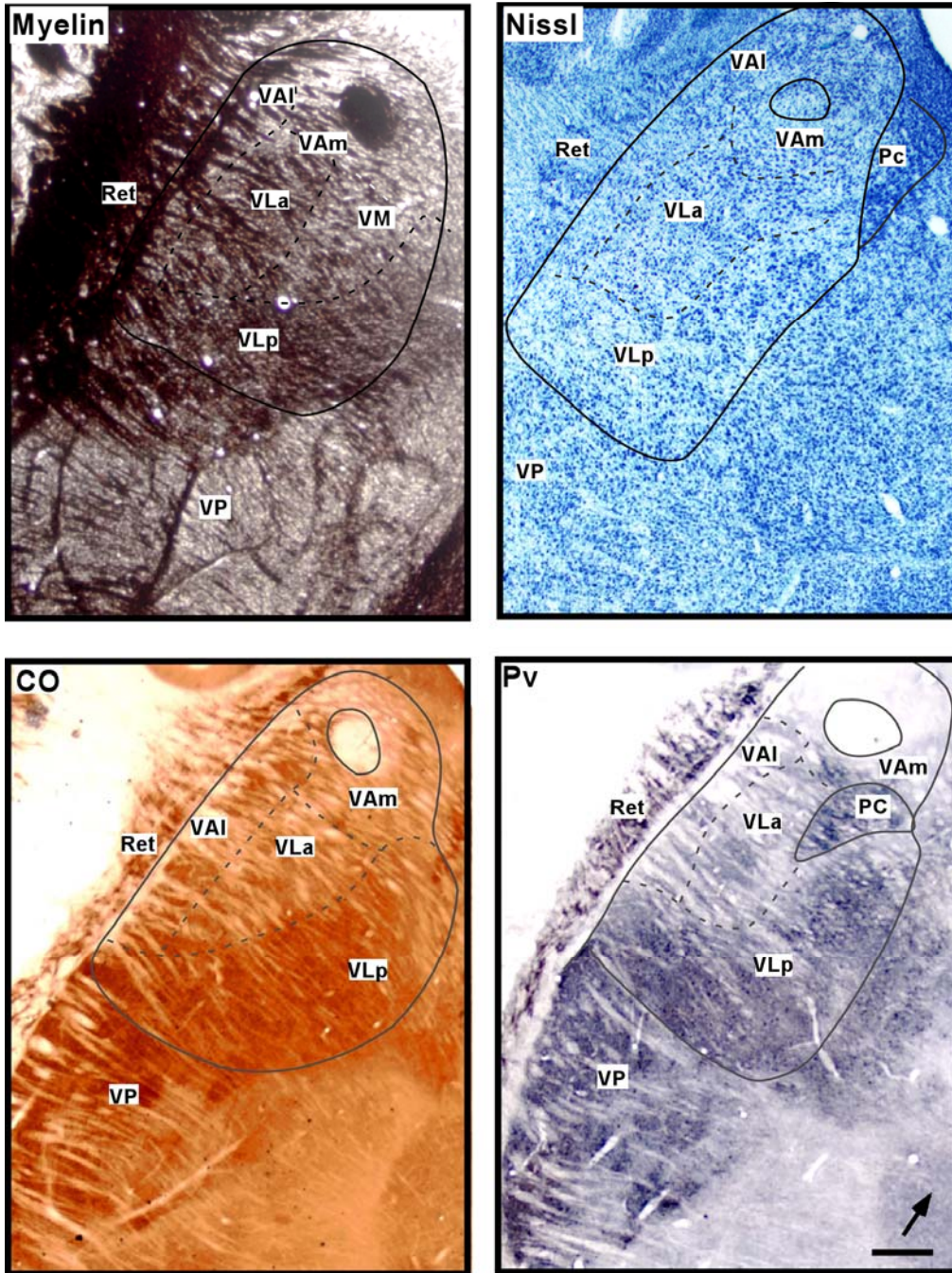
Fig. 2-5. Photomicrographs of horizontally-cut sections stained with myelin, Nissl, CO and Pv preparations. (Top left) The myelinated fibers are travelling in horizontal (latero-medial) orientation and the fibers near the reticular nucleus (Ret) are thicker but sparser than the fibers located in the medial part of the motor thalamus. (Top-right) It is difficult to differentiate subdivisions within the motor thalamus in Nissl stains with this small magnification. (Bottom) The darkly-stained VLp can be distinguished easily in CO and Pv stainings. The solid lines are the boundaries of the motor thalamus, and the dash lines are the borders of the motor thalamic subdivisions. Arrow points to the anterior; Left = lateral; Scale bar = 1mm.
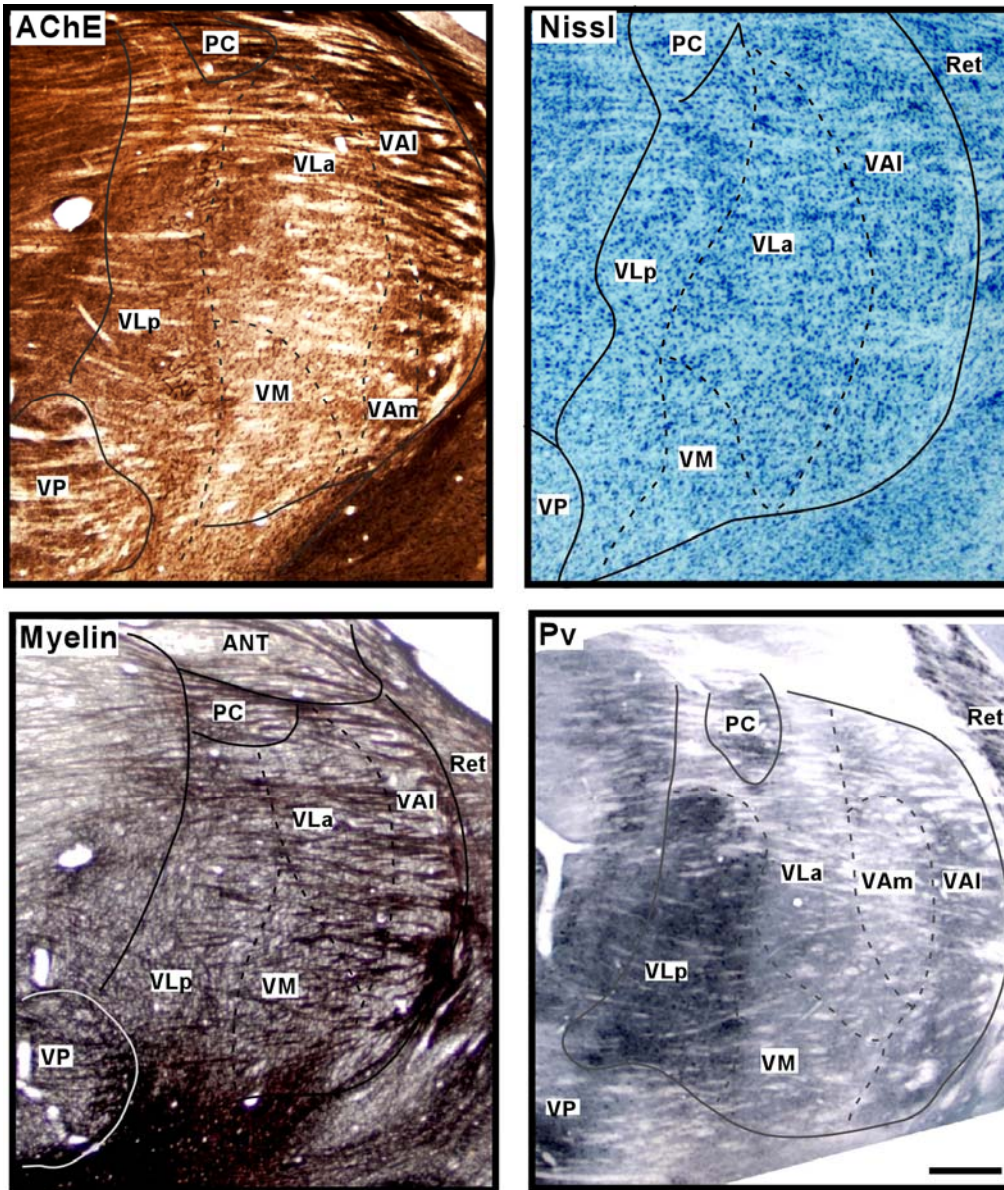
Fig. 2-6. Photomicrographs of sagittally-cut sections stained with AChE, Nissl, myelin, and Pv. In a AChE section (top-left), the major subdivisions of the motor thalamus, VLp, VLa, and VAl can be demarcated easily. However, the border between VLa and VM is difficult to be marked. Similar to the horizontally-cut sections illustrated in Fig. 5, it is difficult to delineate subdivisions in Nissl sections (top-right); however, in Pv staining (bottom-right), only VLp could be distinguished. In myelin-stained sections (bottom-left), unlike the horizontal plane, the border of VAl and VLa, and the border of VLa and VLp somehow could be delineated in sagittal plane. The fibers become thinner and denser as travelling from the anterior motor thalamus (VA) to the posterior motor thalamus (VLp). The solid lines are the boundaries of the motor thalamus, and the dash lines are the borders of the motor thalamic subdivisions. Top = dorsal; Left = posterior; Scale bar = 1mm.

Ventral lateral nucleus, anterior subdivision (VLa)

The anterior subdivision of the VL complex, VLa has an elongated shape that is oriented anterio-posteriorly in horizontal sections. The VLa is not as big as VLp. It protrudes into the ventral anterior region (VA). The VA is like a C-shaped belt that surrounds VLa anterio-laterally. Anteriorly, VLa is adjacent to the medial part of VA (VAm); laterally, VLa is adjacent to the lateral part of VA (VAl); medially and posteriorly to VLp, and ventrally to VM. The horizontal plane (Fig. 2-2) provides the clearest picture of VLa. While VLp can be revealed in most of the staining preparations, VLa can be only seen clearly in the AChE stains. Other stains (CO and Pv) can only weakly reveal VLa.

In AChE preparation, VLa is characterized by its unique moderately to darkly stained cell bodies and lightly stained neuropil (Fig. 2-2). These darkly stained cell bodies make VLa very distinctive from the neighboring structures. While VLp contains darkly stained capillaries and neuropil, VLa lacks of this kind of reticular pattern formed by the capillaries. The VLa is easier to distinguish in horizontal sections than in sagittal (Fig. 2-6) and coronal sections (Fig. 2-7). The cell body pattern is not so clearly revealed in the coronal sections. In Nissl preparations, VLa contains mostly small-sized cells. Majority of these cells is in oval shape, but some are round and multipolar in shape (Fig. 2-4). Compare to VLp, the cells in VLa in Nissl stains are slightly smaller and more sparsely packed. Similar to simian primates, the cells in the VLa are not distributed uniformly, but gather in closely arranged clusters. These clusters are also the characteristic feature of this thalamic region in most primates. The myelin stains reveal VLa with densely packed and darkly stained fibers. As mentioned above, the border between VLa and VLp is not clear; however, the borders of VLa with VA and with VM could be marked easily

(Fig 2-5, 2-6, 2-7). The fibers in VLa are thinner and denser than in VA, but denser and

darker than in VM.
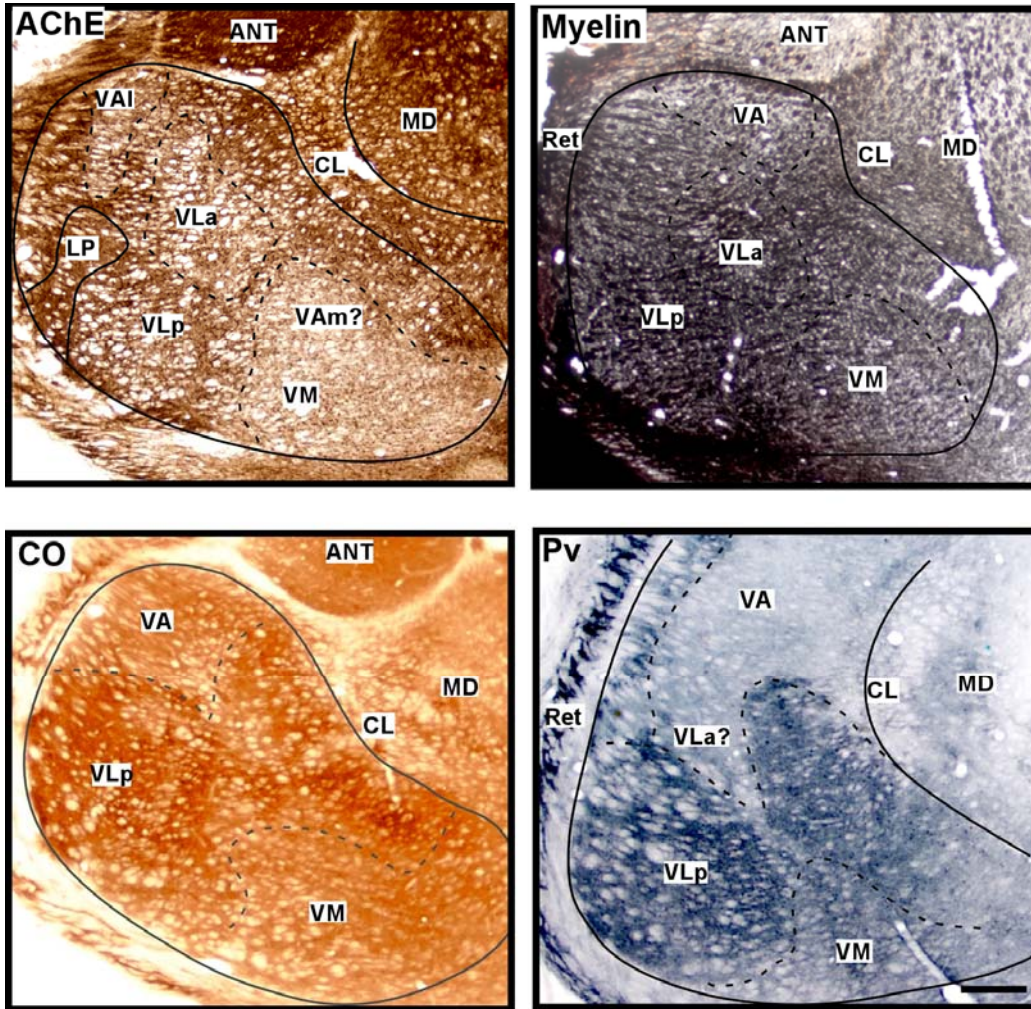
Fig. 2-7. Photomicrographs of coronally-cut sections stained with AChE, myelin, CO and Pv. In a AChE section (top-left), only VLp and VM can be well demarcated. VLp has darkly-stained neuropil and capillaries, and VM has very lightly-stained and densely-packed cell bodies. Similar to the horizontal sections that most of the subdivisions are hard to be distinguished in myelin stains (top-right), except for that the latero-ventral part of VLp is darkly stained. VLa is also darkly stained but the medial sector of VLp adjacent to CL is only a little bit darkly stained compared to the rest of motor thalamic subdivisions. Similar to the horizontal and sagittal planes, in CO (bottom-left) and Pv (bottom-right) sections, only VLp was shown as a darkly-stained structure that is very distinctive from the adjacent structures. The solid lines are the boundaries of the motor thalamus, and the dash lines are the borders of the motor thalamic subdivisions. Top = dorsal; Left = lateral; Scale bar = 1mm.

The Pv and CO preparations display VLa as a lightly stained structure. In both preparations, the neuropil in VLa is stained slightly darker than the anteriorly adjacent pale VA, and is much lighter than the darkly stained posteriorly adjacent VLp (Fig. 2-5, 2-6). So the VLa bordering with VLp is much better marked than bordering with VA. The presence of big darkly stained cell bodies in VLp is another feature that distinguishes VLa from VLp.

Ventral Anterior Region

The AChE staining is the best staining to reveal the VA region and its subdivisions. In AChE preparations, the ventral anterior region (VA) is distinctive from the neighboring nuclei by its appearance of moderately to darkly stained neuropil patches (Fig. 2-1, 2-2). VA is located in the most anterior part of the motor thalamus, and is smaller than the VL region. Similar to VLp, VA is also semi-circular in shape. The overall VA region is lighter than VLp, but darker than VLa in AChE stains. To distinguish the subdivisions, the horizontal and sagittal planes (Fig. 2-6) are the most useful to separate VA from VL. In the coronal sections, it is really difficult to delineate VA from the neighboring structures (Fig. 2-7).

Similar to VL, the overall VA region is not a uniform structure. It can be divided into two subdivisions, lateral (VAl) and medial (VAm) (Fig. 2-2). The lateral VA (VAl) is seen as an anterio-posteriorly elongated structure in the horizontal sections. It is narrower than VLa. It sits medially to the reticular nucleus (Ret), laterally to VLa and VAm, posteriorly to the anterior nucleus (Ant), and anteriorly to VLp. The borders of VAl with the adjacent motor thalamic nuclei are fairly distinctive in horizontal sections in

AChE stains. The medial VA subdivisions, VAm, is also a small subdivision. VAm is

much smaller than VAl. VAm sits medially to the VAl, anteriorly to the VLa, and

ventrally to Ant. In the sagittal and coronal sections, it is difficult to differentiate the

lateral and medial VA.

VAl contains AChE darkly-stained capillary reticular networks and moderately-stained

neuropil. This kind of reticular pattern tends to cluster at the medial sector of VAl where

it is bordering with VAm. The density of the reticular network in VAl is much lower

than in VLp, and the neuropil in VAl is more lightly stained than in VLp (Fig. 2-2).

Within VAl, the dorsal part of VAl is slightly darker than the ventral part. VAm, on the

other hand, is characterized by moderately stained cell bodies and lightly stained neuropil

(Fig. 2-2). This kind of cell body pattern seems to cluster at the lateral sector of VAm

where it is bordering with VAl. Besides, the density of these moderately stained cell

body in VAm is lower than in VLa, and the neuropil in VAm is slightly lighter and

sparser than in VAl. This feature of VAm is very different from VAl that VAl only

displays capillaries and neuropil instead of cell bodies. However, at ventral levels, both

VAm and VAl are somewhat moderately stained, and the detailed AChE features are not

so clear, thus it is difficult to separate VAm and VAl apart at ventral levels.

The Nissl preparations also show the medio-lateral differentiations of cell distribution

within VA. Different from the medial VA that the cells in the lateral VA are smaller and

are elongated and oval in shape (Fig. 2-4). These cells are distributed into small clusters.

These clusters are sparsely distributed among the thick fibers. The overall cell patterns of

VAl and VLa are very similar that the cells in both structures are grouped in clusters.

The differences are that the cells in VLa are rather slightly smaller and round in shape

compared to the cells in VAl. On the contrarily, VAm contains really large round cells (Fig. 2-4) that are even larger than the cells in VAl and other VL subdivisions. These big VAm cells are densely packed and evenly distributed due to thin fibers passing through, which make this subdivision so distinctive and easily to be distinguished from other VL subdivisions. At low magnifications, subdivisions of VA are not apparent in Nissl sections (Fig. 2-5, 2-6). In myelin preparations, VA is characterized by thick and sparsely packed fibers (Fig. 2-5, 2-6). Therefore, unlike AChE and Nissl stains, the myelin staining does not distinguish the subdivisions within VA.

The Cb preparations reveal VA region as a homogeneous dark structure that contrasts to the neighboring pale nuclei. However, the CO and Pv stainings reveal VA as a heterogeneous structure. At dorsal levels, VAm is more darkly stained than VAl; whereas, VAl as well as VLa are revealed as lightly-stained structures. At ventral levels, both VAm and VAl are moderately to lightly stained as homogeneous structures. The appearance of both VAm and VAl is very close to VLa at ventral levels, thus it is difficult to separate them apart (Fig. 2-5). Therefore, the lateral and medial subdivisions of VA can only be distinguished at dorsal levels rather than ventral levels.

Ventral Medial Region

The ventral medial region (VM) sits ventrally to VLa, anteriorly to VLp, and posteriorly to VA. VM is a homogeneous structure that is better visible in AChE preparations. In AChE preparations, VM is a very distinctive structure, especially in coronal sections. VM looks much lighter than the adjacent structures such as VLp (Fig. 2-7). In both coronal and horizontal sections (Fig. 2-3), VM has a mixture of lightly stained and

densely packed cell bodies and neuropil patches. These cell bodies and neuropil are so

densely packed that seem to fill the whole VM region. The cell bodies in VLa are more

darkly stained than in VM. In the sagittal plane, the border between VM and VLa is not

so clear, thus it is difficult to distinguish them (Fig. 2-6). Although Nissl preparations do

not reveal any striking features of the cells in VM, VM is occupied by evenly distributed

round and multipolar cells (Fig. 2-4). These cells are bigger and denser than those in

VLa and VLp, but similar to those in VAm. In myelin stained sections, VM has lightly

stained and densely packed thin fibers (Fig. 2-5, 2-6, 2-7). The overall characteristic of

the myelin pattern in VM is not so different from other VL subdivisions. Therefore, the

borders of VM with VL can not be marked confidently according to AChE stains. In

both CO and Pv preparations, VM is lightly to moderately stained. Thus, VM cannot be

delineated from the adjacent lightly to moderately stained structures such as the VA and

VLa. However, VM contrasts to the darkly stained VLp (Fig. 2-6).

Additional Motor-Related Thalamic Nuclei

Although the ventral lateral, ventral anterior and ventral medial thalamic regions are the

main source of projections to the motor cortical areas, other nuclei in the thalamus that

are related to motor movements also send inputs to the motor cortical areas. In our

thalamocortical connection study, labeled cells were seen in the additional motor-related

thalamic nuclei such as the intralaminar nuclei (IL) and medial dorsal nucleus (MD) after

the neuroanatomical tracers injected in the primary motor area, premotor areas and

supplementary motor area of the motor cortex.

The Intralaminar Nuclei

The intralaminar nuclei in galagos consist of paracentral (Pc), central lateral (CL), central median (CM), and parafascicular (Pf) nuclei. Both Pc and Pf are fairly small structures compared to CL and CM. To differentiate IL nuclei, there is no "one plane" or "one staining method" that works best for all. For example, horizontal and coronal planes are good in revealing the anterior IL subdivisions, and Cat 301 works better than AChE to reveal the posterior IL subdivisions.

Pc and CL are located in the anterio-dorsal thalamus. Pc sits in between VL and CL, and CL sits laterally to medial dorsal nucleus (MD). Both Pc and CL are elongated in shape; however, the anterior part of Pc is wider than its posterior part. The CL is like a C-shaped structure that separates the motor thalamus and medial dorsal nucleus (MD). The Pc is better viewed in the horizontal and sagittal planes, whereas, horizontal and coronal planes reveal better picture of CL. In AChE stained sections, Pc is a really darkly stained structure with dense neuropil and few capillaries (Fig. 2-8). These striking landmarks make Pc so unique and distinctive compared to other IL subdivisions. On the contrary, CL is revealed as a slight darkly stained structure with loosely packed neuropil patches in AChE sections (Fig. 2-8). Few darkly stained cell bodies are seen in the anterior CL, and some darkly stained cell bodies are seen in the posterior CL. Nissl preparation show that Pc contains densely-packed and slightly darkly-stained cells. These cells are medium-sized and elongated-shaped, which make Pc so distinctive from CL that CL contains loosely packed cells. The cells in CL are relatively smaller and lightly stained compared to those in Pc. There are more multipolar cells dominated in the dorsal part of CL, and
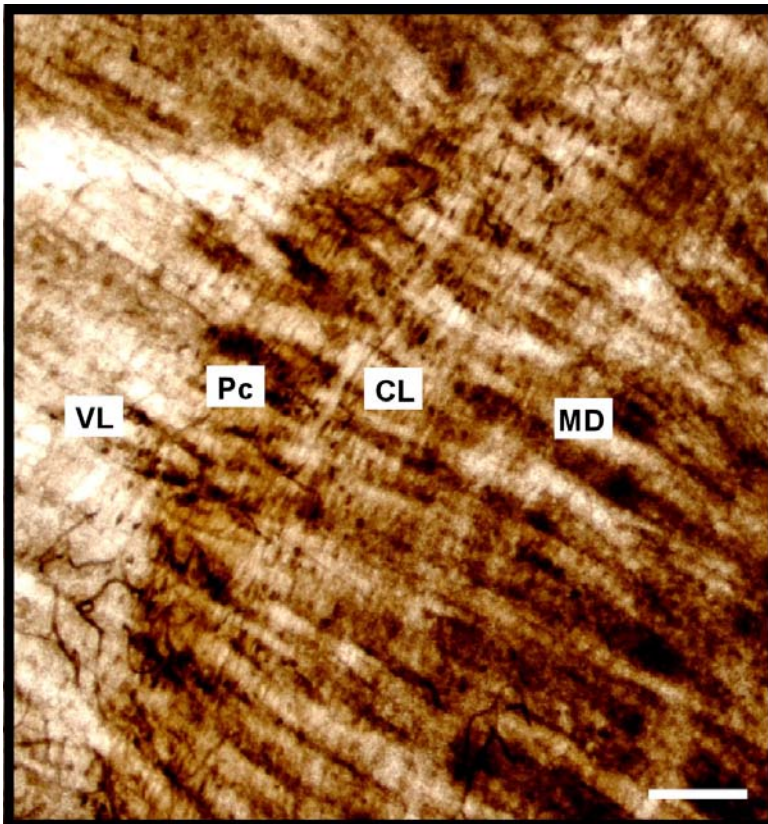
Fig. 2-8. AChE staining reveals two of the intralaminar (IL) subdivisions, Paracentral (Pc) and central lateral (CL), with high magnification. This photo is the same as that in Fig 1 (top-left). Both Pc and CL are localized in the anterior thalamus at dorsal levels. Pc is located medial to the VL, and CL is located lateral to medial dorsal nuclei (MD). Pc has darkly-stained and densely-packed neuropil. The neuropil is clustered in big patches. CL, on the contrary, is more lightly-stained than Pc and is revealed with some small-elongated cell bodies spreading among this sparse neuropil. Top = anterior; left = lateral; scale bar = 0.2 mm.

more elongated cells dominated in the ventral part of CL. These cells are kind of loosely

packed and are orientated parallel to the adjacent structures. CO and

immunocytochemistry preparations (Cb, Pv, and Cat 301) reveal Pc and CL as pale

structures (Fig. 2-9). The myelin staining reveals the myelin pattern of Pc similar to the

adjacent motor thalamic nuclei; whereas, with myelin staining, CL has densely packed

and darkly stained elongated fibers that make it very distinctive from adjacent VLp and MD.

Other two IL subnuclei, CM and Pf, are located in the ventro-posterior thalamus. Both CM and Pf are posteriorly adjacent to MD. CM is a large nucleus compared to other IL subdivisions. The coronal plane reveals CM better than the horizontal and sagittal planes. Pf, on the other hand, is a small structure, which is located medial to CM. Horizontal plane shows better picture of Pf than the coronal plane. In AChE sections, CM has a uniform, lightly-stained neuropil with few darkly stained capillaries (Fig. 9). The overall look of CM is very close to VP, but it is much lighter than LP and MD. Actually, there is a thin septa-like border that separates CM from VP. Thus, it is not so difficult to distinguish CM from the neighboring structures in coronal sections. AChE staining displays Pf with a lot of darkly-stained cell bodies and moderately stained neuropil. Thus, AChE is the best preparation for identifying Pf. In Nissl sections, CM is revealed with medium-sized multipolar and irregular-shaped cells. These cells are not evenly distributed. Some are grouped into clusters and some are darkly stained. The size of the cells is slightly bigger than those in CL, but is close to the size of the cells in the VP and MD. Thus, it is not easy to distinguish the CM from VP and MD in Nissl preparations. Pf has small, elongated and oval-shaped cells. These cells are somewhat loosely packed. In CO, Pv, and Cat 301 preparations, CM is a uniform and darkly-stained structure, very similar to the darkly-stained MDmf in these three preparations (Fig. 2-9). These preparations also reveal some darkly-stained cell bodies in CM. On the contrary, CM is a pale structure in Cb preparations, and Pf is a pale structure in CO, Pv, Cb and Cat 301 preparations. In myelin stained sections, CM is characterized by
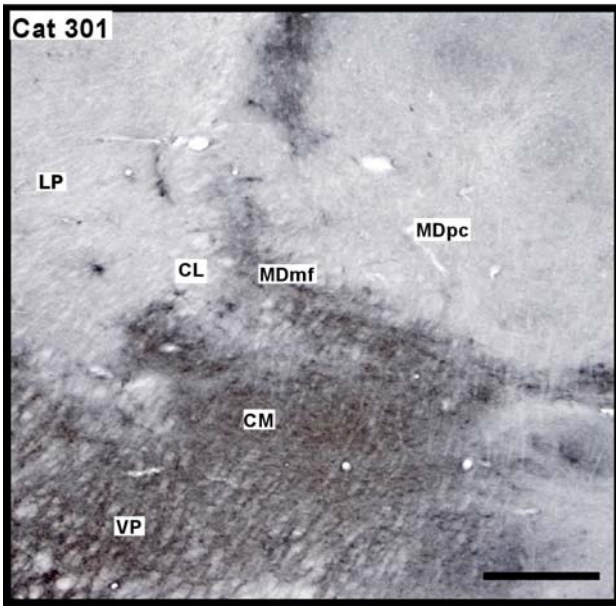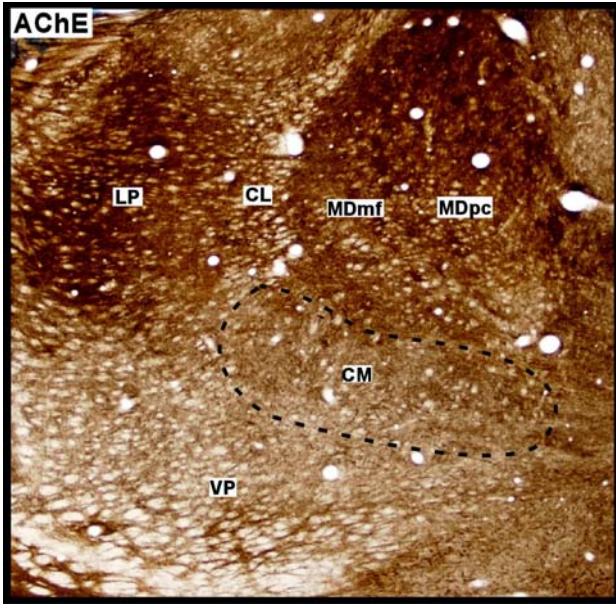
Fig. 2-9. photomicrographs of posterior sections in coronal sections showing the subdivisions of intralaminar (IL) and medial dorsal (MD) that were stained in AChE and Cat 301. In AChE (top), the IL subdivisions, central lateral (CL) and central median (CM) are distinguishable, and the MD subdivisions, multiform (MDmf) and parvocellular (MDpc) are also distinguishable. (Top) CL is much lighter than the adjacent nuclei such as lateral posterior (LP) and MDmf, but slightly darker than CM. CM is seen with some thin reticular network embedded within the light neuropil. MDpc is slightly darkly stained than MDmf. (Bottom) Unlike AChE staining, CM is much darker than CL in Cat 301 sections, but as dark as adjacent VP and MDmf. MDmf is much more darkly stained than the pale MDpc, which is also opposite to the results in AChE sections. The solid lines are the boundaries of the MD and IL, and the dash lines are the borders of the subdivisions within MD. Top = dorsal; Left = lateral; Scale bar = 1mm.

37

densely-packed fibers. These fibers are very thin and look like "wires". It seems that these fibers mingle together and fill in the whole CM region, which contrasts with VP and LP. However, Pf has moderately-stained fine fibers that are not so different from the adjacent structures.

The Medial Dorsal Nucleus

The medial dorsal nucleus (MD) contains three subdivisions: multiform (MDmf) which is the most lateral subdivision adjacent to IL, parvocellular (MDpc) which is located in the central MD, and magnocellular (MDmc) nuclei which is the most medial subdivision. The subdivisions of MD are best seen in the horizontal and coronal sections. Unlike the motor thalamus and IL, each of MD subdivisions could be delineated in most of the preparations we used. The AChE, CO, Pv and Cat 301 preparations are the best stainings to distinguish these subdivisions. MDpc is the most darkly-stained subdivision in AChE preparations, and MDmf is the most darkly-stained in CO, PV, and Cat 301 preparations. Cb staining does not reveal these subdivisions well. The overall MD region looks pale in the Cb sections. In myelin staining, the borders separating these three MD subdivisions are not so clearly marked. The fibers in the lateral MD (mostly in MDmf) are thinner, more densely-packed, and lightly-stained than the fibers in the medial MD (mostly in MDmc) that with thicker and darkly-stained fibers.

MDmf is the smallest structure compared to other two MD subdivisions. It is elongated in shape and extends anterio-posteriorly along the border of IL. The central subdivision, MDpc, is the biggest subdivision that is slightly bigger than MDmc. In horizontal sections, both MDpc and MDmc are seen in rectangular-like shape. MDmf is

characterized by moderately- to lightly-stained neuropil and some darkly-stained capillaries in AChE preparations. MDpc, however, is really darkly stained in the AChE sections that makes it so distinctive compared to the adjacent MDmf and MDmc. AChE stains reveal dark neuropil patches in MDpc, and these neuropil patches are not uniformly-stained, in stead, there are some parts of the nucleus that are much darker than the other parts. AChE preparations reveal uniform, moderately-stained neuropil patches in MDmc that are much lighter than the neuropil patches in MDpc and MDmf (Fig.2-10). Few moderately-stained capillaries are also observed in MDmc.

In Nissl sections, MDmf has medium-sized and densely-packed cells. These cells are mostly multipolar, round or oval in shape, and are evenly-distributed. MDpc contains small-sized cells that are irregular in shape. These densely-packed cells are smaller than those in MDmf. MDmc consists of darkly-stained cells. The majority of these cells are multipolar and round in shape. There are also some irregular-shaped cells mixed with these multipolar and round cells in MDmc. The cells in MDmc are bigger and more loosely-packed than the cells in MDmf and MDpc.

CO and Pv stainings reveal MDmf as a dark structure, MDpc as a pale structure, and MDmc as a moderately dark structure. There are few darkly-stained cell bodies in MDmf and MDmc in CO and Pv stainings. Thus, the borders of pale MDpc with the adjacent MDmf and MDmc are easily marked due to the strong contrast of staining from these two preparations (Fig. 2-10). The immunocytochemical technique, Cat 301, reveals only MDmf as a dark structure but reveals MDpc and MDmc as pale structures that contrast with MDmf.
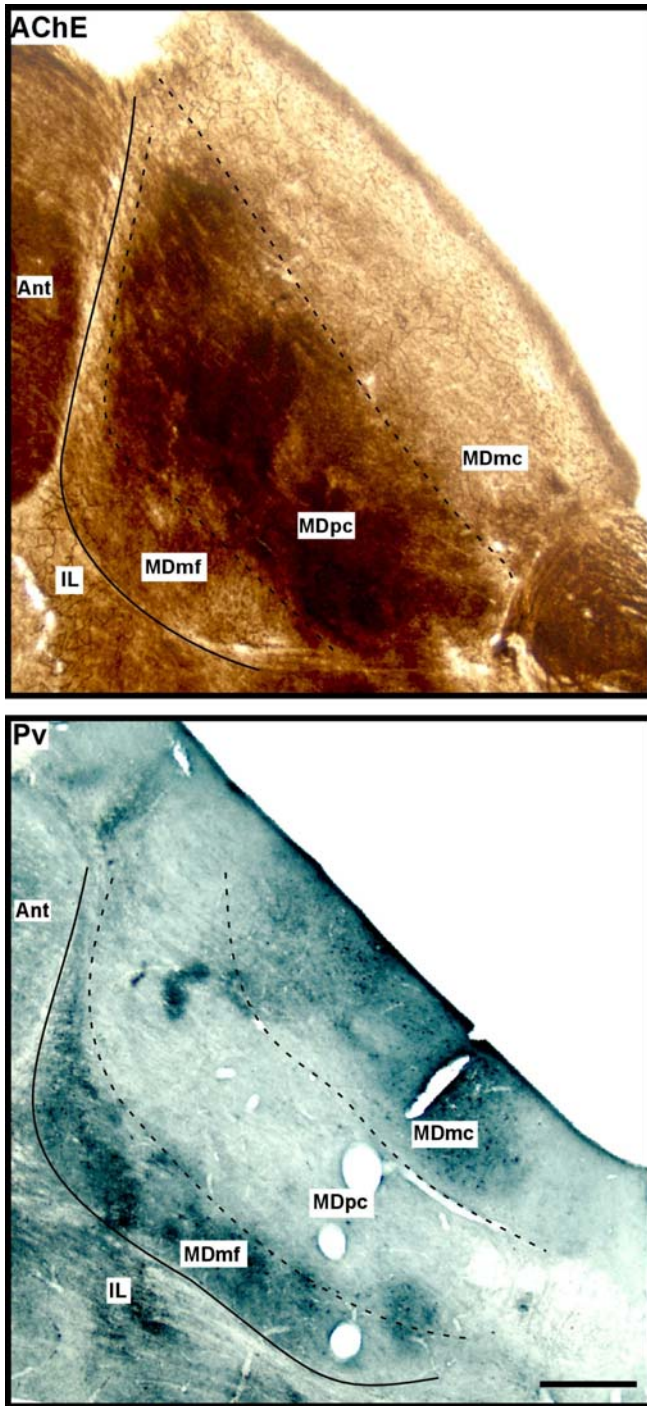
Fig. 2-10. AChE and Pv stainings in the horizontally-cut sections showing the subdivisions of medial dorsal nuclei (MD). Compared to these two stainings, AChE (top) and Pv (bottom), opposite patterns are observed such as MDpc is darkly-stained in AChE, but totally pale in Pv. MDmf is moderately stained in AChE but darkly-stained in Pv, and MDmc is really lightly-stained (almost pale) in AChE but moderately-stained in Pv. The solid lines are the boundaries of the MD and IL, and the dash lines are the borders of the subdivisions within MD. Top = anterior; Left = lateral; Scale bar = 1mm.

Discussion

In this study, we examined the architecture of motor thalamus in prosimian galagos by studying the thalamic sections processed for Nissl, myelin, AChE, CO, Cat 301, Pv and Cb. Based on these preparations, we were able to delineate the VA, VL, and VM in the motor thalamus, Pc, CL, CM and Pf in the intralaminar nuclei (IL), and MDmf, MDpc and MDmc in the medial dorsal nucleus (MD). In general, these subdivisions in prosimian galagos correspond to the architectonic subdivisions found in Old World macaque monkeys and New World owl monkeys. Among these staining preparations, we found AChE was the most useful staining technique in describing these subdivisions. However, CO did not work out so well in identifying motor thalamic subdivisions in galagos. It was not as useful as it was used in owl monkey to differentiate the motor thalamic subdivisions. We also used three cutting planes, and one of them, the horizontal plane, in general, was the most useful plane in revealing the subdivisions.

Parcellation of the Ventral Anterior Thalamus

VA is not a homogeneous structure in prosimian galagos or simian owl monkeys (Stepniewska et al., 1994). VA in galagos and owl monkeys can be divided into two subdivisions, lateral (VAl) and medial (VAm). The VAl and VAm in galagos correspond to VApc and VAmc in owl monkeys, respectively. Both VAm and VAmc (Stepniewska et al., 1994) are characterized by a scattering of cell bodies in AChE sections, and both have large-sized cells in Nissl preparations. In addition, both VAl and VApc (Stepniewska et al., 1994) have a capillary network that is revealed in AChE preparations, and both have small-sized neurons in Nissl preparations. However, the neuropil in VAl is

41

darkly stained in galagos, which is different from the poorly-stained neuropil in VApc in owl monkeys.

Parcellation of the Ventral Lateral Thalamus

The VL complex in both simians (including owl monkeys and macaque monkeys) and prosimian galagos can be divided into anterior (VLa) and posterior (VLp) subdivisions. VLa in owl monkeys and macaque monkeys contains mostly small cells that are clustered in small groups revealed in Nissl sections (Stepniewska et al., 1994; Olszewski, 1952). This is similar to what we found in galagos. However, VLa in owl monkeys has darkly stained capillaries in AChE preparations (Stepniewska et al., 1994), which were not found in VLa of galagos. In galagos, VLa has darkly-stained and densely-packed cell bodies; whereas, the darkly-stained and densely-packed capillary network was mostly found in VLp in galagos. In macaque monkeys, VLa is found to contain dense populations of parvalbumin and calbindin positive cells (reviewed by Jones, 1998a,b), but in our study, we did not see either parvalbumin or calbindin positive cells dominating VLa. In addition, the connectional studies show that VLo (or VLa) rather than VPLo (a subdivision of posterior VLp) sends dominant projections to SMA and PM in macaque monkeys (Kievit and Kuypers, 1977; Schell and Strick, 1984; Darian-Smith et al., 1990; Matelli and Luppino, 1996; Rouiller et al., 1998 & 1999; Matelli et al., 1989;.Luppino et al., 1986; McFarland and Haber, 2000; McFarland and Haber, 2002). Interestingly, we found both VLa and VLp send dominant inputs to the dorsal subdivision of premotor cortex (PMD) and SMA in galagos (see subsequent chapter).

The posterior VL (VLp) in both macaques (reviewed by Jones, 1998a, b) and galagos is dominated by parvalbumin positive cells, which results in darkly stained in Pv preparations. The semi-circular-shaped VLp in galagos extends really anteriorly and sits immediately posteriorly to VAm, which is different from that in simians that the posterior VL (VLp) is exclusively separated from VA by VLa. In addition, unlike simians, VLp in galagos seems to be homogeneous based on histochemistry (including AChE and CO) and immunocytochemistry (Pv, Cb, and Cat 301) stainings. Only in Nissl staining, we found the cells in the medial sector of VLp are larger than the cells in the lateral sector. In owl monkeys and macaque monkeys, Nissl preparations reveal that there are at least three small subdivisions that could be delineated from the posterior VL (Stepniewska et al., 1994; Olszewski, 1952). They are the medial part of VLp (is called VLx in owl monkeys, and area X in macaques) that contains large cells, the dorsal lateral part of VLp (is called VLd in owl monkeys and VLc in macaques) that contains small-sized cells, and the ventro-posterior VLp (is called VLp in owl monkeys and VPLo in macaques) that contains large, darkly-stained multipolar cells. The AChE staining even displays three subdivision differentiations in posterior VL (VLx, VLd, and VLp) in owl monkeys (Stepniewska et al., 1994). Thus, it is possible that the VLp is still not differentiated in galagos compared to VLp in simians. Furthermore, the posterior part of VLp (or VPLo in macaques) is found to be connected strongly with M1. The medial portion of VLp (or area X) at dorsal thalamic levels sends major projections to PMDr, and the medial VLp at ventral levels sends to PMV in macaques (Kievit and Kuypers, 1977; Schell and Strick, 1984; Darian-Smith et al., 1990; Matelli and Luppino, 1996; Rouiller et al., 1998 & 1999; Matelli et al., 1989;.Luppino et al., 1986; McFarland and Haber, 2000; McFarland and

Haber, 2002). As in galagos, we found the similar connection pattern that the posterior

VLp sends major inputs to M1, medial VLp at ventral levels sends to PMV, and anterior

VLp at dorsal levels sends to PMD.

Parcellation of the Ventral Medial Thalamus

There are no further small subdivisions identified in VM in both simian owl monkeys

(Stepniewska et al., 1994) and macaque monkeys (Olszewski, 1952) and prosimian

galagos. However, we noticed that VM sends some projections to M1, PM and SMA,

and there is a topography-like arrangement of these thalamocortical connections. For

example, the anterior VM tends to connect with PM and SMA, and the posterior VM

tends to connections with M1. The topographic relationship of VM and the motor cortex

is not as clear as the topographic relationship of VL and the motor cortex (see

thalamocortical connection chapter).

Parcellation of the Intralaminar Nuclei (IL) and Medial Dorsal Nucleus (MD)

In both owl monkeys and galagos, IL can be demarcated into four subdivisions,

paracentral (Pc), central lateral (CL), central median (CM), and parafascicular (Pf). The

architectonic features in these subdivisions of owl monkeys and galagos are very similar.

For instance, Pc is composed of elongated cells, CL is composed of small cells, and CM

with medium cells that are seen in Nissl stains. The only difference in IL subdivisions

between these two primates is that the Pf in owl monkeys contains large cells

(Stepniewska et al., 1994), but the Pf in galagos consists of small elongated cells. In

addition, AChE preparations also reveal similar features of the IL subdivisions in owl

monkeys and galagos. For instance, in both primates, Pc has darkly-stained neuropil, CL has lightly-stained neuropil patches, CM has uniform, lightly-stained neuropil, and Pf has darkly-stained cell bodies.

In simians, MD is divided into four subdivisions, multiform (MDmf), parvocellular (MDpc), magnocellular (MDmc), and densocellular (MDdc) (Stepniewska et al., 1994; Olszewski, 1952). In our study, we could only identify three subdivisions in MD. They are MDmf, MDpc, and MDmc from lateral to medial. The locations of these subdivisions in galagos correspond to those in simians. Moreover, Nissl staining shows that MDmf in both simians and prosimians is comprised of mostly medium-sized cells, MDpc has mostly small-sized cells, and MDmc has large-sized cells. However, the architectonic features of these subdivisions revealed in AChE sections are quite different in owl monkeys (Stepniewska et al., 1994) and galagos. MDmc in both primates is really lightly stained. MDpc is darkly stained in galagos, but lightly- to moderately-stained in owl moneys. MDmf is moderately-stained in galagos, but darkly-stained in owl monkeys. Our connectional study shows that the lateral MD (mostly MDmf) has the densest connections with the prefrontal cortex in galagos (see subsequent chapter), which also confirms the results in macaque research (Rouiller et al, 1999).

Apparently, the motor thalamus in prosimian galagos is less differentiated compared to the motor thalamus in simians. The overall main subdivisions of the motor thalamus are preserved in galagos similar to those in simians. For example, three main regions: ventral anterior (VA), ventral lateral (VL) and ventral medial (VM) nuclei are seen in both simians and prosimians. In addition, the further subdivisions within VA (lateral and medal in prosimians or parvocellular and magnocellular in simians) and within VL

(anterior and posterior in both prosimians and simians) are also maintained during evolutionary course. The subtle differentiations within the posterior VL (VLp) are not found in galagos, but are found in simians. The posterior VL in simians can be further divided into three small subareas. As for the additional motor-related thalamic nuclei, intralaminar (IL) and medial dorsal (MD) nuclei, it is surprising that these two nuclei that do not play the major roles in sending projections to the motor cortex, are similar in both galagos and simians. The architectonic subdivisions of these two thalamic nuclei in galagos are very close to those in simians. Therefore, the posterior VL that plays an important role in sending projections to the motor cortex is not well differentiated in galagos, and based on the facts of this, we could assume that posterior VL must be involved with some important motor functions in simians, since it is well differentiated into more detailed, small subdivisions in simians.

References

Celio MR. 1990. Calbindin D-28k and parvalbumin in the rat nervous system. Neuroscience 35: 375-475.

Darian-Smith I, Cheema SS, Darian-Smith C. 1990. Thalamic projections to sensorimotor cortex in the newborn macaque. Journal of Comparative Neurology 299: 17-46.

Gallyas F. 1979. Silver staining of myelin by means of physical development. Neurol Res 1: 203-209.

Geneser-Jensen FA, Blackstad TW. 1971. Distribution of acetyl cholinesterase in the hippocampal region of the guinea pig. I. Entorhinal area, parasubiculum, and presubiculum. Z Zellforsch Mikrosk Anat 114: 460-481.

Hassler R. 1959. An introduction to stereotaxy of the human brain., In: Bailey, GSaP. Anatomy of the thalamus. Stuttgart: Thieme. p 230-290.

Hockfield S, McKay RD, Hendry SH, Jones EG. 1983. A surface antigen that identifies ocular dominance columns in the visual cortex and laminar features of the lateral geniculate nucleus. Cold Spring Harb Symp Quant Biol 48: 877-889.

Iuppino G, Sola P, Matelli M, Fogassi L, Rizzolatti G. 1986. Motor thalamus connections with area 4 and 6 in the monkey. BOLLETTINO - SOCIETA ITALIANA BIOLOGIA SPERIMENTALE 62: 1143-1148.

Jones EG. 1998. Viewpoint: the core and matrix of thalamic organization. Neuroscience 85: 331-345.

Jones EG. 1998. A new view of specific and nonspecific thalamocortical connections. Advance Neurology 77: 49-71.

Jones EG. 2001. The thalamic matrix and thalamocortical synchrony. Trends in Neuroscience 24: 595-601.

Kievit J, Kuypers HG. 1977. Organization of the thalamo-cortical connexions to the frontal lobe in the rhesus monkey. Experimental Brain Research 29: 299-322.

Macchi G, Jones EG. 1997. Toward an agreement on terminology of nuclear and subnuclear divisions of the motor thalamus. Journal of Neurosurgery 86: 670-685.

Matelli M, Fogassi L, Luppino G, Rizzolatti G. 1989. Thalamic input to inferior area 6 and area 4 in the macaque monkey. Journal of Comparative Neurology 280: 468-488.

Matelli M, Luppino G. 1996. Thalamic input to mesial and superior area 6 in the macaque monkey. Journal of Comparative Neurology 372: 59-87.

McFarland NR, Haber SN. 2000. Convergent inputs from thalamic motor nuclei and frontal cortical areas to the dorsal striatum in the primate. Journal of Neuroscience 20: 3798-3813.

McFarland NR, Haber SN. 2002. Thalamic relay nuclei of the basal ganglia form both reciprocal and nonreciprocal cortical connections, linking multiple frontal cortical areas. Journal of Neuroscience 22: 8117-8132.

Morel A, Magnin M, Jeanmonod D. 1997. Multiarchitectonic and stereotactic atlas of the human thalamus. Journal of Comparative Neurology 387: 588-630.

Olszewski J. 1952. The Thalamus of Macaca Mulatta, In: Olszewski, J. Basel: Karger. p 93.

Rouiller EM, Tanne J, Moret V, Kermadi I, Boussaoud D, Welker E. 1998. Dual morphology and topography of the corticothalamic terminals originating from the primary, supplementary motor, and dorsal premotor cortical areas in macaque monkeys. Journal of Comparative Neurology 396: 169-185.

Rouiller EM, Tanne J, Moret V, Boussaoud D. 1999. Origin of thalamic inputs to the primary, premotor, and suppleentary motor cortical areas and to area 46 in macaque monkeys: A multiple retrograde tracing study. Journal of Comparative Neurology 409: 131-152.

Schell GR, Strick PL. 1984. The origin of thalamic inputs to the arcuate premotor and supplementary motor areas. Journal of Neuroscience 4: 539-560.

Simmons RMT. 1980. The morphology of the diencephalon in the Prosimii. II. The Lemuroidea and Lorisoidea. Part I. Thalamus and Metathalamus. Journal fur Hirnforschung 21: 449-491.

Stepniewska I, Preuss TM, Kaas JH. 1994. Architectonic subdivisions of the motor thalamus of owl monkeys: Nissl, acetylcholinesterase, and cytochrome oxidase patterns. Journal of Comparative Neurology 349: 536-557.

Wong-Riley M. 1979. Changes in the visual system of monocularly sutured or enucleated cats demonstrable with cytochrome oxidase histochemistry. Brain Res 171: 11-28.

**THALAMIC INPUTS TO PREMOTOR CORTEX IN PROSIMIAN GALAGOS:
ANALYSES OF MULTIPLE RETROGRADE LABELED CELLS**

Introduction

The motor cortex of simian primates can be divided into three main areas, primary motor

cortex (M1), supplementary motor area (SMA), and premotor cortex (PM) based on

differences in the functional and anatomical properties. The PM can be further divided

into dorsal (PMD) and ventral (PMV) subdivisions. Furthermore, in the macaque

monkeys, both PMD and PMV can be divided into smaller rostral and caudal

subdivisions. These motor cortical areas are different from each other not only that the

neurons in different parts of the areas are involved in different parts of body movements,

but also different amplitude levels of the threshold are required to initiate the movements

(Gentilucci et al., 1988; Rizzolatti et al., 1988; Godschalk et al., 1995; Fujii et al, 2000).

Moreover, the architectonic characteristics are varied among the subdivisions of motor

cortical areas (Matelli et al., 1985; Matelli et al., 1991; Gabernet et al., 1999; Geyer et al.,

2000). In addition, different motor cortical areas receive connections from different

cortical (Arikuni et al., 1980; Goldschalk et al., 1984; Matelli et al., 1986; Barbas and

Pandya, 1987; Kurata, 1991; Luppino et al., 1990; Ghosh andGattera, 1995; Matelli et al.,

1998; Luppino et al., 2000; Tanne-Gariepy et al., 2002) and thalamic regions (Darian-

Smith et al., 1990; Matelli and Luppino, 1996; Rouiller et al., 1999).

Studies showed that microstimulating the motor thalamus initiates body movements. The

neurons in the lateral motor thalamus can evoke leg movements, the neurons in the

medial motor thalamus can evoke arm movements, and the neurons in the most medial

motor thalamus can evoke face movements (Strick, 1976a; Vitek et al., 1996; Macchi et

al, 1997 review). These parts of the motor thalamus from lateral to medial, which are

related to the leg, arm and face movements, are connected with the hindlimb, forelimb

and orofacial representations, respectively, in M1 (Strick, 1976b; Jones et al., 1979;

Kunzle, 1978; Ghosh et al., 1987; Matelli et al., 1989).

The motor thalamus of the Old World monkeys such as macaque monkeys (Olszewski,

1952) and the New World monkeys such as owl monkeys (Stepniewska et al, 1994) can

be divided into several subdivisions based on the cytoarchitectonic and histochemical

features. In macaque monkeys, the motor thalamus consists of ventral anterior (VA),

ventral lateral (VL), and ventral posterior (VP) regions. VA consists of magnocellular

(VAmc) and parvocellular (VApc) subdivisions. VL consists of anterior and posterior

nuclei. The anterior VL consists of nucleus pars oralis (VLo), nucleus pars caudalis

(VLc), and nucleus anterior medial (area X). The medial VL nucleus is called VLm, and

the posterior VL nuclei include nucleus pars postrema (VLps), nucleus oral ventral

posterior lateral (VPLo) and nucleus caudal ventral posterior lateral (VPLc) (Olszewski,

1952). The motor thalamus in owl monkey can be divided into ventral anterior (VA),

ventral lateral (VL) and ventral medial (VM, correspond to VLm in macaques) regions.

VA similar to that in macaques can be divided into magnocellular (VAmc) and

parvocellular (VApc) subdivisions, and VL can be divided into anterior (VLa, correspond

to VLo in macaques) and posterior subdivisions. The posterior VL is further divided into

dorsal (VLd, correspond to VLps in macaques), medial (VLx, correspond to area X in

macaques) and principle (VLp, correspond to VPLo in macaques) (Stepniewska et al,

1994). The organization of the motor thalamus in macaques and owl monkeys are really similar; however, the organization of motor thalamus in galagos is only similar to that in simians to some degree, as there are clear differences between prosimian galagos and simians. In galagos, the motor thalamus includes the ventral anterior nucleus (VA) that can be further separated into medial (VAm) and lateral (VAl) divisions. The ventral lateral nucleus can be divided into anterior (VLa) and posterior (VLp) divisions, and the ventral medial nucleus (VM) is a homogeneous structure (see previous chapter). VAm and VAl in galagos correspond to VAmc and Vapc, respectively, in simians. VLa in galagos corresponds to VLo in macaques and VLa in owl monkeys, and VM in galagos corresponds to VLm in macaques and VM in owl monkeys. The posterior VL in galagos is rather a uniformed area and no subdivision are obvious, which is unlike the posterior VL of simians, which has several subdivisions.

In order to study the origins of the thalamic inputs to the motor cortex, multiple tracers were placed into the motor cortical areas. In Old World monkeys, M1 receives thalamocortical projections mostly from VPLo and some are from VLo. SMA and caudal PMD (PMDc) receive inputs mostly from VLo, and some are from VPLo, VLm, VLc and mediodorsal nuclei (MD). The thalamic inputs to PMV are mainly from Area X and VLo, and some are from VPLo, VLc, VLm, and MD. The rostral PMD (PMDr) receives inputs mainly from Area X, and additional inputs are from VA, VLc, VLo, and MD (Strick, 1976; Matelli et al., 1989; Darian-Smith et al., 1990; Matelli and Luppino, 1996; Rouiller et al., 1998; Rouiller et al., 1999; Huffman and Krubitzer, 2001; McFarland and Haber, 2002). There is a one-to-one point topographic organization of the thalamocortical connections of the motor thalamus and the motor areas. The anterior parts of the motor

cortical areas receive inputs mostly from the anterior thalamic nuclei, and the posterior cortical areas receive mostly from the posterior motor thalamic nuclei. The dorsal parts of motor cortical areas receive major projections from the dorsal VL complex, and ventral cortical areas receive major inputs from the ventral VL complex (Matelli et al., 1989; Matelli and Luppino, 1996; Rouiller et al., 1998; Rouiller et al., 1999; McFarland and Haber, 2002). Apparently, each motor cortical area receives inputs from distinct motor thalamic nuclei; however, there is some degree of overlap in thalamocortical projections. SMA and caudal PMD share largest degree of overlap in projections from the motor thalamus, but the thalamocortical projections to SMA and to M1 are overlap only a little bit. The overlap of thalamocortical inputs between PM and M1 is very limited, too (Rouiller et al., 1999).

The currently known thalamocortical connections are basically from the studies in simian primates. There is no information on prosimian primates so far. Thus, we investigated the thalamocortical connections between the motor cortical areas and subdivisions of the motor thalamus in galagos. Multiple tracers were placed into the cortical motor areas and prefrontal cortex following the intracortical microstimulation mapping, and retrograde labeled cells in the motor thalamic subdivisions and other thalamic nuclei were analyzed. The results show that the thalamocortical connections of prosimian primates share some degree of similarity with those of simian primates.

Methods

Eight prosimian galagos (*Galago garnetti*) were used in this study. All animals were received injections of neuroanatomical tracers into the prefrontal and premotor (PM) cortex following intracortical microstimulation identifying the areas of interest. The retrograde labels in the thalamus were analyzed after several days of allowing the tracers to transport. All experimental procedures followed the guidelines of the National Institutes of Health and Vanderbilt University for the care and use of animals in research.

Surgery, Intracortical Microstimulation (ICMS), and Tracer Injections

The animal was anesthetized with 2% isoflurane during the surgery. The skull above the prefrontal and frontal cortex was opened and the bones were removed. After the dura was cut, isoflurane was switched off and the animal was switched to intravenous injection with ketamine hydrochloride 30-60 mg/kg/hr, or was injected ketamine hydrochloride 10-30 mg/kg intramuscularly during the intracortical microstimulation session. The animal was also received xylazine (0.4mg/kg) intramuscularly injections every hour. A low impedance tungsten microelectrode (1.0MΩ) was mounted on the electrode holder and perpendicularly lowered into the cortex to a depth of 1.5-1.8mm from the cortical surface. The monophasic pulses of electrical current in a 60 msec train of 0.2 msec duration pulses were delivered at 300 Hz to the cortex to initiate movements. The subdivisions of PM was demarcated based on the types of the movements and the thresholds that initiate the movements (Wu et al., 2000). The mapping session was kept as short as possible to minimize the damage to the cortex.

Different tracers were loaded into either 1 μl or 2 μl Hamilton syringes. The syringe was mounted onto the electrode holder and lowered into 2 different depths (1.5mm and 1.0mm) of the cortex. The tracer was pressure injected into each depth of the cortex. The fluorescent tracers included fast blue (FB, 3% in distilled water), diamidino yellow (DY, 2% in distilled water), fluororuby (FR, 10% in distilled water, Molecular Probes, Inc.), and fluorescein-dextran (FE, 10% in distilled water, Molecular Probes, Inc.). The nonfluorescent tracers were wheat-germ agglutinin conjugated to horseradish-peroxidase (WGA-HRP, 2% in distilled water, Sigma, Inc.), biotinylated dextran amine (BDA, 10% in phosphate buffered saline) and cholera toxin B subunit (CTB, 1% in distilled water). For each fluorescent and CTB tracer, a total of 1.0 μl was injected; for WGA-HRP, a total of 0.03 μl was injected; and for BDA, a total of 1.6 μl was used. Each animal received up to 4 different tracer injections into different motor areas (see Table 3-1). After injections, the cortex was covered with gelatin film, the opening in the skull was closed with dental acrylic, and the skin was sutured. The animal was carefully monitored during the recovery period.

Abbreviations 3-1. Abbreviations of tracers, cortical areas and thalamic nuceli

Tracers:
FB   Fast blue
DY   Diamidino yellow
FR   Fluororuby
FE   Flurescein-dextran
WGA-HRP   Wheat-germ agglutinin conjugated to horseradish-peroxidase
BDA   Biotinylated dextran amine
CTB   Cholera toxin B subunit

Cortical Areas:
M1   Primary motor area
PMD   Dorsal premotor area
PMV   Ventral premotor area
SMA   Supplementary motor area
FEF   Frontal eye field
PFC   Prefrontal cortex
FSa   Frontal sulcus, anterior
FSp   Frontal sulcus, posterior
Tk/HL   Trunk and hindlimb movements
FL   Forelimb movements
OF   Orofacial movements
EM   Eye movements
Mix   Shoulder, trunk, neck, ear, eye lid and eye movements

Thalamic nucleus:
VA   Ventral anterior
VAl   Ventral anterior, lateral subdivision
VAm   Ventral anterior, medial subdivision
VL   Ventral lateral
VLa   Ventral lateral, anterior subdivision
VLp   Ventral lateral, posterior subdivision
VM   Ventral medial
MDmf   Medial dorsal, multiform subdivision
IL   Intralaminar
CL   Central lateral
CM   Central median
Pc   Paracentral
Pf   Parafascicular
ANT   Anterior nucleus
LP   Lateral posterior
VP   Ventral posterior

Table 3-1. Summary of experimental cases in this study. The total of 8 animals was used and the areas of injection and tracers were listed. Multiple tracers were placed into different regions of the motor cortex and prefrontal cortex (not shown). FR was placed into the Frontal Eye Field (FEF) and FE was placed in the cortex rostral to PMD overlapped with FEF in case 00-79, .CTB was placed into the area rostral to PMD and BDA was placed into the area rostral to PMV in the prefrontal cortex.
Fast blue (FB, 3% in distilled water). Diamidino yellow (DY, 2% in distilled water). Fluororuby (FR, 10% in distilled water). Flurescein-dextran (FE, 10% in distilled water). Wheat-germ agglutinin conjugated to horseradish-peroxidase (WGA-HRP, 2% in distilled water, Sigma, Inc.). Biotinylated dextran amine (BDA, 10% in phosphate buffer). Cholera toxin B subunit (CTB, 1% in distilled water). The tracers injected in the PMD were mainly located in the central (^{2}) part of PMD, some were in the more rostral (^{1}) part of PMD, and some were in the more caudal (^{3}) part of PMD.

Case number	Tracers injected in						Plane of section in thalamus
	M1			PM		SMA (forelimb)	
	trunk	forelimb	orofacial	PMD (forelimb and mix)	PMV (orofacial)		
03-65	CTB		DY	^{2}FR	BDA		Horizontal
03-74		FE		^{2}CTB		FR	Horizontal
99-75		WGA-HRP	FB	^{2}FR			Coronal
00-79		DY		$^{1\,2}$WGA-HRP	FB		Coronal
01-39		DY			WGA-HRP		Coronal
01-98				^{1}DY	WGA-HRP		Coronal
01-123				^{3}WGA-HRP, ^{1}FE			Coronal
03-11		FR		^{2}FE			Coronal

Comprehensive ICMS, Lesions, Histology and Data Analysis

After about 5 to 9 days of survival time, more comprehensive mapping was carried out.

The same cortical region of those animals that earlier received frontal stimulations was

re-exposed, and additional sites were stimulated for a more comprehensive motor map.

The spacing between each penetration site was about 1.0 mm. In order to avoid the blood

vessels, the spacing varied slightly. At the end of the mapping session, continuous

electrolytic lesions, 5 µA of DC current from 2.0 mm deep to the surface of the cortex,

marked the physiological borders between the motor cortex subdivisions. Finally, the

animal was given a lethal dose of barbiturate and perfused with saline, followed by 2%

paraformaldehyde, and 2% paraformaldehyde with 10% sucrose. The brain was removed

and blocked. The thalamus was separated from the cortex, and was stored in 30%

sucrose overnight.
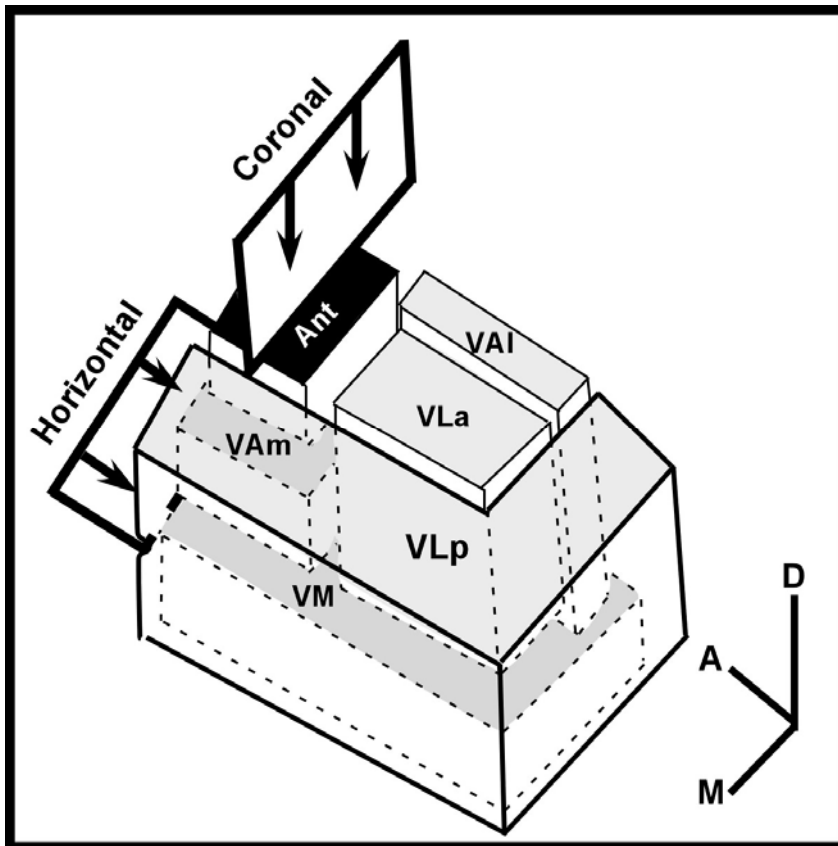
Fig. 3-1. The 3D structure of the motor thalamus. The motor thalamus consists of VA, VL and VM. VA is further divided into lateral (VAl) and media (VAm), and VL is further divided into anterior (VLa) and posterior (VLp). VLp is the largest subdivision among these subnuclei that surrounds the edge of the motor thalamus medially and posteriorly. The drawing also illustrates the cutting planes, coronal and horizontal, used in this study. D = dorsal; M = medial; A = anterior.

The thalamus was cut coronally or horizontally (Fig. 3-1) at either 40 or 50 μm thickness.

One series of the thalamic sections was mounted unstained for fluorescent microscopy.

Second series was processed to reveal WGA-HRP (Gibson et al., 1984), BDA (Veenman

et al., 1992; Sakai et al., 2000), or CTB label (Bruce and Grofova, 1992; Sakai et al., 2000). An additional series was stained to reveal architectonic features. The staining techniques included Nissl preparations, histochemical stainings for acetylcholinestrase (AChE) (Geneser-Jensen and Blackstad, 1971), myelin (Gallyas, 1979), or cytochrome oxidase (CO) (Wong-Riley, 1979), and immunocytochemical procedures for parvabumine (Pv) (Celio, 1990), Calbindin D-28K (Cb) (Celio, 1990), and Cat-301 (Hockfield et al., 1983; Hendry et al., 1988).

In the thalamic sections, the fluorescent label was plotted on a fluorescent microscope. BDA- and CTB-labeled cells were plotted on a brightfield light microscope, and WGA-HRP-labeled cells were plotted on a darkfield light microscope. The sections processed with the Nissl, myelin, histochemical (CO, AChE) and immunocytochemical (Pv, Cb, and Cat 301) procedures for thalamic architecture were analyzed on a brightfield microprojector or microscope. Adjacent sections with the labeled cells and the architectonic features were superimposed, based on superimposing the blood vessel patterns. The architectonic borders of the nuclei were delineated and compared across the various stainings.

Results

The patterns of thalamocortical connections were established after four fluorescent (FB, DY, FR, and FE) and three non-fluorescent (WGA-HRP, BDA, and CTB) tracers were placed into the various motor areas, including the primary motor area (M1), the supplementary motor area (SMA), and subdivisions of the premotor cortex (PMD and PMV), as these areas were defined by intracortical microstimulation (ICMS) mapping. A

few injections were also made in the prefrontal cortex. A summary of injections by cases

in this study is listed in Table 3-1, and a summary of injections by areas and mean

diameter of the uptake zones is listed in Table 3-2. Ideally, the tracer injections were to

Table 3-2. Summary of the number of the injections and mean diameter of the uptake zones in each
cortical area. The mean diameter was estimated based on the plotting results from the cortical sections.
Most of the uptake zones were in round shape, except for 6 injections that the uptake zones were elongated
in shape. The diameters of these 6 injections were taken into account and those were measured based on
the longest distance. The prefrontal injections included injections in the frontal eye field, the area rostral to
PMD and the area rostral to PMV.

Cortex	Number of injections	Mean diameter of the uptake zone (mm)
M1 trunk	1	2
M1 forelimb	5	2.5
M1 face	2	5
PMD	8	1.8
PMV	4	2.2
SMA	1	2
PFC	4	2.7

be placed in the central part of the cortical subdivisions, with some exceptional instances

(Fig. 3-2). The retrograde labeled neurons (Fig. 3-3 and 3-4) were assigned to the

thalamic nuclei differentiated architectonically. The distributions of the cells in the

motor thalamus (VA, VL, and VM) and other motor-related nuclei (IL and MD) were

determined, but the distributions of terminals and double-labeled cells were not analyzed.

The architectonic subdivisions of the motor thalamus were most clearly defined in the

horizontally-cut sections.
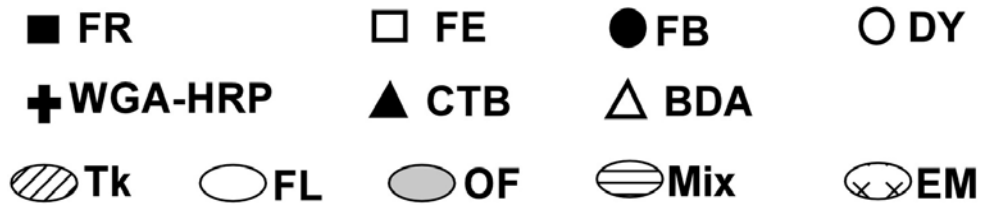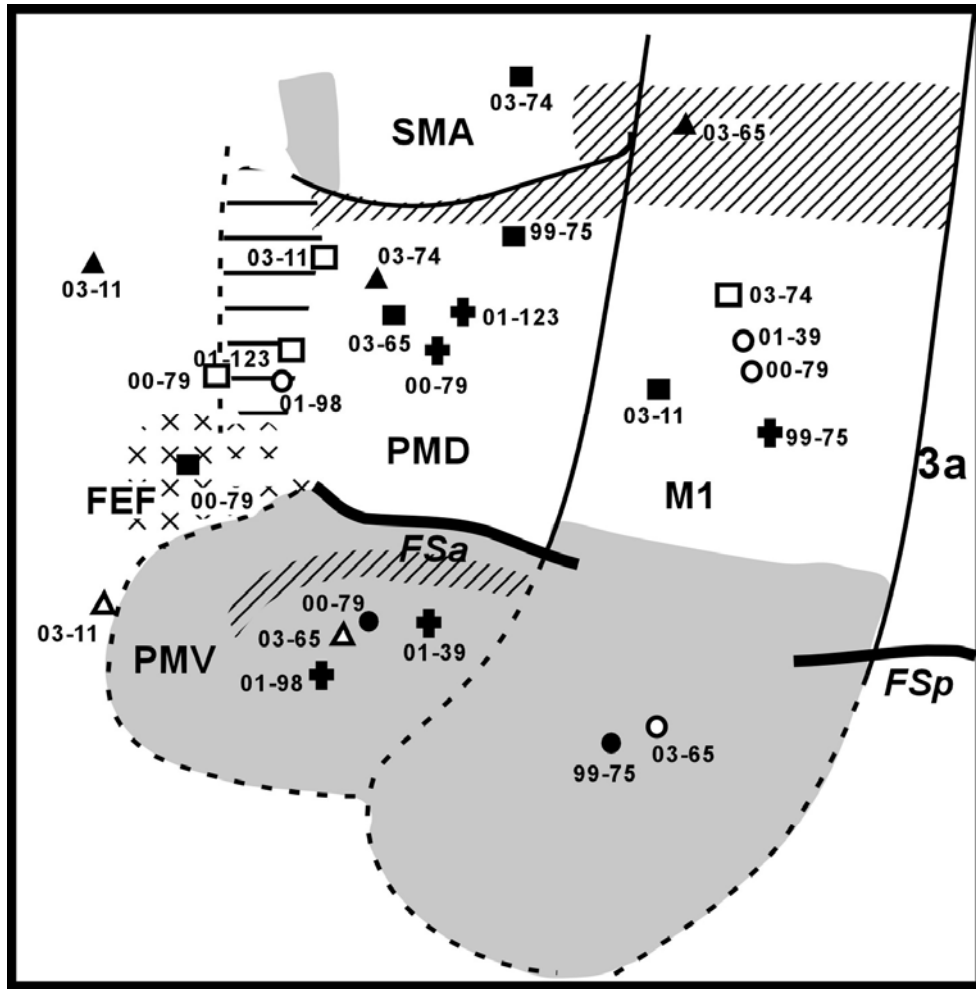
Fig. 3-2. Locations of the injections made in the cortex of 8 animals. The number of injections in each cortical area was listed in Table 2. Ideally, the injections were planned to be placed in the central region of each cortical area. Solid lines indicate the borders derived from intracortical microstimulation mapping and/or architectonic myelin staining. Dash lines are the estimated borders based on the study by Wu et al (2000). Each symbol represents different injected dyes and different background indicates different body movement representation. TK = trunk; FL = forelimb; OF = orofacial; Mix = trunk, shoulder, neck, ear, eye lid and eye movements; EM = eye movement.
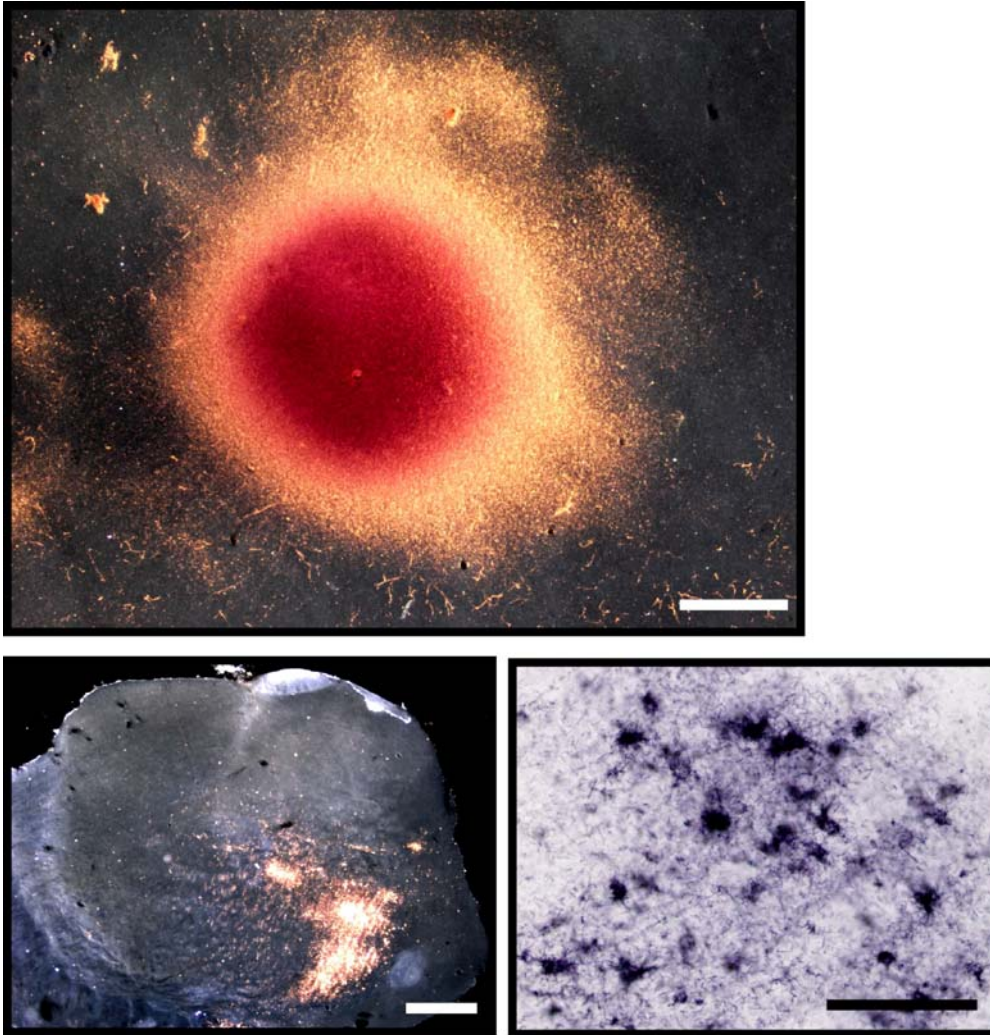
Fig. 3-3. Photomicrographs of WGA-HRP injection in case 01-98. (Top) The injection site was in the orofacial representation of PMV. The dense core in the center is surrounded by the outer uptake ring. The perikarya are a little bit more visible in the outer ring than in the central core. The transport of dye is much better visible in the cortex away from the injection site. Scale bar = 1mm. (Bottom left) Retrograde labeling in the thalamus is shown in a coronal thalamic section following the injection in the cortex. Dense labeling appears in the ventral medial part of thalamus (VLp) and intralaminar nucleus. Top = dorsal; Left = lateral.; Scale bar = 1mm. (Bottom right) Higher magnification showing the retrograde labeled cells in the motor thalamus. The perikarya are filled with WGA-HRP and the proximal dendrites are visible in most of the cells. Scale bar = 100µm.

Each cortical motor area has its dominant connections with different regions of the motor

thalamus. In the motor thalamus, VL (including VLa and VLp) is the region that

provides strongest inputs to the cortical motor areas. The connections between the VL

complex and the cortical motor areas are topographically arranged. Generally, the
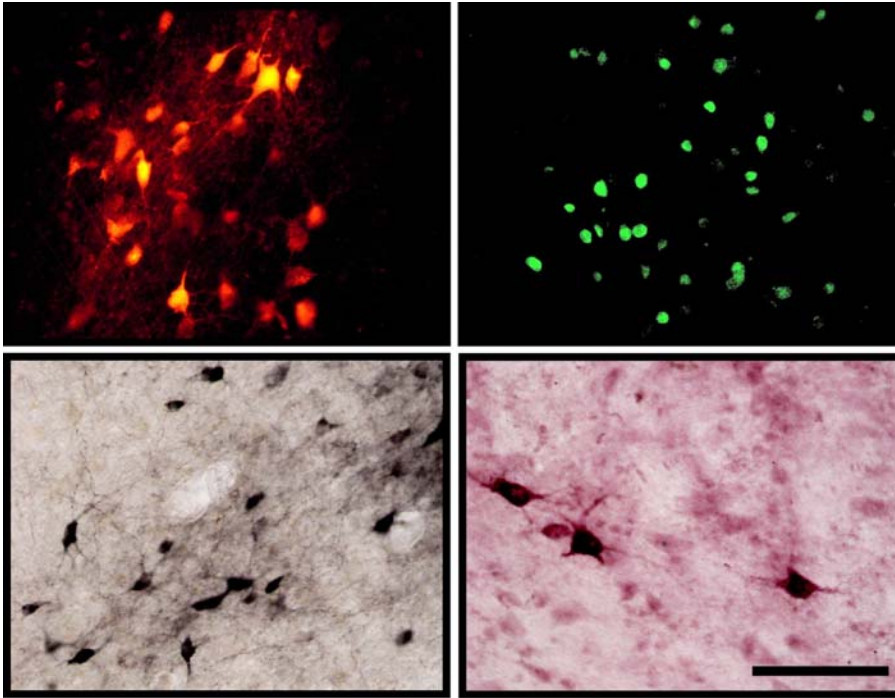
Fig.3-4. Photomicrographs of labeled cells in the thalamus after the injections made in the motor cortex. (Top left) The cell bodies and dendrites of the intralaminar thalamic cells labeled by FR placed into PMD in case 03-65. (Top right) The nucleus of the motor thalamic cells labeled by DY placed into M1 orofacial area in case 03-65. (Bottom left) The cell bodies and dendrites of the motor thalamic cells labeled by BDA made in PMV in case 03-65. (Bottom right) The cell bodies and proximal dendrites of the motor thalamic cells labeled by CTB injected in PMD in case 03-74. Scale bar = 100 μm.

anteriorly located motor areas such as PM and SMA connect mainly with the anterior

parts of the VL region (VLa and anterior VLp), and the more posterior motor area such as

M1 connects mainly with the posterior parts of the VL region (posterior VLp). Moreover,

the dorsal PM (PMD) receives dominant thalamocortical projections from the dorsal parts

of VL, and the ventral PM (PMV) receives dominant projections from the ventral parts of VL.

Thalamocortical Connections with M1

Eight injections were placed in M1. Based on physiological mapping, one of these injections was in the trunk, five in the forelimb, and two in the orofacial representations (Table 3-2). The CTB injection was in M1 trunk representation in case 03-65 (Fig. 3-2). The injection was not confined to M1, and overlapped partly with the trunk representation of SMA and forelimb representation of M1. Most of the labeled neurons were found in VLp and VLa, and Figure 3-5 shows their distribution in the horizontally-cut thalamic sections. The labeled cells were mostly concentrated in the posterior part of these nuclei although some labeled cells were diffusely distributed in the medial VLp. Many labeled cells were also seen in the posterior VAl where it is bordered with VLa. Lots of labeled cells were seen in the lateral VM. Numerous labeled cells spread all over the central median nucleus (CM) and the posterior central lateral nucleus (CL) and the parafascicular nucleus (Pf), and some were in ventral posterior nucleus (VP), the multiform subdivision of medial dorsal nucleus (MDmf), and maybe pulvinar. The label found in VA, Pf and MD might be caused by the involvement of SMA in injection site. Thus, based on the results of case 03-65, the motor thalamic VLp and VLa, as well as CM send major inputs to the M1 trunk representation.
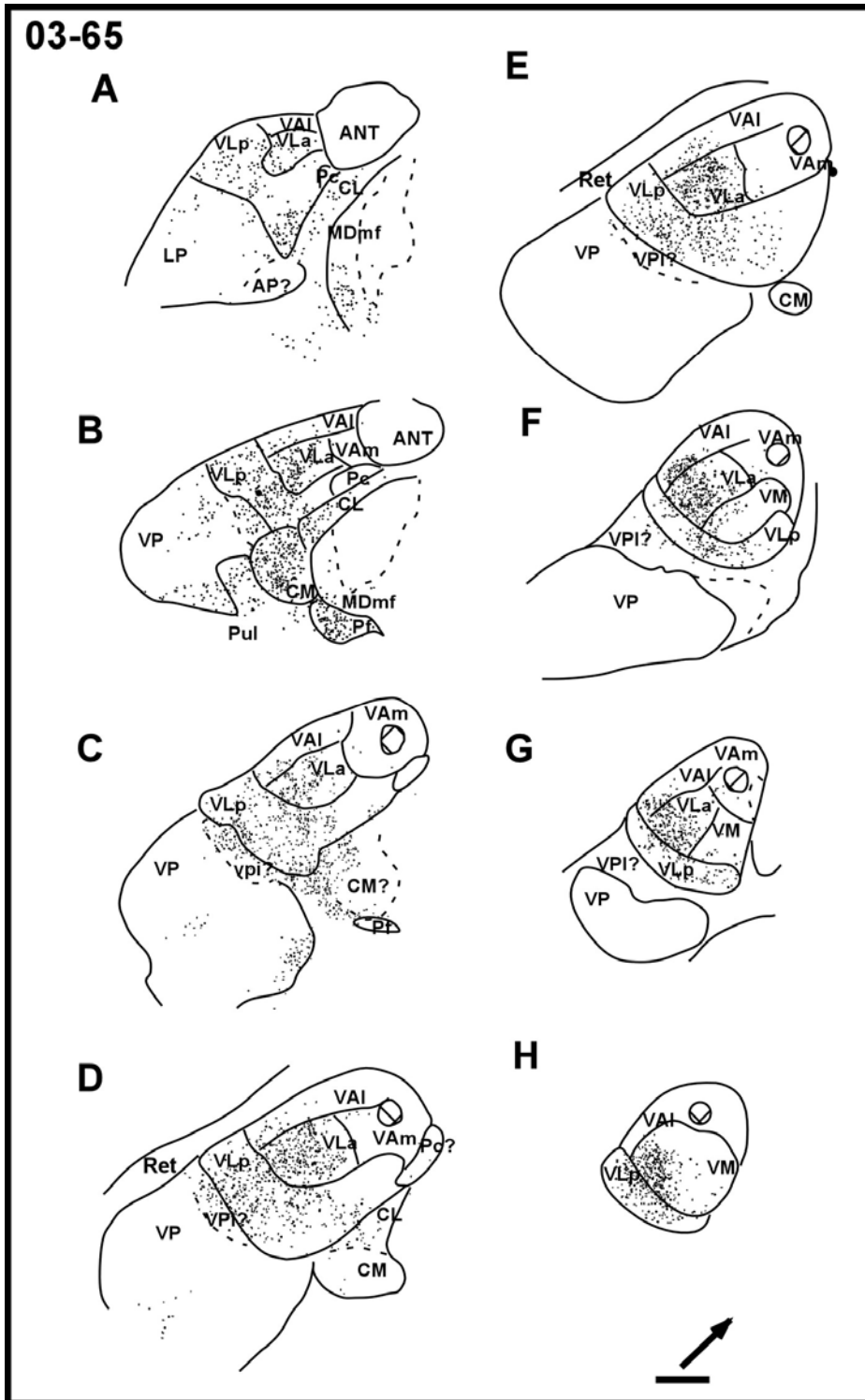
Fig. 3-5. Series of horizontal sections from dorsal (A) to ventral (H) of the thalamus in case 03-65 showing the distribution of CTB labeled cells. CTB was injected into the trunk representation of M1. The injection site in the cortex involved partly SMA trunk and M1 forelimb representations. Each dot represents a single labeled cell. The arrow points at anterior. Scale bar = 1 mm.

Five animals received tracer injections in the M1 forelimb representation (Fig. 3-2). The FE injection in case 03-74 and WGA-HRP in 99-75 were both within the forelimb area. The DY injection in case 01-39 and FR in case 03-11 spread somewhat into the rostrally adjacent PMD, and the DY injection in case 00-79 spread into both PMD and caudally adjacent area 3a. The distribution of the label was very similar in all cases with forelimb injections (Fig. 3-6), and was also similar to the pattern in case 03-65 with trunk injection that most labeled neurons were found in the posterior VL (VLp) and then VLa and CM. The difference is that the label following forelimb injection was concentrated in the medial part of VL, while label following the trunk injection was concentrated in the lateral part of VL.

Figure 3-6A illustrates the distribution of the labeled cells in selected horizontal sections of case 03-74 with a small injection in the forelimb representation in M1. The labeled cells mainly occupied the posterior part of VLp. Some labeled cells were found in VLa and VM of the motor thalamus. These cells were not diffusely distributed, but were concentrated in the central and posterior parts of the motor thalamus. Some labeled cells were also found in CL and CM of IL. The label in the CL was concentrated in the very posterior part and the label in the CM was diffusely distributed. Very few labeled cells were observed in the medial part of posterior VAl where it is bordered with VLa. Due to the use of horizontally-cut sections that reveal the clearest motor thalamic subdivisions, the numbers of the labeled cells in the motor thalamic subdivisions in case 03-74 with confined tracer injection were determined. Following the FE injection in M1 forelimb representation in case 03-74, the total of labeled cells in VLp (247) divided by the total
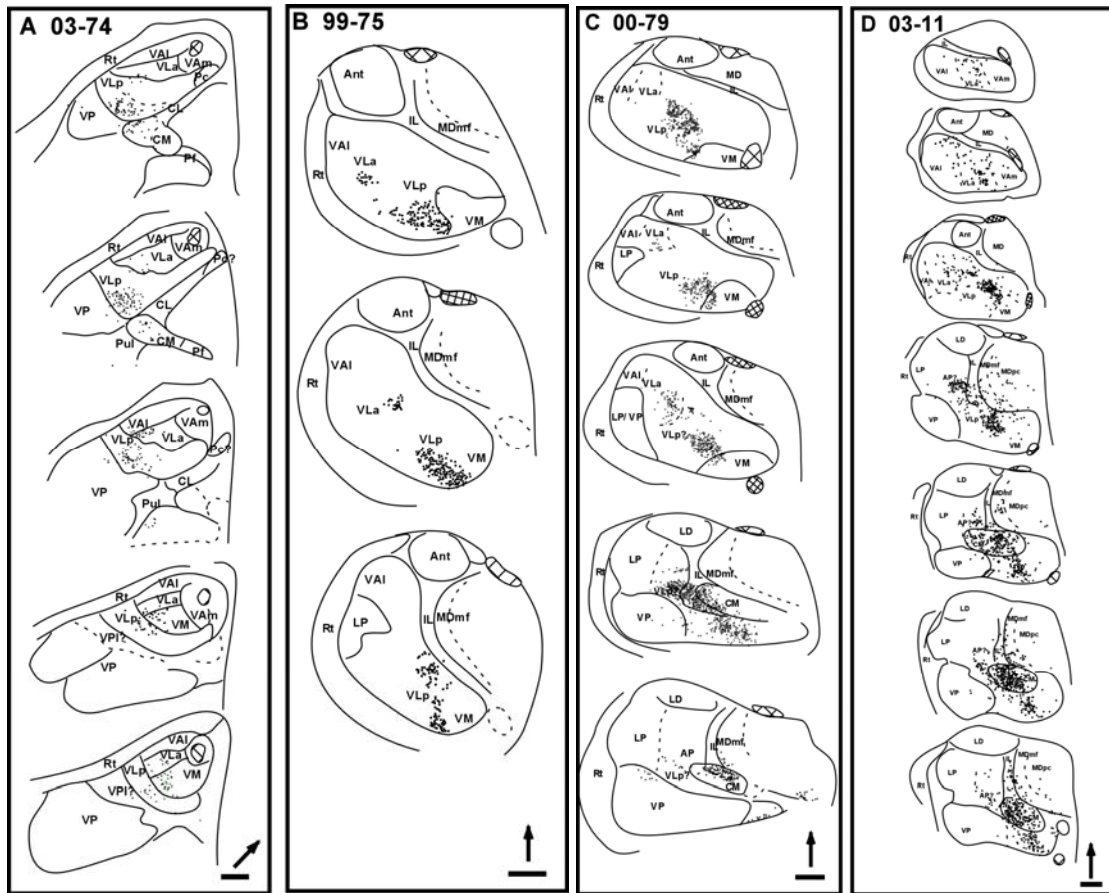
Fig. 3-6. Series of thalamic sections of 4 animals that received tracer injections in M1 forelimb area. (A) Retrograde label is shown in the horizontal sections from dorsal (top) to ventral (bottom) following the placement of FE, which was confined to the M1 forelimb area in case 03-74. Arrows points at anterior. (B) Retrograde labeled cells shown in the coronal sections from anterior (top) to posterior (bottom) after WGA-HRP was placed and restricted in the forelimb representation of M1 in case 99-75. Arrows points at dorsal. (C) Distribution of labeled cells in the coronal sections in case 00-79. The DY injection was not restricted to the M1 forelimb area, but involved partly with PMD and area 3a. Arrow points at dorsal. (D) Distribution of labeled cells in the coronal sections in case 03-11. The uptake zone of the FR injection involved PMD. Arrow points at dorsal. Scale bar = 1 mm.

number of labeled cells in the whole motor thalamus (366) (include VLp, VLa, VM, VAl

and VAm) across all thalamic sections derives the percentage of cells in VLp (67.5%)

(Table 3-3). This means that M1 forelimb has connections with the motor thalamus, and

67.5% of the connections come from VLp. Whereas, only 27% (68 out of 366 labeled

cells) of the connections come from VLa and 12% (44 out of 366) come from VM that

projects to M1 forelimb. There are almost no connections between VA (1.9% from VAl

and 0% from VAm) and M1 forelimb representation.

Table 3-3. Summary of the number of the injections and mean diameter of the uptake zones in each cortical area. The mean diameter was estimated based on the plotting results from the cortical sections. Most of the uptake zones were in round shape, except for 6 injections that the uptake zones were elongated in shape. The diameters of these 6 injections were taken into account and those were measured based on the longest distance. The prefrontal injections included injections in the frontal eye field, the area rostral to PMD and the area rostral to PMV.

Motor Cotex

Motor Thalamic Nuclei — M1, PMV, PMD, SMA

| 20 40 60 80 | | 80 | | 80 | | 80 (%) |

(Bar chart showing distributions for VLa, VLp, VAl, VAm, VM across M1, PMV, PMD, SMA)

Motor Thalamus \ Motor Cortex	M1	PMV	PMD	SMA
VLa	68 (27.5)	105 (31.0)	538 (35.65)	621 (40.1)
VLp	247 (67.5)	205 (64.5)	612 (42.25)	725 (46.9)
VAl	7 (1.9)	2 (0)	179 (12.95)	86 (5.6)
VAm	0 (0)	4 (1.2)	44 (2.85)	6 (0)
VM	44 (12.0)	23 (6.8)	88 (6.35)	109 (7.0)
Total	366	339	1461	1547
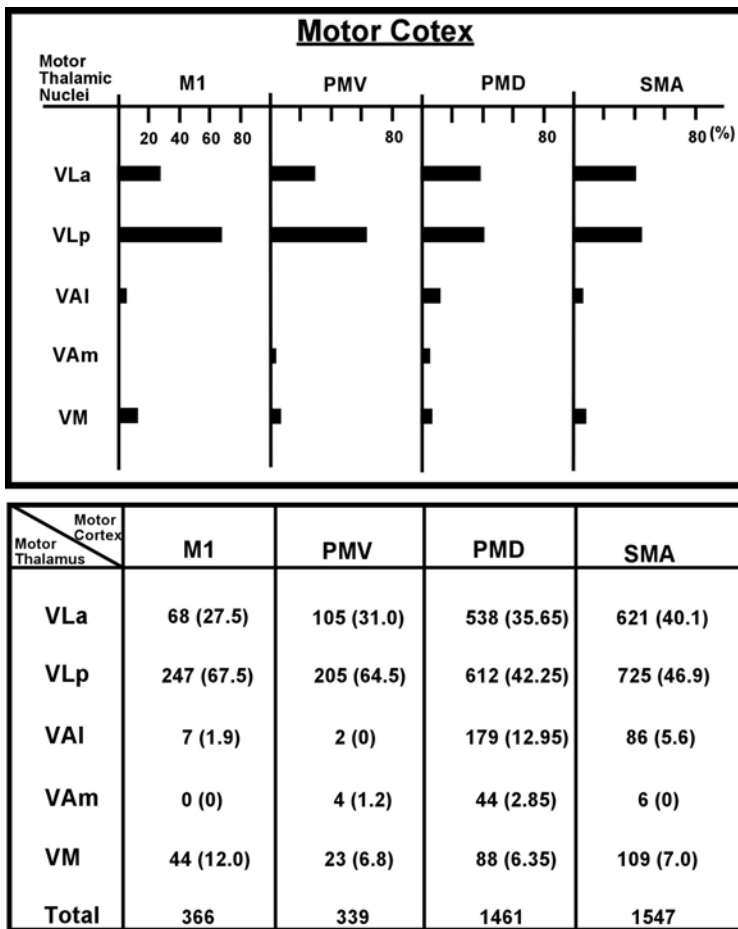
The distributions of the label of case 99-75 (Fig. 3-6B), case 00-79 (Fig. 3-6C) and case

03-11 (Fig. 3-6D) were very similar to the that of case 03-74. However, some labeled

cells were found in MDmf and CL in case 00-79 and 03-11, which might result from the

contamination of the uptake zones with PMD, and very few labeled cells were seen in VP, which might result from the involvement of the uptake zone of case 00-79 with somatosensory area 3a. In addition, compared to the label in VLp in case 00-79 with case 99-75, the label in case 00-79 was somewhat located a little bit more dorsally than the label in case 99-75. This might be because the injection in the cortex in case 00-79 was made more dorsally than the injection in case 99-75.

DY was placed into the orofacial representation in case 03-65 and FB was placed into the orofacial representation in case 99-75 (Fig. 3-2). Both injections were large and involved adjacent areas. The DY injection covered part of PMV and area 3a, and the FB injection covered part of PMV. Similar to the injections made in the trunk and forelimb representations, VLp was the main nucleus sending projections to the M1 orofacial area. Other than VLp, CM and VLa also connect with M1 orofacial area. However, compared to the distributions of the label following the forelimb injections, the main population of the label following the orofacial injections was located in the more medial and ventral part of the VL complex. Figure 3-7 shows the pattern of the labeled cells after the tracers were placed into the M1 orofacial area. It is clear that VLp was the most densely labeled nucleus, and the label was concentrated in the posterior VLp. VLa was also labeled with densely-packed cells that were concentrated in the anterior sector. There were also many labeled cells appeared in the posterior sector of VLa (Fig. 3-7 Case 03-65). These densely-packed cells in the anterior VLa might result from the involvement of the uptake zone of the injection with PMV. Some labeled cells were found in VM, and these cells tended to cluster in the posterior sector in both cases. The subdivision of IL, CM, was found with dense labeled-cells, and these cells were scattered and distributed all over the

CM region. Labeled cells were also found in VP, CL, MDmf, Pf and pulvinar, which might be because of the involvement of the injection with PMV and area 3a in case 03-65. In summary, in the motor thalamus, the posterior VLp, sends the most dominant inputs to M1 trunk, forelimb and orofacial representations. The posterior VLa also sends dense inputs, and the posterior VM sends some inputs to these three body-movement representations in M1. Of other thalamic nuclei, CM, has dense connections with M1. The neurons in CM sending projections to M1 were scattered distributed through the whole region. To compare the thalamocortical connections with these body-movement representations, the trunk representation receives strong inputs from the lateral part of the motor thalamus, the forelimb representation receives from the medial part, and the orofacial representation from the most medial part of the motor thalamus. In addition, the more dorsal part of the thalamus has more connections with the forelimb representation, and the ventral part of the thalamus has more connections with the orofacial representation.
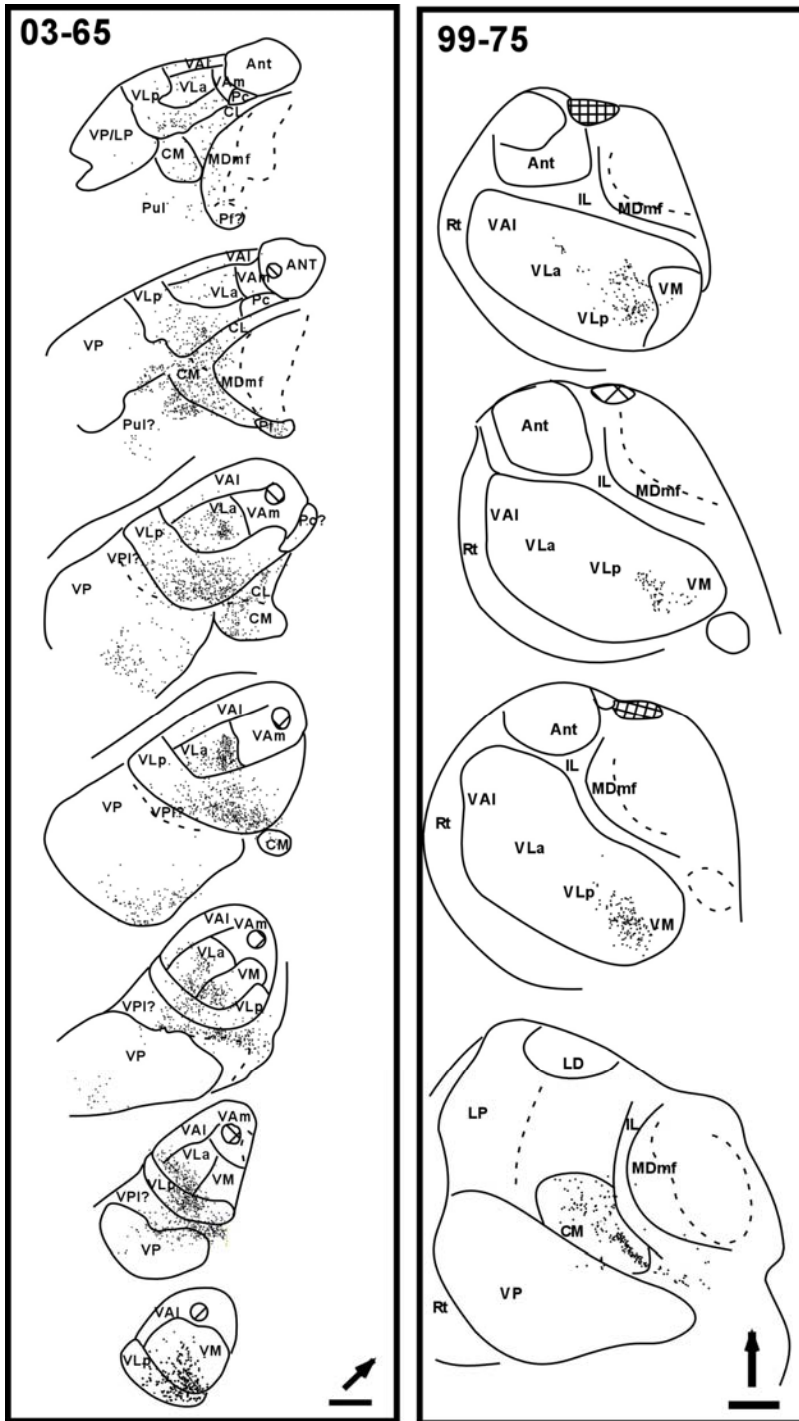
Fig. 3-7. Distribution of labeled cells shown in the 2 cases following the injection of fluorescent tracers in the M1 orofacial representation. Both injections are big and the uptake zones cover PMV. The DY injection in case 03-65 (right) also covers area 3a. (Left) Horizontal sections from dorsal to ventral in case 03-65. Arrow points at anterior. (Right) Coronal sections from anterior to posterior in case 99-75 that received FB injection. Arrow points at dorsal. Scale bar = 1 mm.

Thalamocortical Connections with PM

Nine tracers were placed into PMD in 7 animals and four tracers were placed into PMV in 4 animals. In general, PMD receives strong inputs from the dorsal part of the thalamus, and PMV from the ventral part. Moreover, the thalamic projections from the motor thalamus to PMD seem to be denser than the projections to PMV. Similar to the connections of M1 with the motor thalamus, there is also somatotopic relationship related to the body-movement representations of PM with the motor thalamus that the forelimb representation in PM receives dominant inputs from the medial part of the thalamus, and the orofacial representation from the most medial part of the thalamus.

Projections to PMD

Most of the tracers were mainly placed into the central part of PMD, three were placed in the more rostral part, and only one was in caudal part of PMD (Fig. 3-2). The tracers were mostly placed into the proximal forelimb representation of PMD, but the zone of uptake in some cases might have covered other body movement representations such as ear or neck. Compared to the thalamocortical connections of M1 forelimb area that has the densest connections with the posterior VLp, PMD forelimb area receives dense inputs from both VLa and anterior VLp. Figure 3-8A to 3-8D show the distributions of the cells after the tracers were placed in the central PMD. In general, the labeled cells were mainly concentrated in VLa and VLp. These cells were concentrated in the anterior sectors of VLa and VLp, and both VLa and VLp seemed to contain equally dense population of labeled cells. Some labeled cells were seen clustered in the anterior VAl,

71

and some were scattered distributed in VM at ventral levels. Table 3-3 shows the strength of inputs from the motor thalamic nuclei to PMD in these two animals: case 03-74 and 03-65. The percentage of labeled cells was averaged from two cases with confined PMD injections (CTB in case 03-74 and FR in case 03-65) shows that PMD has strong connections with the motor thalamus. Among these connections with the motor thalamus, 42.25% (39.2% in case 03-65 and 45.3% in case 03-74) of the connections is from VLp and 35.65% (45.8% in case 03-65 and 25.5% in case 03-74) is from VLa. There are 12.95% of the inputs from VAl, 6.35% from VM and 2.85% from VAm. Within the IL subdivisions, CL was densely labeled, and the distribution of these labeled cells was arranged like an elongated belt along with CL from anteriorly to posteriorly. A few cells were found in CM and possibly in Pf. In MD, only MDmf was labeled, and these cells tended to cluster in the posterior part of MDmf where it is adjacent to pulvinar. A very small population of labeled cells was seen in lateral posterior nucleus (LP) and pulvinar.

The uptake zones in case 03-65 with CTB injection and in case 03-74 with FR injections were confined to PMD. Compared the pattern of the labeled cells in these two cases, a little bit more labeled cells were observed in VAl in case 03-74. In addition, there were a few labeled cells in VAm, and lots of labeled cells were found in Pc, where it is anterior to CL at the ventral levels (Fig. 3-8B). These additional labeled regions, only found in case 03-74, might result from the FR injection site in case 03-74 being slightly rostral to the CTB injection in case 03-65 (Fig. 2). The distribution of the labeled cells in case 99-75 was similar to other cases with PMD injections, although the zone of uptake in case 99-75 was slightly larger and it might involve SMA.

The injections in rostral part of PMD with a mixed movement representation (proximal

limb, ear and eye lid), also resulted in patterns of the labeled cells that were similar to

those resulted from the injections in the central PMD. VLa, VLp and MDmf were the

main nuclei sending inputs to the rostral PMD (Fig. 8E). A WGA-HRP tracer was made

into the caudal part of PMD in case 01-123, and the large injection core covered not only

M1 but also a little bit of SMA. The distribution of the label was similar to other cases

following injections in the central PMD, except that VM and CM in case 01-123 were

more densely labeled than in the other cases.

In conclusion, there is not much difference in thalamocortical connections of different

parts of PMD. The distributions of the labeled cells were very similar after injections in

the central, rostral, or caudal parts of PMD. In the motor thalamus, the anterior sectors of

VLa and VLp were the most densely labeled nuclei. In other motor-related thalamic

nuclei, CL as well as MDmf were also densely labeled. VAl and VM only have sparse

connections with PMD. CM and VAm have very few connections with PMD. The

projections from VAm only go to the rostral part of PMD.
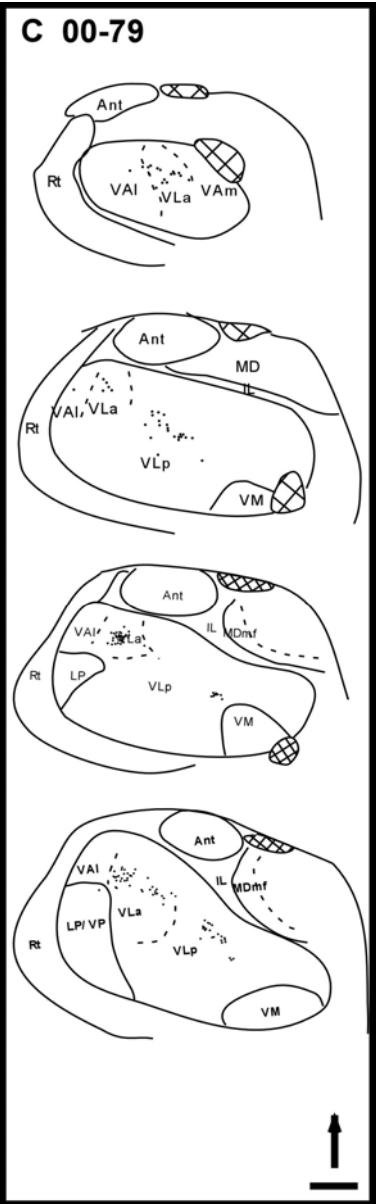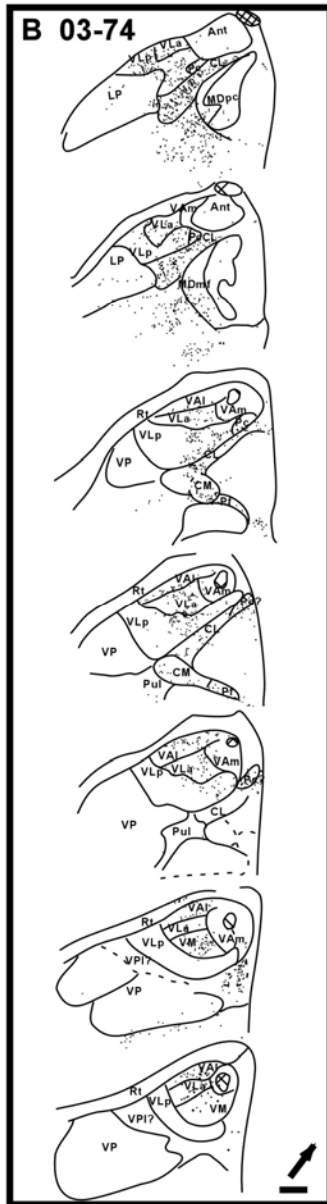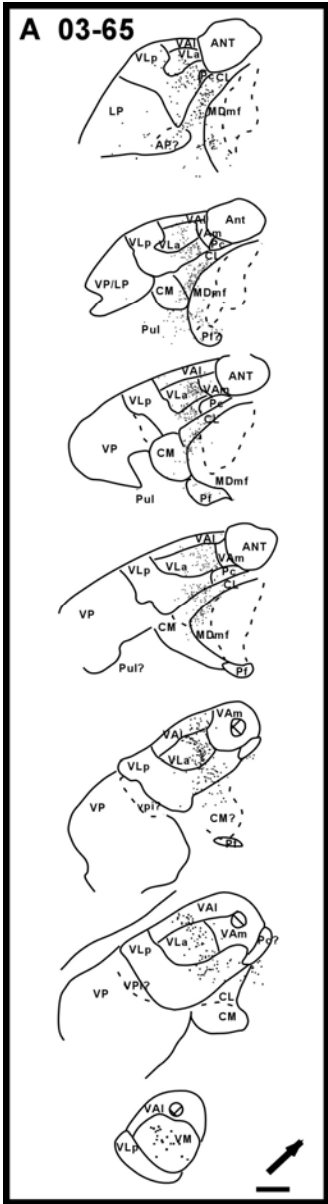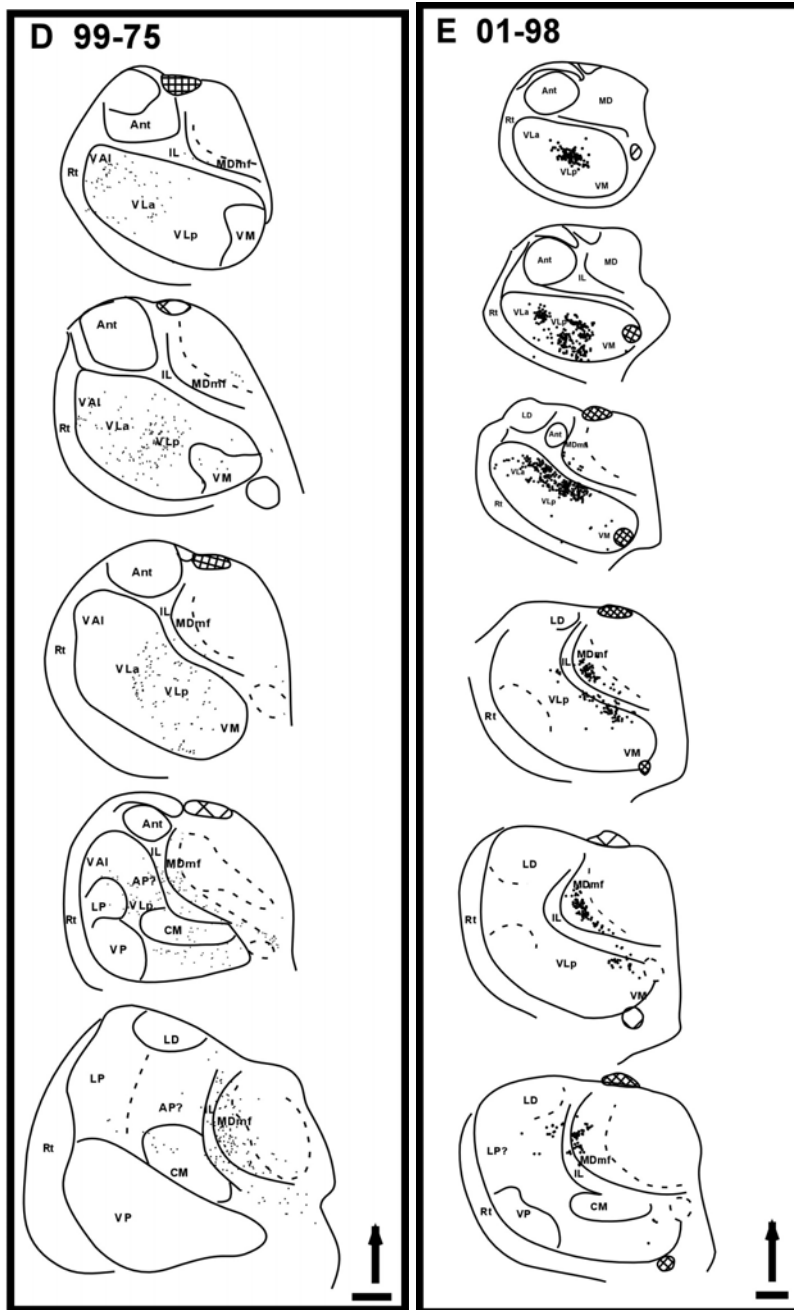
Fig. 3-8. Distribution of labeled cells in the thalamus following tracer injections in PMD of 5 animals. Four tracers were placed in the central PMD with forelimb representation (A to D), and one tracer was placed in the rostral sector of PMD with mix of proximal forelimb, neck, ear, eye lid movement and eye movement representations (E). All injections are supposed to be confined within PMD. (A and B) Showing horizontal thalamic sections from dorsal to ventral. Case 03-65 received FR and case 03-74 received CTB injections. Arrows points at anterior. (C to E) Showing coronal sections from anterior to posterior. WGA-HRP was placed into the central PMD. FR was placed into the central PMD in case 99-75 and DY was placed into the rostral PMD in case 01-98. Arrow points at dorsal. Scale bar = 1mm.

Projections to PMV

Whereas the dorsal motor thalamus tends to connect with PMD, the ventral motor

thalamus tends to connect with PMV. The thalamocortical connections were revealed by

placing tracers into the orofacial representation of PMV. The whole PMV area was not

mapped thoroughly, and only the medial border of PMV with PMD and the caudal border

of PMV with M1 were defined electrophysiologically. The anterior and lateral borders of

PMV were approximated based on the study by Wu et al (2000). The anterior border of

PMV is about 4 mm anterior to M1 face representation, and the lateral border is about 3

mm lateral to FSa. Thus, the injections in case 03-65, 00-79, and 01-39 were confined to

the previously established territory of PMV. In case 01-98, the zone of uptake might

have contaminated M1 face representation (Fig. 3-2).

The distribution of thalamic label following PMV injections are very similar to those

following M1 injections. VLp and VLa were the major motor thalamic nuclei that send

projections to PMV. VLp had denser connections with PMV than VLa (Fig. 3-9). The

label in both VLp and VLa was concentrated in the medial sector. Figure 3-9A shows the

distribution of the label following BDA injection in case 03-65. The number of labeled

cells in the motor thalamic subdivisions was determined, and shows that PMV receives

major projections from the motor thalamus: 64.5% (205 out of 339) of the projections

comes from VLp, 31% (105 out of 339) comes from VLa, and 6.8% (23 out of 339)

Fig. 3-9. Distribution of labeled cells in the thalamic sections following injections in PMV orofacial representation in 4 animals. (A) Retrograde labeled cells in the horizontal sections from dorsal to ventral after BDA injection in case 03-65. Arrow points at anterior. (B to D) Retrograde labeled cells in the coronal sections from anterior to posterior in animal 00-79 with FB injection, animal 01-39 and 01-98 with WGA-HRP injections. Arrow points at dorsal. Scale bar = 1 mm.

comes from VM (Table 3-3). However, there are almost no connections between PMV and VA (0% from VAl and 1.1% from VAm). Similar to the thalamocortical connections of PMD, MDmf sent dense, CL sent some, and VAm only sent very few projections to PMV. The labeled cells were located in the posterior ventral MDmf and CL. The additional label in CM in case 01-98 with the WGA-HRP injection (Fig. 3-9D) might result from the contamination of the uptake zone with M1. Overall, the results indicate

77

that the thalamocortical connections of PMV share some similarities with the thalamocortical connections of both M1 and PMD.

Thalamocortical Connections with SMA

Similar to the thalamocortical projections to PMD, the direct projections from the motor thalamus to SMA mostly originate from the VL complex, VLa and VLp. VAl sends some projections to SMA, but VAm almost does not send projections to SMA. Case 03-74 received a FR injection that was restricted in the forelimb representation of SMA (Fig. 3-2). The labeled cells were observed predominately in VLa and VLp, and they were clustered in the central parts of these nuclei (Fig. 3-10). It seems that there were slightly more labeled cells in VLp than VLa. Some labeled cells were found scattered in the medial VLp, VM and VAl at ventral levels. The label in VM was spread-out in the whole area. Very few labeled cells were seen in VAm. There were 46.9% (725 out of 1547) of labeled cells in VLp and 40.1% (621 out of 1547) in VLa. On the other hand, there were only 7% (109 out of 1547) of labeled cells in VM, 5.5% (86 out of 1547) in VAl and 0% in VAm (Table 3-3). Very dense labeled cells were found in CL and these labeled cells were arranged following the orientation of CL. Some labeled cells were also seen in CM and they were spread-out all over this nucleus. Very few labeled cells were found in MDmf, which is contrary to the results with PM injections where dense label was seen in MDmf. There were a very few cells in pulvinar and other regions of the very medial part of the thalamus.
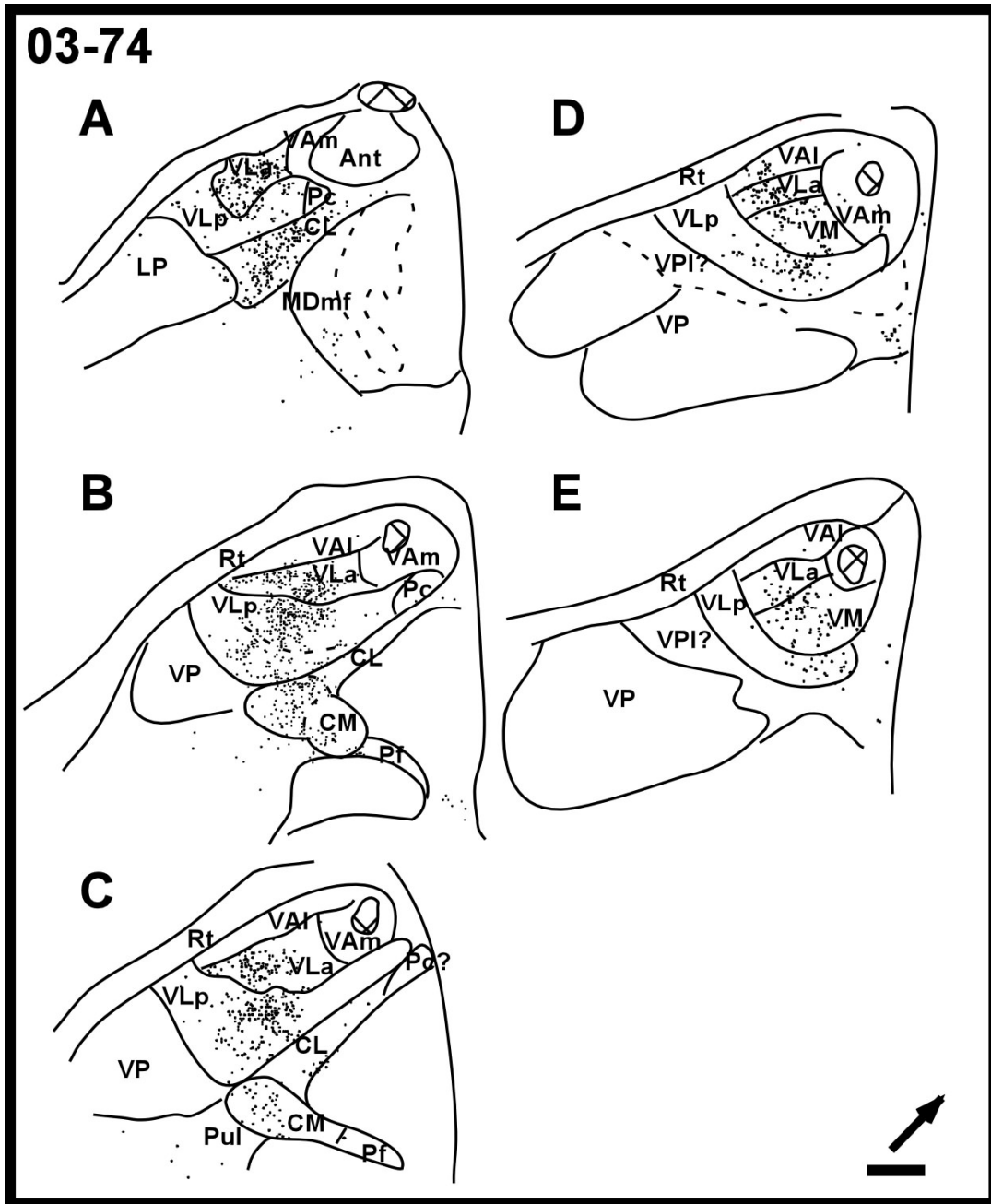
Fig. 3-10. Series of horizontal sections from dorsal (A) to ventral (E) of the thalamus in case 03-74 showing the distribution of FR labeled cells. The FR was placed into the forelimb representation of SMA, and the uptake zone was confined within this region. Arrow points at anterior. Scale bar = 1mm.

Thalamocortical Connections with Prefrontal Cortex

The thalamocortical connections of the motor cortex are different from those of the

prefrontal cortex. The anterior and medial parts of the thalamus, such as VAm and MD,

had predominant connections with the prefrontal cortex; whereas the VL complex of the

motor thalamus, rather than MD, had the predominant connections with the motor cortex.

A FR tracer was injected in the frontal eye field (FEF), and a FE tracer was injected into

the cortex rostral to FEF (Fig. 2) in case 00-79. This small injection was confined to FEF

based on the estimation of electrophysiological boundaries of motor areas by Wu et al.

(2000). The distribution of the thalamocortical labeled cells is shown in figure 3-11A

and 11B. The motor thalamic subdivisions, VAm and VLp, as well as MD subdivision,

MDmf, were the main nuclei that sent projections to FEF. A CTB tracer was placed into

an area rostral to PMD, and a BDA tracer was placed into an area rostral to PMV in the

prefrontal cortex in case 03-11 (Fig. 3-2). These two prefrontal areas were rostral to

premotor cortex in that no obvious movements were observed with microstimulation

currents as high as 300µA. The large CTB injection might include FEF and other frontal

cortical areas. Compared to the distribution of the labeled cells following PM injections,

the labeled cells tended to cluster in the anterior thalamic regions following prefrontal

injections, which is similar to the distribution from FEF injection. However, MD nuclei

rather than VL complex contributed the major inputs to the prefrontal cortex. The

majority of CTB labeled cells were found in MDmf. Lots of labeled cells were also

found in anterior VA (mostly in VAm) and VLp. Some were seen in MDpc, and few

were in VLa, CL and CM (Fig. 3-11B). Similarly, the majority of BDA labels were
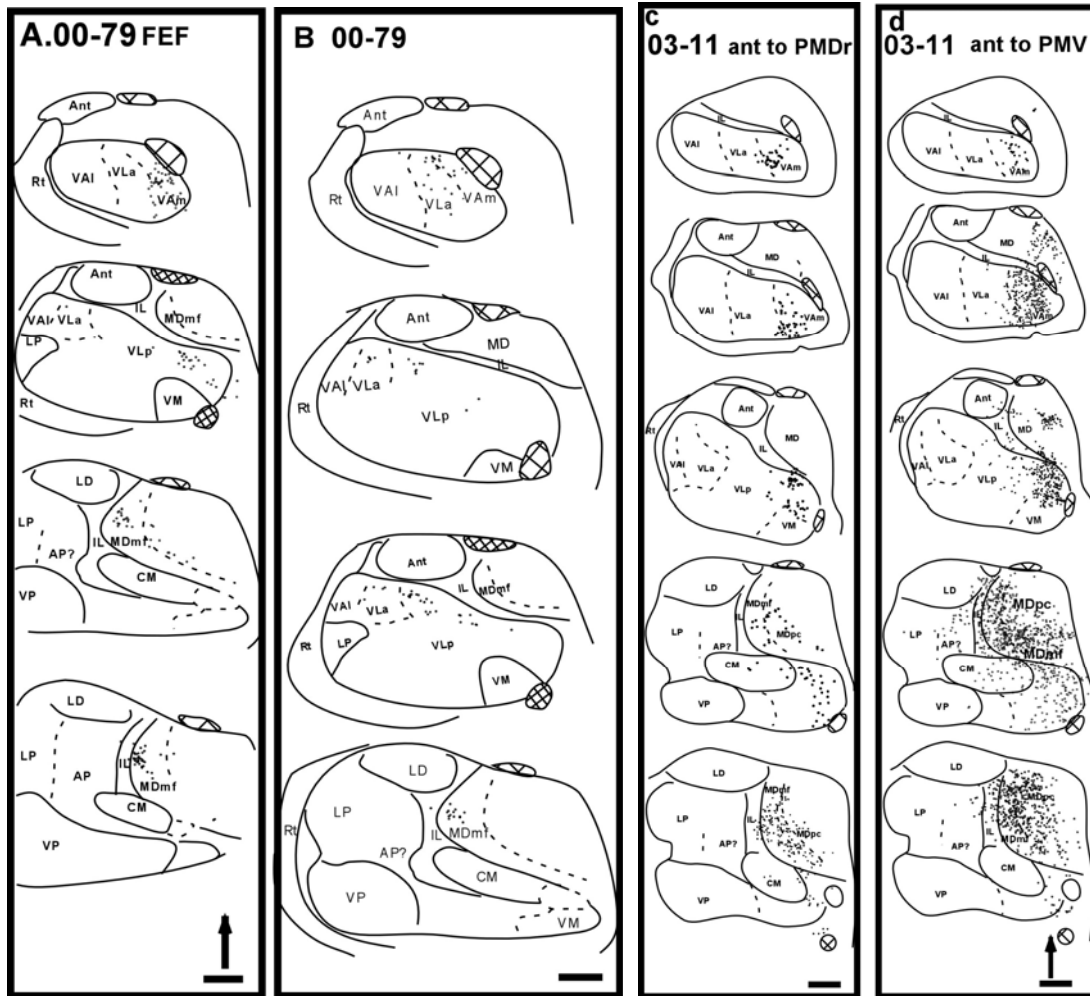
Fig. 3-11. Series of thalamic sections with coronally-cut from anterior to posterior. Four tracers were placed in the prefrontal cortex in 2 animals. A FR injection was made into the FEF (a), and a FE injection was made into the cortex rostral to FEF (b) in case 00-79. The uptake zone is confined within the area. Animal 03-11 received CTB injection in the area rostral to PMD (c) and BDA injection in the area rostral to PMV (d). Arrow points at dorsal. Scale bar = 1mm.

found in MDmf and MDpc. Thus, VAm and VLp of the motor thalamic subdivisions,

and MDmf of the MD subnucleus were the main nuclei that had dense connections with

the prefrontal cortex. The IL nuclei subdivisions (CL and CM) and VLa only sent sparse

inputs to the prefrontal cortex (Fig. 3-11C).

Summary for the Thalamocortical Connections of the Motor Thalamus

Both M1 and PMV share very similar patterns of thalamocortical connections. Both receive really strong inputs from VLp, and then VLa. Both receive some inputs from VM, and very few (or almost none) from VA of the motor thalamic subdivisions. The differences were found in the connections with other motor related thalamic nuclei such as IL and MD. M1 receives dense inputs from CM, while PMV receives dense inputs from MDmf and some from CL. PMD and SMA, which are located anterior to M1 and medial to PMV, are connected with both VLa and VLp with almost equal strengths of connections. Both PMD and SMA receive some inputs from VAl and VM, and very few from VAm of the motor thalamus. Also, both receive dense projections from CL. The differences in the thalamocortical connections between these two are that PMD has dense connections with MDmf and very few connections with CM; whereas, SMA has dense connections with CM, and very few connections with MDmf (Fig 3-12). The VL complex of the motor thalamus is the major region of connections with the frontal motor areas (PM, M1 and SMA), whereas the MD subdivision, MDmf, is the main region sending inputs to the prefrontal areas that are adjacent to PM. In addition, the medial subdivision (VAm) of the anterior motor thalamus (VA) sends strong inputs to the prefrontal cortex rather than the frontal cortex.
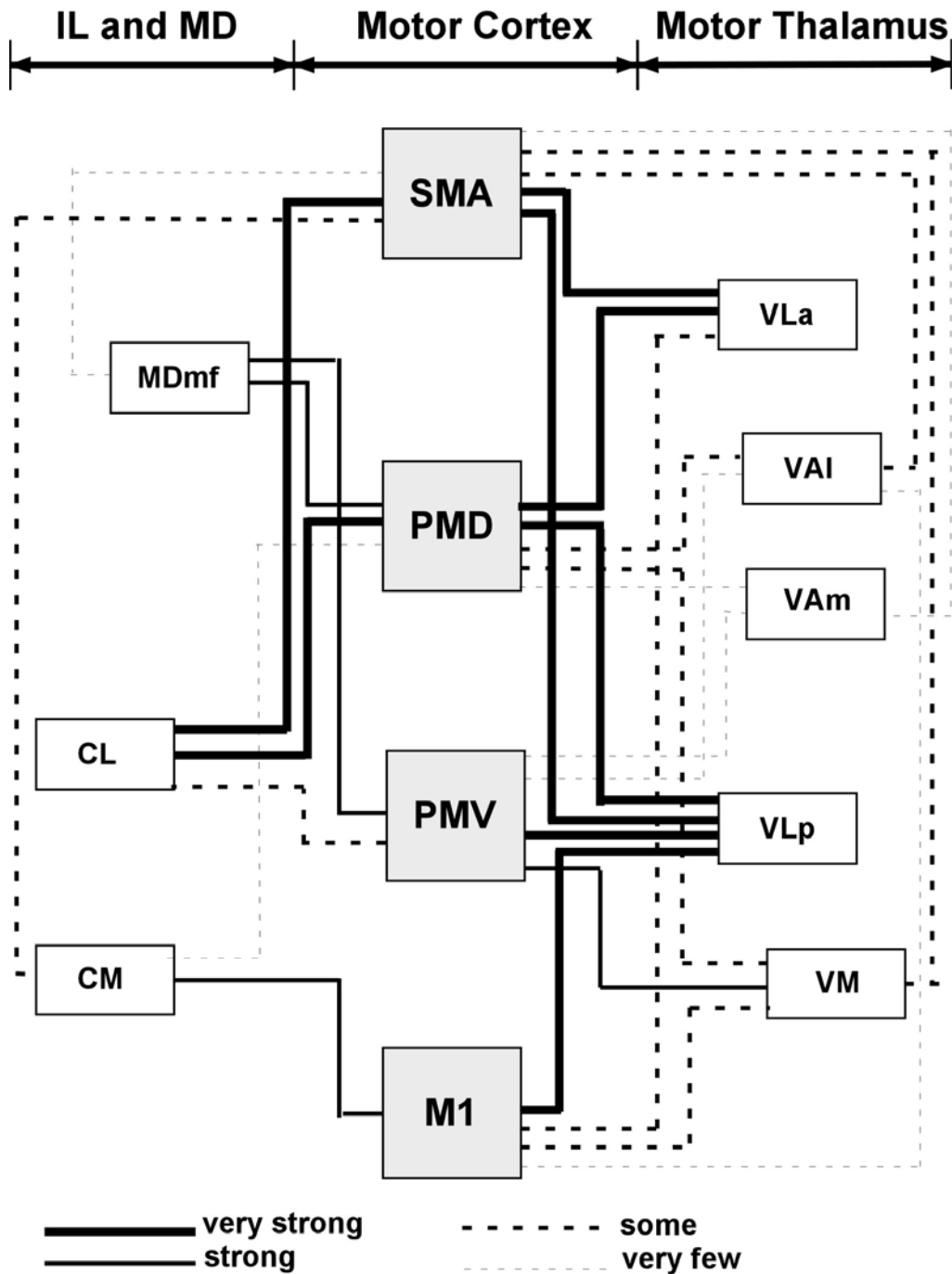
Fig. 3-12. Summary of the projections from the thalamus to the motor cortex including M1, PM and SMA. The inputs from the motor thalamus are illustrated in the right panel, and the inputs from the intralaminar nucleus and medial dorsal nucleus are illustrated in the left panel. Different thickness of the lines represents different degree of strengths of connections. The thickest line indicates the strongest projection, and the thin line indicates the moderate strong connections. The thick-dashed line indicates some connections and the thin-dashed line indicates very few or almost no connections.

Topography of Thalamocortical Connections

M1 contains three main body-movement representations from medial to lateral. They are

hindlimb/trunk, forelimb and orofacial representations. These representations in M1 are

connected with VL complex in a topographic pattern. The hindlimb/trunk area receives

inputs from the lateral part of VL, the forelimb area receives from the medial part of VL,

and the orofacial area receives from the most medial part of VL. Thus, in VL, from

medial to lateral, have connections with orofacial, forelimb and hindlimb/trunk

representations, respectively, in M1 (Fig. 3-13B).

Moreover, the thalamocortical connections of the premotor and motor areas of cortex

have a topographically organized patterns of connections with the VL complex (Fig. 3-

13C). M1, located in the posterior part of the frontal cortex, receives inputs from the

posterior sectors of the VL complex (posterior VLp and VLa). The PMD, which sits

anterior to M1, receives inputs from the anterior sectors of the VL (VLa and anterior

VLp). PMV, located lateral to PMD, receives inputs from medial parts of the VL (medial

VLp and VLa). SMA, just medial to PMD and rostral to M1, receives projections from

the central parts of the VL between the anterior part of VL that projects to PMD and the

posterior part of VL that projects to M1. In the horizontal dimension, this kind of highly

organized topography of the thalamic cells were most obvious in VL, but less clearly

obvious in VM, which also sends inputs to M1, PM and SMA. The cells in VM

projecting to the motor cortex are more widely distributed. Other thalamic nuclei, CM,
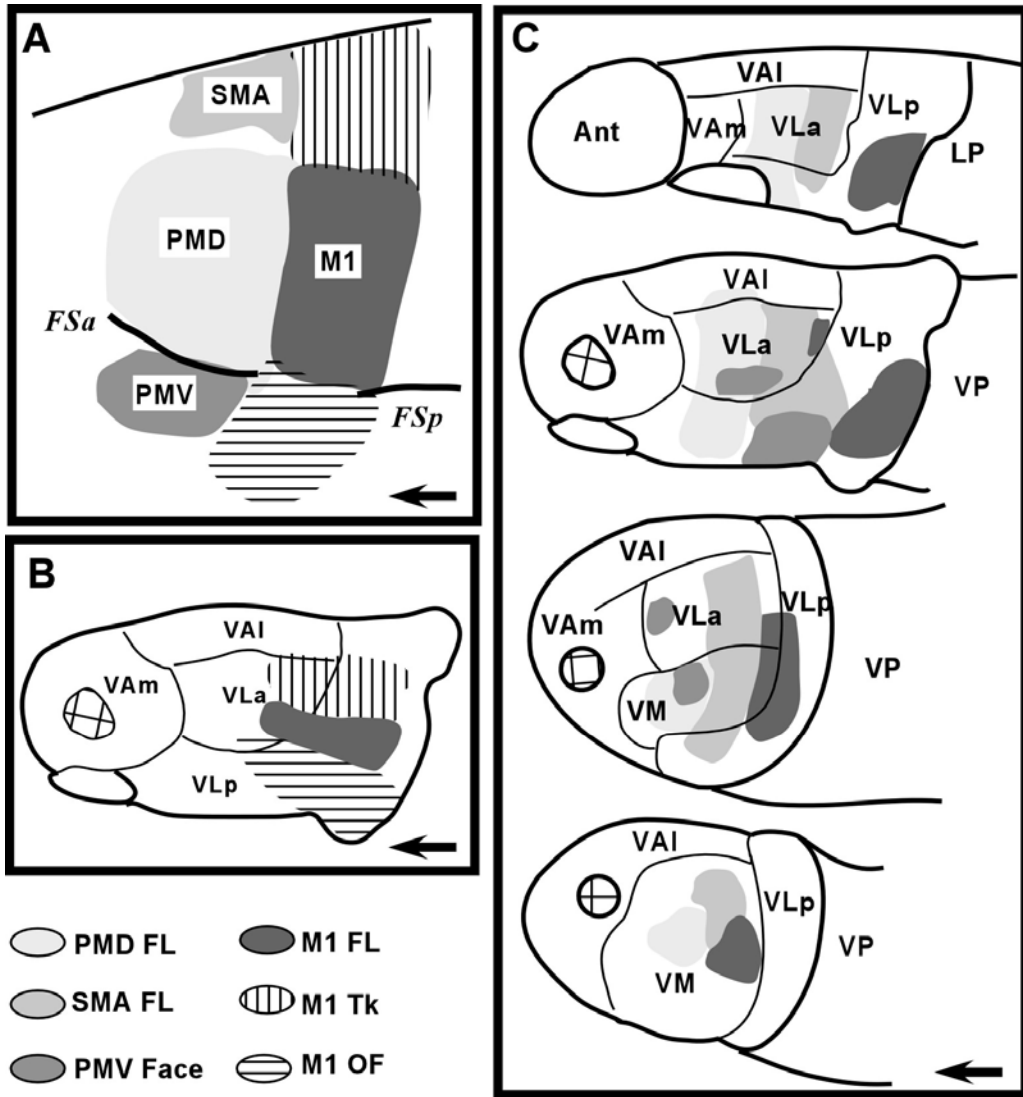
Fig. 3-13. The topographic organization of the thalamocortical connections. Different motor cortical areas shown in (A) have dominant connections from different regions in the thalamus shown in (B and C). (B) Somatotopic organization shows that the M1 trunk representation receives dominant connections from the lateral sector of VL, the forelimb receives connections mostly from the medial sector of VL, and the orofacial receives from the most medial VL. (C) As for the topographic organization, in general, M1 has strong connections with the posterior part of the motor thalamus, VLp. PM has strong connections with the anterior part of the motor thalamus (anterior VLa and anterior VLp). The central part of the VL complex project to SMA. In addition, PMD has stronger connections with the dorsal part of the motor thalamus, and PMV with the ventral part of the thalamus. In (A), arrow points at rostral. Top = medial. In (B and C), horizontal thalamic sections are presented. Arrow points at anterior and the top of each section indicates lateral. The thalamic sections in (C) are arranged from dorsal to ventral.

CL and MD also send projections to these multiple motor cortical areas, but the projections are not as well segregated as the projections from the VL complex to the motor cortical areas. The labeled cells were found spread all over these nuclei (CM, CL and MD) following the injections in these motor cortical areas. As for the vertical dimension, the dorsal PM (PMD) has denser connections with the dorsal parts of VL and the ventral PM (PMV) has denser connections with the ventral parts of VL.

Thus, it is clear that the projections from the motor thalamus (especially VL complex) to motor cortical areas (M1, PMD, PMV, and SMA) are well segregated. Each motor area in the cortex receives dominant projections from these segregated regions.

Discussion

Body Movement Representations in the Motor Cortical Areas

There is a similar point-to-point topographic organization found in both macaque monkeys and prosimian galagos. Thus, in macaques, the neurons in the lateral part of the VL complex project to the leg representation of the motor cortex, the neurons in the medial part of the VL complex project to the forelimb representation of the motor cortex, and the neurons in the most medial VL project to the face representation of the motor cortex (Strick, 1976b; Jones et al., 1979; Kunzle, 1978; Ghosh et al., 1987; Matelli et al., 1989). We found the similar topographic organization of the connections of VL and M1 in galagos, neurons located from the lateral to medial VL send inputs to the hindlimb/trunk, forelimb and orofacial representations, respectively, of M1. The results are consistent with the findings in thalamic stimulation studies in macaques that

stimulating the neurons in the lateral VL complex evoke leg movements, stimulating the

neurons in the medial VL evoke arm movements, and stimulating the most medial VL

initiate face movements (Strick, 1976a; Vitek et al., 1996).

Following tracers injected into PMD and SMA forelimb representations, labeled cells

were concentrated in the medial part of VL in case 03-74 and 03-65, which suggests that

neurons in the medial VL in galagos are related to forelimb movements, although this

part of the motor thalamus was not stimulated. However, the labeled thalamic cells were

found in the most medial part of VL after the tracers placed into PMV. The injections

were placed in the orofacial representation of PMV, but the zone of uptake spread over

most of PMV in cases 00-79 and 01-98. The distributions of these labeled cells were not

different from that of case 03-65 with a smaller zone of uptake where the labeled cells

were also mainly clustered in the most medial VL. There were no labeled cells found in

the central and lateral VL. In addition, few labeled cells were observed in the lateral VL

in case 99-75 with a FR injection in the forelimb PMD as the zone of uptake in this case

was big and it also involved the hindlimb/trunk representation. If the topographical

organization of the body-movement in M1 described above is also preserved in PM, we

may assume that PMV might not contain leg and arm movement neurons since the

neurons in the VL that are related to leg and arm movements located in the lateral and

medial VL, respectively, do not connect with PMV. This hypothesis could be further

confirmed with detailed and complete microstimulation in PMV. PMV was

microstimulated intracortically in these galagos for tracer injection purpose, but the very

anterior and lateral boundaries of PMV were not electrolytic explored because we did not

plan to delineate these borders since these anterior and lateral borders have been defined

by Wu et al. (2000). The penetrations we had in PMV area in all cases were mostly related to orofacial movements, and few penetrations were related to ear movements (3 cases), but only one case had few trunk movements.

In macaques, the posterior VL subdivisions, VPLo and area X, receive dense inputs from the cerebellum, which also send inputs to the caudal part of M1 and the rostral part of PMV where the digital forelimb movements are dominant (Jones et al., 1979; Kunzle, 1978; Matelli et al., 1989). The anterior motor thalamic nuclei, VA and VLo, receive major inputs from the basal ganglia, which also send inputs to the rostral part of M1, PMD, and caudal PMV where the proximal forelimb movements are dominant (Jone et al., 1979; Kunzle, 1978; Matelli et al., 1989). This kind of connection pattern is basically similar to, but slightly different from, what we found in galagos. In galagos, posterior VLp sends main projections to M1 and PMV, and the VLa and anterior VLp send main projections to PMD and SMA. But, we do not know the connections of the motor thalamus with cerebellum and basal ganglia. Thus, based on the macaque data, if it is also true in galagos that VLp receives inputs from cerebellum and VLa from basal ganglia, can we hypothesis that distal movements are dominant in M1 and PMV in galagos, since both nuclei receive strong inputs from VLp. In our mapping results, we only found few digital movements in M1 and none in PMV, we saw mostly proximal forelimb movements (such as shoulder and arm) in the forelimb representations in M1, PMD and SMA. We did not find any forelimb movement in PMV. This raises the possibility that the connections of cerebellum and basal ganglia with the motor thalamus in galagos differ from what we see in macaques.

Delineating cortical motor areas based on their thalamocortical connections

There are more similarities than the differences in the thalamocortical connections of the

motor thalamus and motor cortex in macaques (Schell and Strick, 1984; Darian-Smith et

al., 1990; Matelli and Luppino, 1996; Rouiller et al., 1999) and galagos. There is a

topographical relationship of the thalamocortical connections related to body movement

in both species. Moreover, the rostral motor cortical areas (SMA and PMD) receive

strong inputs from the anterior parts of the motor thalamus, and the caudal motor cortical

areas (M1) receive strong inputs from the posterior parts of the motor thalamus. The

dorsal motor cortical area (PMD) receives strong projections from the dorsal part of the

VL complex, and the ventral motor cortical area (PMV) receives projections from the

ventral VL complex.

In galagos and macaques, M1 receives the strongest inputs from the posterior VLp (VPLo

in macaques), less strong inputs from VLa (VLo in macaques), some from VM (VLm in

macaques), and none from VA. PMV receives the strongest inputs from the medial

region of VLp (maybe area X in macaques), less strong inputs from VLa (VLo in

macaques), VM (VLm in macaques) and MDmf (lateral MD in macaques), and very

sparse from VA in galagos. In macaques as in galagos, PMV receives strong inputs from

VLo, area X, VLc, VLm and MD, but not from VA.

PMD of galagos has the strongest connections with VLa and anterior VLp, less strong

connections with MDmf, some with VAl and VM, and very few with VAm. In macaques,

the caudal PMD (PMDc) has the strongest connections with VLo (corresponds to VLa in

galagos), but less strong connections with the posterior VL (including VPLo and VLc),

VLm (corresponds to VM in galagos) and MDmf. PMDc has very few connections with

VA. On the other hand, the rostral PMD (PMDr) has the strongest connections with area X (part of posterior VL), VA and MDmf, and few with VLc and VLo. Thus, if we combine the distribution of the thalamocortical connections of PMDc and PMDr in macaques, we will notice that VLo as well as posterior VL send the densest projections to PMD, and much less from VA to PMD. We are not sure whether there are rostral and caudal differentiations in PMD in galagos.

SMA of galagos receives the densest projections from VLa and central VLp, some from VAl and VM, and very few from VAm and MDmf. In macaques, the SMA-proper receives the strongest inputs from VLo (corresponds to VLa in galagos), less strong inputs from the posterior VL (including VPLo and VLc), VLm (corresponds to VM in galagos) and MD, and very few from VA. As we have noticed here, there are some differences between these two primates in that in galagos, the connections of SMA with VLp are as strong as the connections with VLa, and there are very few inputs (almost none) projecting from MDmf to SMA. However, we had only one injection in SMA and we might need more injections to see if these discrepancies do exist.

Although in galagos the thalamocortical connections of the motor thalamus with the cortical motor areas are similar to those of macaques, there are some distinguishable differences in these connections. In both primates, M1 and PMV have the strongest connections with VLp, and less with VLa, and PMD and SMA have the strongest connections with VLa, as well as with VLp. However, differences are observed in the connections of these cortical areas with MD or IL. M1 has strong connections with CM (a subdivision of IL), but not with MDmf (a subdivision of MD), and PMV has strong connections with MDmf, but not with CM. Although both PMD and SMA are strongly

connected with CL, PMD has additional strong connections with MDmf, but SMA has very few (or almost none) connections with MDmf. In galagos, M1 receives densest inputs from the posterior VL complex, PMD from the anterior VL complex, and SMA from the central VL. Besides, compared the connections of PMD and PMV with the VL complex, PMD has the strongest connections with the VL at dorsal levels, and PMV with the VL at ventral levels. Apparently, thalamocortical connections from the VL complex to these four motor areas (M1, PMD, PMV and SMA) are highly segregated and there is almost no overlap. This is slightly different from the results found in macaques where the thalamocortical projections to SMA-proper and PMDc are highly overlapped, and there are limited overlapped projections from the motor thalamus to M1 and PM (or SMA) (Rouiller et al., 1999). Due to the high degree of segregation of the thalamocortical inputs of the motor thalamus with the motor cortex, we assume that the information may not be integrated in the motor thalamus before being processed in the motor cortex. In addition, due to this segregation, we suggest that the motor cortex in galagos is not homogeneous. There are multiple individual subdivisions in the motor cortex including M1, PMD, PMV and SMA. These four areas are related, because they all receive the strongest inputs mainly from the VL complex of the motor thalamus. However, the cortical areas that are rostral to PM have the strongest inputs from MDmf rather than from the VL complex. So we could further suggest that these prefrontal areas are not included in motor cortex.

References

Arikuni T, Sakai M, Hamada I, Kubota K. 1980. Topographical projections from the prefrontal cortex to the post-arcuate area in the rhesus monkey, studied by retrograde axonal transport of horseradish peroxidase. Neuroscience Letters 19: 155-160.

Barbas H, Pandya DN. 1987. Architecture and frontal cortical connections of the premotor cortex (area 6) in the rhesus monkey. Journal of Comparative Neurology 256: 211-228.

Bruce K, Grofova I. 1992. Notes on a light and electron microscopic double-labeling method combining anterograde tracing with Phaseolus vulgaris leucoagglutinin and retrograde tracing with cholera toxin subunit B. Journal of Neuroscience Methods 45: 23-33.

Celio MR. 1990. Calbindin D-28k and parvalbumin in the rat nervous system. Neuroscience 35: 375-475.

Darian-Smith I, Cheema SS, Darian-Smith C. 1990. Thalamic projections to sensorimotor cortex in the newborn macaque. Journal of Comparative Neurology 299: 17-46.

Fujii N, Mushiake H, Tanji J. 2000. Rostrocaudal distinction of the dorsal premotor area based on oculomotor involvement. Journal of Neurophysiology 83: 1764-1769.

Gabernet L, Meskenaite V, Hepp-Reymond MC. 1999. Parcellation of the lateral premotor cortex of the macaque monkey based on staining with the neurofilament antibody SMI-32. Experimental Brain Research 128: 188-193.

Gallyas F. 1979. Silver staining of myelin by means of physical development. Neurol Res 1: 203-209.

Geneser-Jensen FA, Blackstad TW. 1971. Distribution of acetyl cholinesterase in the hippocampal region of the guinea pig. I. Entorhinal area, parasubiculum, and presubiculum. Z Zellforsch Mikrosk Anat 114: 460-481.

Gentilucci M, Fogassi L, Luppino G, Matelli M, Camarda R, Rizzolatti G. 1988. Functional organization of inferior area 6 in the macaque monkey. I. Somatotopy and the control of proximal movements. Experimental Brain Research 71: 475-490.

Geyer S, Matelli M, Luppino G, Zilles K. 2000. Functional neuroanatomy of the primate isocortical motor system. Anatomy & Embryology 202: 443-474.

Ghosh S, Brinkman C, Porter R. 1987. A quantitative study of the distribution of neurons projecting to the precentral motor cortex in the monkey (M. fascicularis). Journal of Comparative Neurology 259: 424-444.

Ghosh S, Gattera R. 1995. A comparison of the ipsilateral cortical projections to the dorsal and ventral subdivisions of the macaque premotor cortex. Somatosensory and Motor Research 12: 359-378.

Gibson AR, Hansma DI, Houk JC, Robinson FR. 1984. A sensitive low artifact TMB procedure for the demonstration of WGA-HRP in the CNS. Brain Res 298: 235-241.

Godschalk M, Lemon RN, Kuypers HG, Ronday HK. 1984. Cortical afferents and efferents of monkey postarcuate area: an anatomical and electrophysiological study. Experimental Brain Research 56: 410-424.

Godschalk M, Mitz AR, van Duin B, van der Burg H. 1995. Somatotopy of monkey premotor cortex examined with microstimulation. Neuroscience Research - Supplement 23: 269-279.

Hockfield S, McKay RD, Hendry SH, Jones EG. 1983. A surface antigen that identifies ocular dominance columns in the visual cortex and laminar features of the lateral geniculate nucleus. Cold Spring Harb Symp Quant Biol 48: 877-889.

Huffman KJ, Krubitzer L. 2001. Thalamo-cortical connections of areas 3a and M1 in marmoset monkeys. Journal of Comparative Neurology 435: 291-310.

Jones EG, Coulter JD, Wise SP. 1979. Commissural columns in the sensory-motor cortex of monkeys: Differential thalamic relationships of sensory-motor and parietal cortical fields in monkeys. Journal of Comparative Neurology 188: 113-135.

Kunzle H. 1978. An autoradiographic analysis of the efferent connections from premotor and adjacent prefrontal regions (areas 6 and 9) in macaca fascicularis. Brain, Behavior & Evolution 15: 185-234.

Kurata K. 1991. Corticocortical inputs to the dorsal and ventral aspects of the premotor cortex of macaque monkeys. Neuroscience Research - Supplement 12: 263-280.

Luppino G, Matelli M, Rizzolatti G. 1990. Cortico-cortical connections of two electrophysiologically identified arm representations in the mesial agranular frontal cortex. Experimental Brain Research 82: 214-218.

Luppino G, Rizzolatti G. 2000. The organization of the frontal motor cortex. News Physiological Science 15: 219-224.

Macchi G, Jones EG. 1997. Toward an agreement on terminology of nuclear and subnuclear divisions of the motor thalamus. Journal of Neurosurgery 86: 670-685.

Matelli M, Luppino G, Rizzolatti G. 1985. Patterns of cytochrome oxidase activity in the frontal agranular cortex of the macaque monkey. Behavioural Brain Research 18: 125-136.

Matelli M, Camarda R, Glickstein M, Rizzolatti G. 1986. Afferent and efferent projections of the inferior area 6 in the macaque monkey. Journal of Comparative Neurology 254: 460-492.

Matelli M, Fogassi L, Luppino G, Rizzolatti G. 1989. Thalamic input to inferior area 6 and area 4 in the macaque monkey. Journal of Comparative Neurology 280: 468-488.

Matelli M, Luppino G, Rizzolatti G. 1991. Architecture of superior and mesial area 6 and the adjacent cingulate cortex in the macaque monkey. Journal of Comparative Neurology 311: 445-462.

Matelli M, Luppino G. 1996. Thalamic input to mesial and superior area 6 in the macaque monkey. Journal of Comparative Neurology 372: 59-87.

Matelli M, Govoni P, Galletti C, Kutz DF, Luppino G. 1998. Superior area 6 afferents from the superior parietal lobule in the macaque monkey. Journal of Comparative Neurology 402: 327-352.

McFarland NR, Haber SN. 2002. Thalamic relay nuclei of the basal ganglia form both reciprocal and nonreciprocal cortical connections, linking multiple frontal cortical areas. Journal of Neuroscience 22: 8117-8132.

Olszewski J. 1952. The Thalamus of Macaca Mulatta, In: Olszewski, J. Basel: Karger. p 93.

Rizzolatti G, Camarda R, Fogassi L, Gentilucci M, Luppino G, Matelli M. 1988. Functional organization of inferior area 6 in the macaque monkey. II. Area F5 and the control of distal movements. Experimental Brain Research 71: 491-507.

Rouiller EM, Tanne J, Moret V, Kermadi I, Boussaoud D, Welker E. 1998. Dual morphology and topography of the corticothalamic terminals originating from the primary, supplementary motor, and dorsal premotor cortical areas in macaque monkeys. Journal of Comparative Neurology 396: 169-185.

Rouiller EM, Tanne J, Moret V, Boussaoud D. 1999. Origin of thalamic inputs to the primary, premotor, and suppleentary motor cortical areas and to area 46 in macaque monkeys: A multiple retrograde tracing study. Journal of Comparative Neurology 409: 131-152.

Sakai ST, Stepniewska I, Qi HX, Kaas JH. 2000. Pallidal and cerebellar afferents to pre-supplementary motor area thalamocortical neurons in the owl monkey: a multiple labeling study. Journal of Comparative Neurology 417: 164-180.

Schell GR, Strick PL. 1984. The origin of thalamic inputs to the arcuate premotor and supplementary motor areas. Journal of Neuroscience 4: 539-560.

Stepniewska I, Preuss TM, Kaas JH. 1994. Architectonic subdivisions of the motor thalamus of owl monkeys: Nissl, acetylcholinesterase, and cytochrome oxidase patterns. Journal of Comparative Neurology 349: 536-557.

Strick PL. 1976. Activity of ventrolateral thalamic neurons during arm movement

Anatomical analysis of ventrolateral thalamic input to primate motor cortex. Journal of Neurophysiology 39: 1032-1044.

Tanne-Gariepy J, Bello A, Fadiga L, Rizzolatti G. 2002. Parietal inputs to dorsal versus ventral premotor areas in the macaque monkey: evidence for largely segregated visuomotor pathways. Neuropsychologia 40: 492-502.

Veenman CL, Reiner A, Honig MG. 1992. Biotinylated dextran amine as an anterograde tracer for single- and double-labeling studies. Journal of Neuroscience Methods 41: 239-254.

Vitek JL, Ashe J, DeLong MR, Kaneoke Y. 1996. Microstimulation of primate motor thalamus: somatotopic organization and differential distribution of evoked motor responses among subnuclei. [erratum appears in J Neurophysiol 1997 Jun;77(6):2857; J Neurophysiol 1997 Mar;77(3):1049.]. Journal of Neurophysiology 75: 2486-2495.

Wong-Riley M. 1979. Changes in the visual system of monocularly sutured or enucleated cats demonstrable with cytochrome oxidase histochemistry. Brain Res 171: 11-28.

Wu CW, Bichot NP, Kaas JH. 2000. Converging evidence from microstimulation, architecture, and connections for multiple motor areas in the frontal and cingulate cortex of prosimian primates. Journal of Comparative Neurology 423: 140-177.

CHAPTER IV

IPSILATERAL CORTICAL PROJECTIONS TO THE
ELECTROPHYSIOLOGICALLY IDENTIFIED PREMOTOR CORTEX IN THE
PROSIMIAN GALAGOS

Introduction

The primate motor cortex refers to areas 4 and 6, based on the cytoarchitectonic study by

Brodmann in 1905. Area 6 is located anterior to area 4, and unlike area 4, area 6 lacks

Betz cells in macaque monkeys. Area 6 is also known as a part of the non-primary motor

cortex. Area 6, which is involved in preparation of voluntary movements, is comprised

of the premotor area (PM) and the supplementary motor area (SMA). These areas have

been identified in cytoarchitectonic, electrophysiological and functional studies.

According to Brodmann, area 6, which includes the premotor area, is a fairly uniform

cytoarchitectonic region, just rostral to agranular area 4 (Brodmann, 1909). However,

PM is not a uniform architectonic region, and it has been divided into different areas via

various technical research methods. In 1919, Vogt and Vogt divided PM, based on its

cytoarchitecture, into several subdivisions such as areas 6aα and 6aβ that are medial to

the spur of the arcuate sulcus, and areas 6bα and 6bβ that are lateral to the spur of the

arcuate sulcus. A few decades later, PM was again divided into superior and inferior

parts based on cytoarchitectonic features. The superior PM was called FB, and the

inferior PM was further separated into FBA and FCBm by Von Bonin and Bailey (1947).

According to the cytochrome oxidase (CO) histochemistry and Cat 301

immunocytochemistry study by Matelli et al. (1985), the dorsal portion of PM with the

expression of low enzyme activity was named F2, and the ventral portion of PM with the expression of high enzyme activity was further divided into F4 and F5. In 1987, Barbas and Pandya divided PM into 6DR, 6DC, and 6DV based on the characteristics of cytoarchitecture, myelination, and corticocortical connections. For instance, highly myelinated 6DC contains large pyramidal cells, but lacks a granular layer IV. Just rostral to 6DC, 6DR has only median or small-sized pyramidal cells, and 6V just lateral to 6DC has a thin granular layer IV.

Moreover, in accordance with the electrophysiological data, PM has been divided into dorsal and ventral portions in macaque monkeys. Microstimulating the neurons in the dorsal PM (PMD) evokes hindlimb, trunk and forelimb movements, and microstimulation in the ventral PM (PMV) evokes forelimb, neck, head, and face movements (Woolsey et al., 1951; Goldschalk et al., 1981; Rizzolatti et al., 1981b, c). Similarly, a microstimulation study in owl monkeys also showed that there are different body movement representations in PM subdivisions. The caudal PM (PMDc) contains complete body movement representation, proceeding across hindlimb, trunk, forelimb, and face (also including neck and eye movement) representations from dorsomedial to ventrolateral. However, stimulating rostral PMD (PMDr) only elicited face, neck, and eye movements, and stimulating PMV evoked forelimb and orofacial movements (Preuss et al., 1996). The current threshold that is required to initiate the movements in PMDc is higher than in PMV, and in PMDr is even higher than in PMDc. As for the functional differences in PM subdivisions in macaque monkeys, the neurons in the superior area 6 (PMD) are active during the preparation for action before the actual movements. These neurons are activated independent of physical movements. However, the neurons in the

inferior area 6 (PMV) are active not only before but also during the actual movements. These neurons also respond to the somatosensory and visually-cued stimuli (Kurata, 1991; Tanji, 1982; Weinnich and Wise, 1982; Wise et al., 1983).

The corticocortical connection studies in macaque monkeys also suggest that PM consists of more than one subdivision. PMV receives inputs mostly from the prefrontal cortex such as the areas in the dorsal (area 46) and ventral bank of the principal sulcus, other motor areas in both prefrontal and frontal cortex, and somatosensory areas in the parietal cortex. PMDc, on the other hand, receives projections largely from other motor areas in the caudal part of the frontal cortex, and somatosensory areas in the intraparietal sulcus. PMDr receives strong inputs basically from the prefrontal cortex such as area 46 and frontal eye field (FEF), and areas in the medial section of the intraparietal sulcus and the visual area (7m) in the parietal cortex (Barbas and Pandya, 1987; Ghosh and Gattera, 1995; Kurata, 1991; Matelli et al., 1986; Godschalk et al., 1984). In addition, areas that share the same functions are connected with each other. For example, the forelimb and face representations of PMV connect with the forelimb and face representations, respectively, of M1.

Most of the research related to PM has been conducted in simian primates, especially macaque monkeys. Very little research was carried in the prosimian primates. The most recent study by Wu et al (2000), successfully studied the connections of M1 with tracer injections, and defined the subdivisions of PM with intracortical microstimulation methods. PMV sits rostral to M1 orofacial representation, and consists of trunk, forelimb and orofacial representations but lacks a hindlimb representation. PMDc lies rostral to the hindlimb/trunk and forelimb representations of M1, and consists of hindlimb/trunk

and forelimb representations from medial to lateral. On the contrary, PMDr, which is located rostral to PMDc, consists of the mixed representations of hindlimb, trunk, forelimb, orofacial and eye movements (Wu et al., 2000). To initiate the movements, PMDr requires higher electric currents than PMV and PMDc. Moreover, the cytoarchitectonic characteristics of PM subdivisions in galagos are similar to those in simian primate studies (Wu et al., 2000). That is, PMDc is agranular and has median pyramidal cells in layer V, and both PMV and PMDr have small pyramidal cells in layer V; whereas, the layer IV in PMV is thicker than the layer IV in dysgranular PMDr. The goal of this study was to examine the organization of PM cortex in galagos, and compare it to the studies in simian primates. We examined the corticocortical connections of PM via tracer injection method, and the architecture of PM via various staining preparations. Multiple neuroanatomical tracers were injected into M1, PM subdivisions, FEF, prefrontal cortical areas and areas in the parietal cortex following the intracortical microstimulation mapping. Our anatomical results were related to the electrophysiological results in galagos that divided PM into several subdivisions, including dorsal (PMD) and ventral (PMV) premotor areas. The corticocortical connections of these subdivisions are organized similar to simian primates. Thus, the basic pattern of motor system organization might appear early in the course of primate evolution.

Methods

Ten adult galagos (Galago garnetti) were used in this study, and these animals were also

used for thalamocortical connection and architecture studies. The cortex of each animal

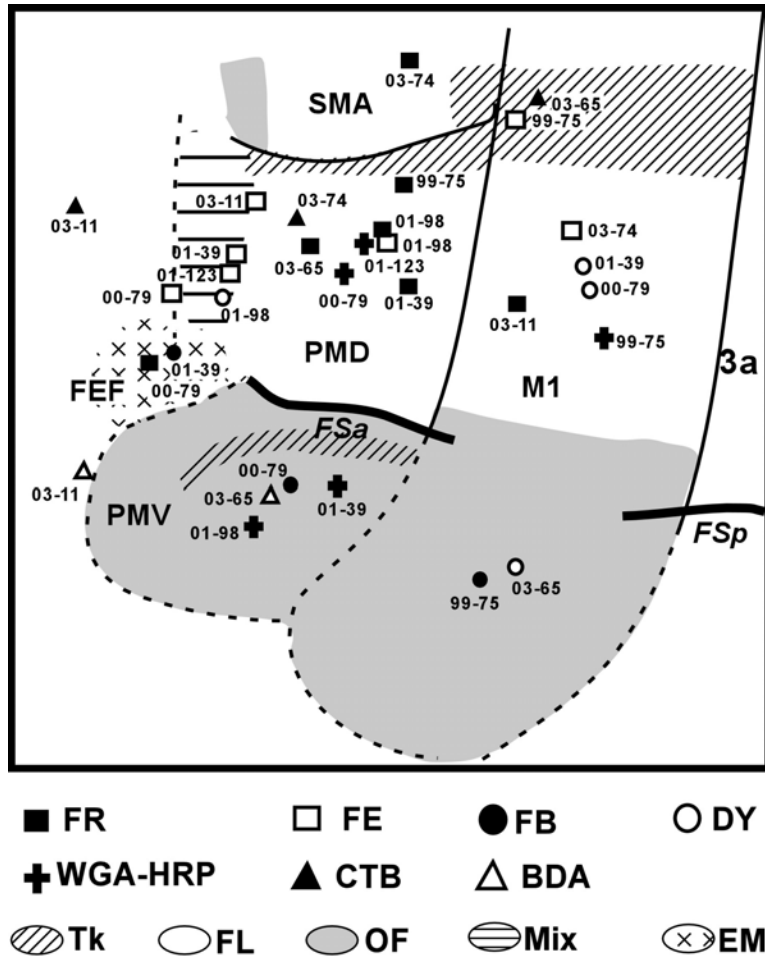was explored with the microelectrode stimulation for tracer injections. Multiple

Fig 4-1. Summary of locations of the injection sites in the motor cortex and prefrontal cortex of 8 cases. The solid lines are electrophysiological borders defined based on intracortical microstimulation (ICMS) mapping and the dash line indicates the cortical borders estimated from the study by Wu et al (2000). The numbers represent the case numbers of the animals, and the symbols represent the tracers (FR, FE, FB, DY, WGA-HRP, CTB, and BDA) used in this study. The tracers were injected in the cortical regions (M1, PMD, PMV, SMA, and FEF) where different parts of body movements could be evoked via ICMS. Tk, trunk; FL, forelimb; OF, orofacial; Mix, mix movements including shoulder, neck, and ear movements; EM, eye movement. Left, rostral; top, medial.

neuroanatomical tracers were placed into the frontal lobe including the motor cortex and

prefrontal cortex in 8 animals (Fig. 4-1), and into the parietal cortex in 2 animals (Table

4-1). The procedures formatting the frontal injections were described in the previous

chapters on thalamocortical connections. The procedures for the parietal

injections were similar. In brief, after the tracers were injected into the cortex and after 5

to 9 days of survival, the animals went through a comprehensive ICMS mapping sessions

of the motor cortex in order to get a more complete motor map. After the animals were

sacrificed, the cortex was separated from the thalamus. The cortices of 9 animals were

flattened and cut horizontally from white matter to pia surface, and the cortex of 1 animal

was cut sagittally from lateral to medial. One series of sections was mounted unstained

for fluorescent microscopy. A second series was processed to reveal WGA-HRP (Gibson

et al., 1984), or BDA (Veenman et al., 1992; Sakai et al., 2000) and CTB label (Bruce

and Grofova, 1992; Sakai et al., 2000). One or more additional flattened or sagittal series

were stained to reveal architectonic features, including myelin (Gallyas, 1979), or

cytochrome oxidase (CO) (Wong-Riley, 1979). Other sagittal sections were stained for

Nissl substance or SMI-32 (Campbell and Morrison, 1989) for architecture. The borders

among the motor cortical subdivisions were based on the electrophysiological borders

from ICMS and anatomical borders from architecture and connections of the motor

cortex. Sometimes, the borders had to be adjusted a little bit to match each other, but

most of time, the electrophysiological borders corresponded very well with the

anatomical borders. Data analysis was the same described in previous thalamocortical

connection study.

Table 4-1. Summary of experimental cases in this study. All cortex of the animals was flattened, except for case 01-39 that was cut sagittally. A fluoro-ruby tracer was injected in the frontal eye field (FEF) in case 00-79, and a fast blue tracer was injected in the FEF in case 01-39 that are not listed. A Fluorescein-dextran tracer was placed into the cortex rostral to PMD but overlapped with FEF in case 00-79. Fast blue (FB, 3% in distilled water). Diamidino yellow (DY, 2% in distilled water). Fluoro-ruby (FR, 10% in distilled water). Fluorescein-dextran (FE, 10% in distilled water). Wheat-germ agglutinin conjugated to horseradish-peroxidase (WGA-HRP, 2% in distilled water, Sigma, Inc.). Biotinylated dextran amine (BDA, 10% in phosphate buffer). Cholera toxin B subunit (CTB, 1% in distilled water). The tracers injected in the PMD were mainly located in the central ([2]) part of PMD, some were in the more rostral ([1]) part of PMD, and some were in the more caudal ([3]) part of PMD.

Case Number		Tracers injected in the motor cortex						
		M1			PMD	PMV	SMA	FEF
		Trunk/hindlimb	forelimb	orofacial	forelimb	orofacial	forelimb	
1	03-65	CTB		DY	[2] FR	BDA		
2	03-74		FE		[2] CTB		FR	
3	99-75	FE	WGA-HRP	FB	[2] FR			
4	00-79		DY			FB		FR/FE
5	01-39		DY		[1] FE	WGA-HRP		FB
6	01-98				[3] FE/FR, [1] DY	WGA-HRP		
7	01-123				[3] WGA-HRP, [1] FE			
8	03-11		FR		[2] FE			

Case Number		Prefrontal cortex		Posterior parietal cortex (PPC)					
		Anterior to PMD	Anterior to PMV	Anterior to IPS (area 1+2)	Superior PPC		Inferior PPC		Posterior tip of IPS
					Superior PPC (area 5)	Upper bank of IPS	Inferior PPC (area 7)	Lower bank of IPS	
	03-11	CTB	BDA						
9	02-25				WGA-HRP		DY		FB
10	02-68			FB,FR	DY	BDA		FE	

Abbreviations 4-1. Abbreviations of sulci, cortical areas and body movements

Sulci:
FSa   Frontal sulcus, anterior
FSp   Frontal sulcus, posterior
IPS   Intraparietal sulcus
LS   Lateral sulcus
OS   Orbit sulcus
CgS   Cingulate sulcus

Cortical subdivisions:
M1   Primary motor area
PMD   Premotor area, dorsal subdivision
PMV   Premotor area, ventral subdivision
SMA   Supplementary motor area
FEF   Frontal eye field
CSMA   Cingulate sensory motor area
sPPC   Posterior parietal cortex, superior subdivision
iPPC   Posterior parietal cortex, inferior subdivision

Intracortical microstimulation (ICMS) mapping body movements:

Hindlimb (HL) and trunk (tr)

ak	ankle		ck	cheek
kn	knee		fc	face
hp	hip		jw	jaw
l.tr	lower trunk		l.l	lower lip
to	toe		mo	mouth
u.tr	upper trunk		nk	neck
i.	ipsilateral		no	nose
b.	bilateral		tg	tongue
			th	throat
			u.l	upper lip

Orofacial (OF) heading appears at top right of the second column.

Forelimb (FL)
    am arm
    el elbow
    fa forearm
    dg digit
    sh shoulder
    wr wrist

Eye and ear
    eb eye blink
   ed eye lid
    em eye movement
    er ear

Results

The distribution of the labeled cells in the ipsilateral cortex with multiple

neuroanatomical tracer injections was analyzed in ten adult prosimian galagos. The

frontal cortex of 8 galagos and the posterior parietal cortex of 2 galagos were explored

with intracortical microstimulation (ICMS) mapping for tracer injections. The frontal

cortex of all animals underwent more comprehensive ICMS mapping before the animals

were sacrificed. The cortex of 9 animals was flattened and cut horizontally from white

matter to pia surface, and the cortex of one animal was cut sagittally from lateral to

medial. The subdivisions of the motor cortex in the frontal lobe were identified

according to the electrophysiological results from the ICMS compared with the

architectonic borders from the histological myelin staining. Four motor areas were

identified in the motor cortex including the primary motor cortex (M1), the premotor

cortex (PM), and the supplementary motor area (SMA). The PM could be separated into

the dorsal (PMD) and ventral (PMV) subdivisions. The retrograde labeled cells in the

cortex were analyzed, which established the afferent projections to the motor cortical

subdivisions in eight animals and to the posterior parietal cortex in two animals. In this

study, the ICMS mapping, the architecture of the frontal cortex, and the ipsilateral

cortical connections with the motor areas will be described separately.

Intracortical Microstimulation Mapping

The ICMS session was carried out in 10 animals. The motor cortex in the frontal lobe of

the left hemisphere of the animals was explored, and among these animals, two of them

that received tracer injections in the posterior parietal cortex (PPC). Their PPC around

the intraparietal sulcus was also stimulated with short train duration (60 ms) monophasic

microcurrents. No obvious motor movement was observed with stimulation in the PPC

even that the currents were as high as 250 µA. The microstimulation in the frontal motor

cortex delineated the electrophysiological borders of four motor areas. The primary

motor cortex (M1) sits between the anterior frontal sulcus (FSa) and posterior frontal

sulcus (FSp), the dorsal premotor cortex (PMD) is located medial to FSa and rostral to

M1, the ventral premotor cortex (PMV) is lateral to FSa and rostral to M1 orofacial

representation, and the supplementary motor area (SMA) is located medial to PMD. Our

ICMS results are basically very similar to the study by Wu et al (2000).

The elicited body movements were mostly contralateral to the stimulation hemisphere.

The movements were elicited with the lowest threshold in M1 compared to other motor

cortical areas. The threshold could be as low as 3 µA. In addition, M1 consists of

complete body movement representations, trunk/hindlimb, forelimb, and orofacial

representations, from medial to lateral. Few ipsilateral hindlimb movements were

observed near the border of trunk/hindlimb and forelimb representations and few digit

movements were found in the forelimb representation near the forelimb-orofacial border

(Fig. 4-2a-d). In the forelimb representation, proximal body movements (shoulder) were

found more often than elbow and hand movements. The somatosensory area 3a located

caudally to M1 could also be evoked some body movements (such as shoulder

movement), which required higher currents than M1. Thus, the border between M1

forelimb representation and area 3a could be delineated based on the threshold levels
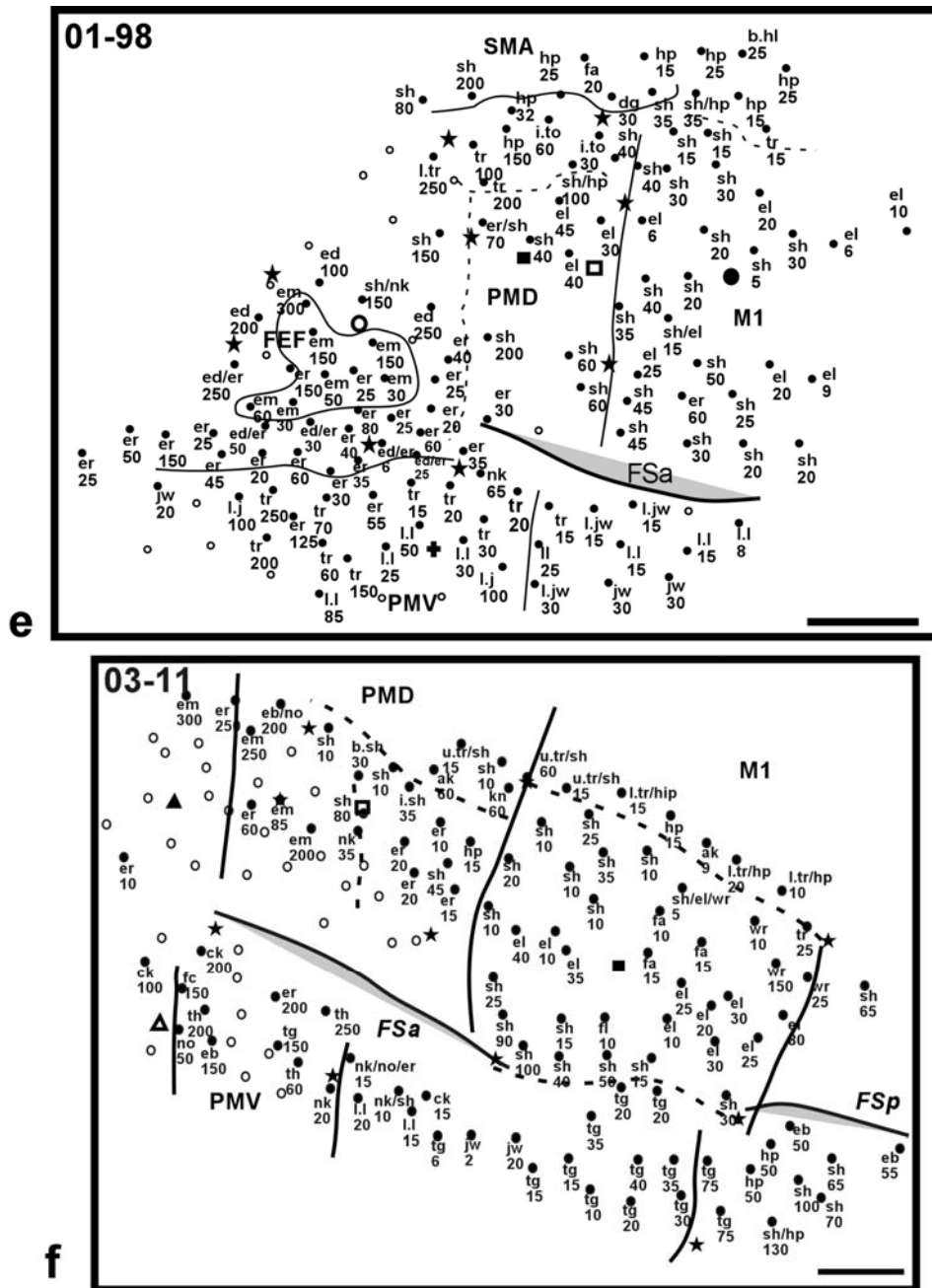
from ICMS mapping.
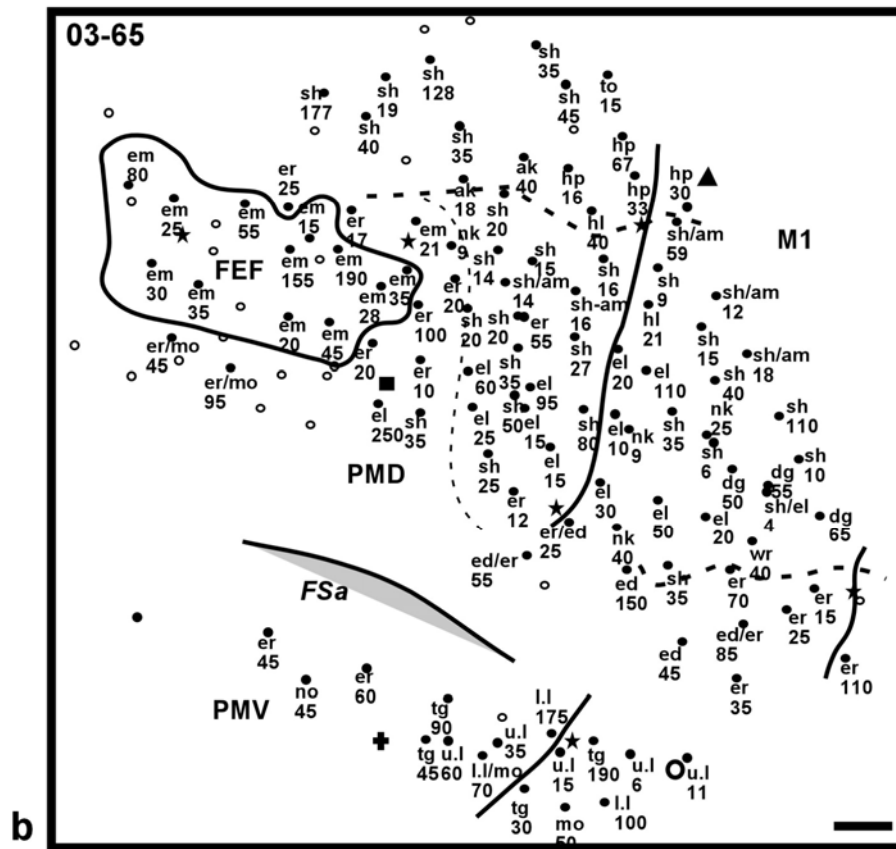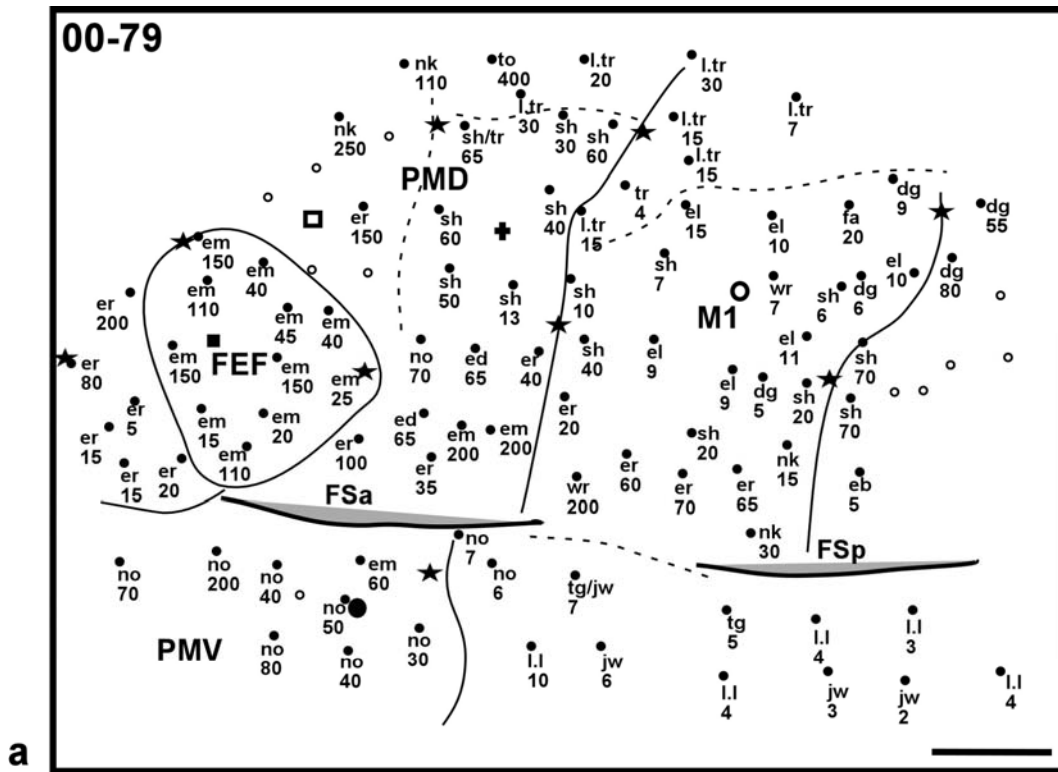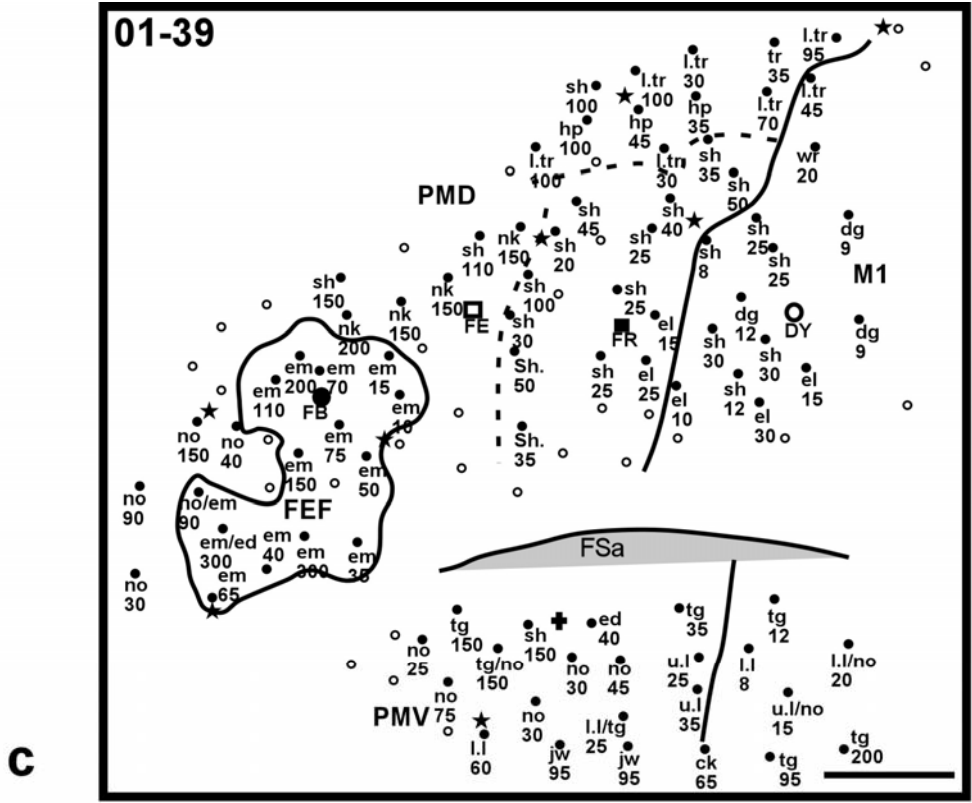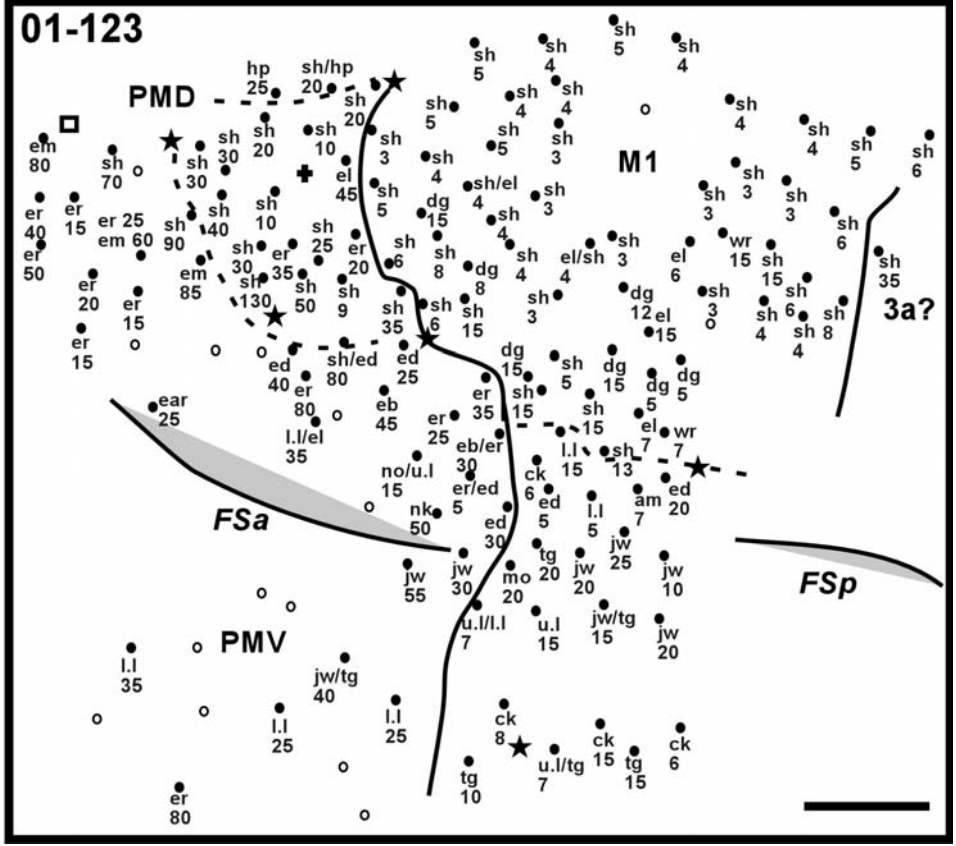
Fig. 4-2. Results of intracortical microstimulation mapping in 6 cases (2a-2f). The mapping covered the motor cortical subdivisions (M1, PMD, PMV and SMA), FEF and regions rostral to PMD and caudal to M1. The purpose of mapping procedure here was to delineate the electrophysiological borders (solid and dash lines) between the subdivisions. The numbers indicate the threshold of the lowest electric currents that could evoke the reliable body movements. The borders were marked based on the levels of the threshold and types of body movements, and these borders were also compared with the architectonic borders (shown in next figure), both electrophysiological and architectonic borders corresponded very well in most of the cases. In general, M1 is located in between FSa and FSp, and PMD is medial to FSa; whereas PMV is lateral to FSa. Each solid dot indicates one penetration with movement response, and the open circle indicates the penetration with no response. Left, rostral; top, medial. Scale bar= 1mm. Refer to the abbreviation list for the body movement.

The cortical area rostral to M1 required higher currents to initiate movements. The dorsal premotor cortex (PMD) consisted of mostly shoulder movements with a mix of some trunk/hindlimb movements in medial PMD and some ear movements in the lateral PMD (Fig. 4-2). The proximal forelimb movements dominated the whole region but the digit movements were not observed. The forelimb, trunk/hindlimb and ear movements were not as discrete as those found in M1. In PMD, these movements were mixed with each other at some point. We saw few neck, eye movements and eye lid movements in the lateral part of PMD. Although we were not able to identify whether there were rostral and caudal differentiations in PMD based on the electrophysiological results, we noticed that the thresholds in the rostral part of PMD were higher than more caudal part of PMD. There were few trunk, shoulder, neck, eye-lid, ear and eye movements were found in the rostral PMD. Most of time, we did not get any movement response in this rostral region of PMD even though the electrical currents were raised to 250 or 300 µA. The ventral PM (PMV) contained mostly orofacial movements (Fig. 4-2). Few upper trunk movements were found in two cases and these movements mix with orofacial movements (Fig. 4-2e). One shoulder movement was found in one of these two cases. We did not explore the very rostral and lateral portions of PMV since our purpose here was to identified the borders of PMV with PMD and M1 for tracer injections. The thresholds that were needed to elicit movements in PMV were just slightly higher than those needed to initiate orofacial movements in M1. Therefore, it was not so easy to mark the border of PMV with M1 based only on physiological mapping results.

A small region, which might be frontal eye field (FEF), located anterior to the tip of FSa and in between PMD and PMV was also distinguished. Stimulating this region with

threshold currents ranging from 20 µA to 300 µA, saccade eye movements were observed (Fig. 4-2a to c,e). SMA contained the body movement representations with the trunk/hindlimb in the caudal part and forelimb in the rostral part. The thresholds in SMA were much lower than those in PMD, but slightly higher than that in M1. The borders of SMA with PMD and M1 could be distinguished easily according to the level of the threshold and somatotopic representations of the body movement. Again, we did not stimulate the entire SMA region. For our purpose, we just had to identify the physiological borders of SMA with PMD and M1.

Architecture of the Motor Cortical Areas

In order to relay the cortical labeled neurons, the architecture of the motor cortex had to be studied, and also, the architectonic borders could be compared with the physiological borders to further confirm the boundaries of the motor cortical subdivisions. The cortex of 9 animals was flattened and cut parallel from white matter to pia surface. The flattened sections were stained with myelin and CO. The CO staining did not show clear subdivisions in the frontal lobe. The myelin stained sections showed better subdivisions of some cortical areas. The area 3b in the anterior parietal cortex was darkly stained. It was revealed as an elongated region extending from the medial wall to the lateral part of the hemisphere near the lateral sulcus (Fig. 4-3). The middle sector of area 3b (perhaps the forelimb representation) was about 2.5 mm to 3 mm wide which was the most darkly stained, and the isolated oval structures in the most lateral part of area 3b (perhaps orofacial representation) were also visible. There was a septa-free region near the FSp,

which might be the hand-face border of area 3b. Another less dark region located

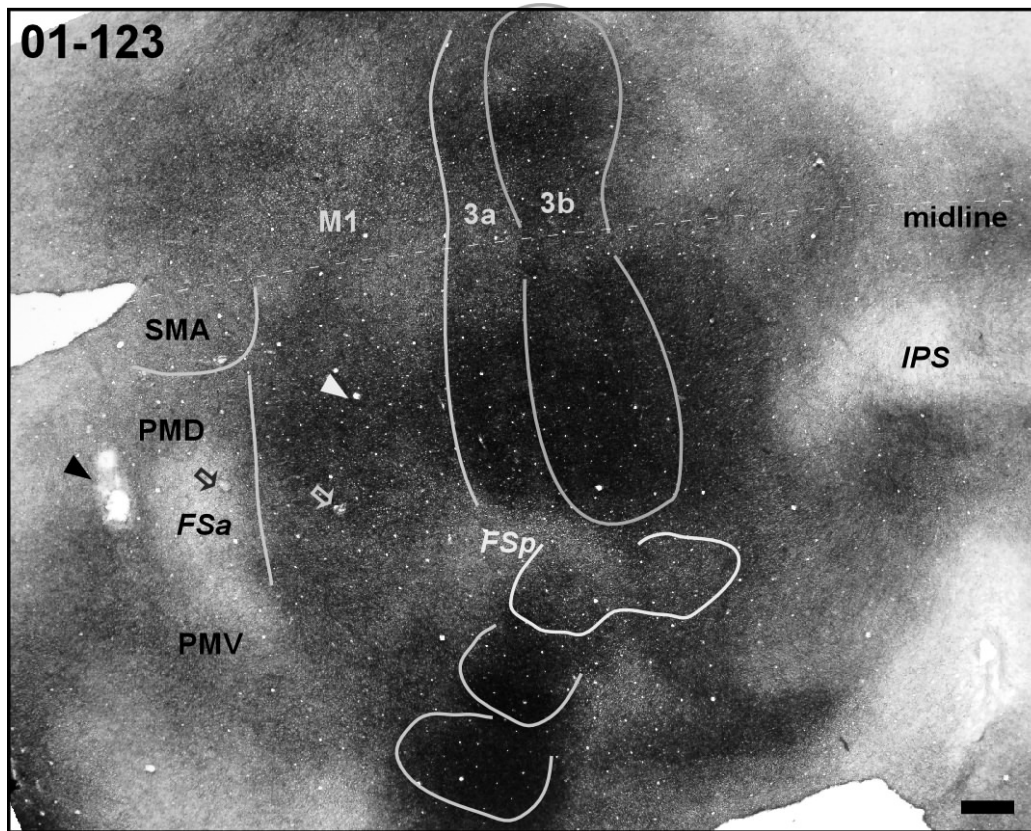adjacent and rostral to area 3b was area 3a. Area 3a was about 1.5 mm, which extended

Fig. 4-3. Photomicrograph of flattened cortex stained with myelin preparation in case 01-123. Somatosensory area 3b was the most darkly stained structure including hindlimb/trunk, forelimb and orofacial subdivisions from medial (top) to lateral (bottom). Somatosensory area 3a was also darkly stained, and only hindlimb/trunk and forelimb subdivisions were darkly stained. The FSp roughly separated the hand and face representations in both 3a and 3b. Rostral to area 3a was M1, which was less darkly stained compared to 3a, however, M1 was slightly more darkly stained than the premotor areas and SMA. In M1, only forelimb representation rather than the hindlimb/trunk and orofacial representations was darkly stained. The premotor areas, PMV and PMD, were generally as light as other frontal cortical regions, thus, the myelin staining was not sufficient to mark the borders of the premotor areas and frontal regions. Based on the results from ICMS, we were able to separate PMD from PMV according to the location of FSa. SMA, located medial to PMD, was slightly more darkly stained than PMD, but more lightly stained than M1. The solid lines indicate the architectonic borders that correspond very well with the electrophysiological borders defined via ICMS. The solid arrow points at the tracer injection site, and the open arrow indicates the lesion marked by the hand-face border in M1. Scale bar=1 mm.

from the mesial wall to FSp along with area 3b. Unlike area 3b, the orofacial area of area 3a was not distinct. Rostral to area 3a was M1, which was more lightly stained than area 3a. M1 was a medio-lateral elongated structure, too, sitting between FSa and FSp. M1 was larger than area 3a and 3b, which was about 3mm to 4 mm wide. Unlike area 3a and 3b, within the whole M1 region, only the middle sector of M1 that responded to forelimb movement was darkly stained. The very medial part (hindlimb representation) of M1 in the medial wall and orofacial representation in the lateral part of M1 were much lighter. The rostral motor areas, PMD and PMV, were not identified with myelin staining. Both PMD and PMV as well as the areas in the prefrontal cortex were lightly stained compared to M1. The prefrontal region and PM looked homogeneous and uniformly light in myelin preparation. Thus, we used the pattern of sulcus locations to identify the subdivisions of PM. Normally, PMD and PMV were separated by FSa according to the physiological results. SMA was slightly darkly stained compared to M1 trunk/hindlimb representation and PMD, therefore, SMA could be distinguished in myelin staining. There was a region rostral to the tip of IPS and caudal to area 3b, which was darkly stained but not as dark as area 3b. This region might be the forelimb representation of somatosensory 1 and 2. Thus, the myelin staining was able to delineate the borders between the major subdivisions of the motor cortex and somatosensory cortex.

The cortex of one animal, 01-39, was cut sagittally and the sections were processed with immunocytochemical SMI-32, histochemical CO and myelin, and cytoarchitectonic Nissl stainings. In the lateral sections, PMV, the orofacial representation of M1, area 3a and 3b (perhaps the orofacial representation), were distinguished in these preparations. Layer IV of somatosensory area 3b (perhaps orofacial representation) was darkly stained in these
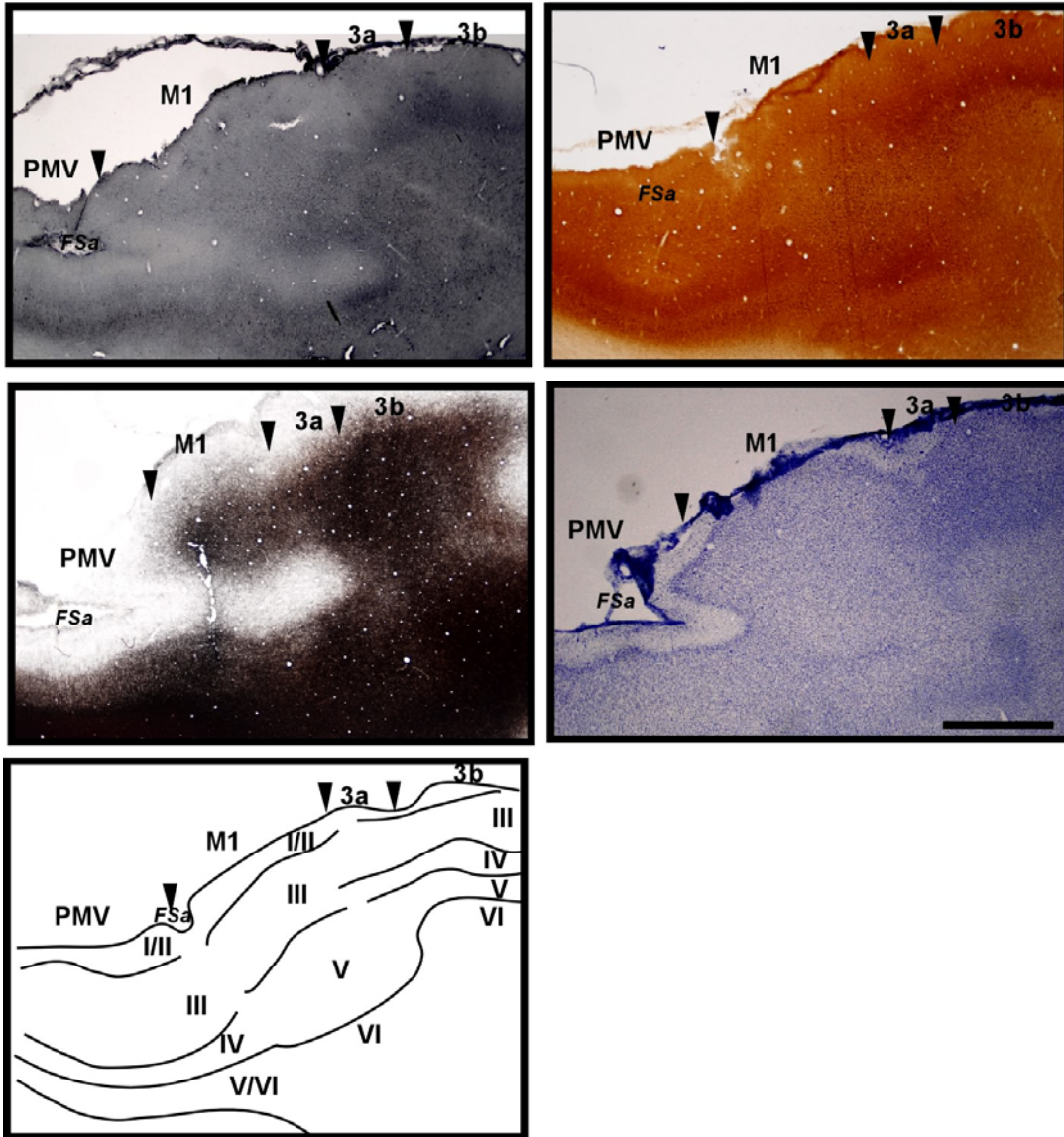
112

Fig. 4-4. Brightfield photomicrographs of the cortical subdivisions shown in SMI-32 (top-left), CO (top-right), myelin (central-left), and Nissl (central-right) stainings, and the drawing of the lamination (bottom). These lateral sagittal sections were from case 01-39. The layer IV of somatosensory area 3b was very darkly stained indicating that area 3b contained a high density of neurofilament structure revealed in SMI-32, high level of mitochondria activity revealed in CO stain, high density of myelinated fibers revealed in myelin stain, and high density of Nissl substances revealed in Nissl stain. Area 3a was more lightly-stained than area 3b in these stainings. As for M1, it was much lighter than area 3a due to lack of layer IV in M1. Rostral to M1 was PMV, which was more darkly stained than M1 in these preparations. The arrow marks the architectonic borders. Left, rostral; top, dorsal. Scale bar= 500μm.
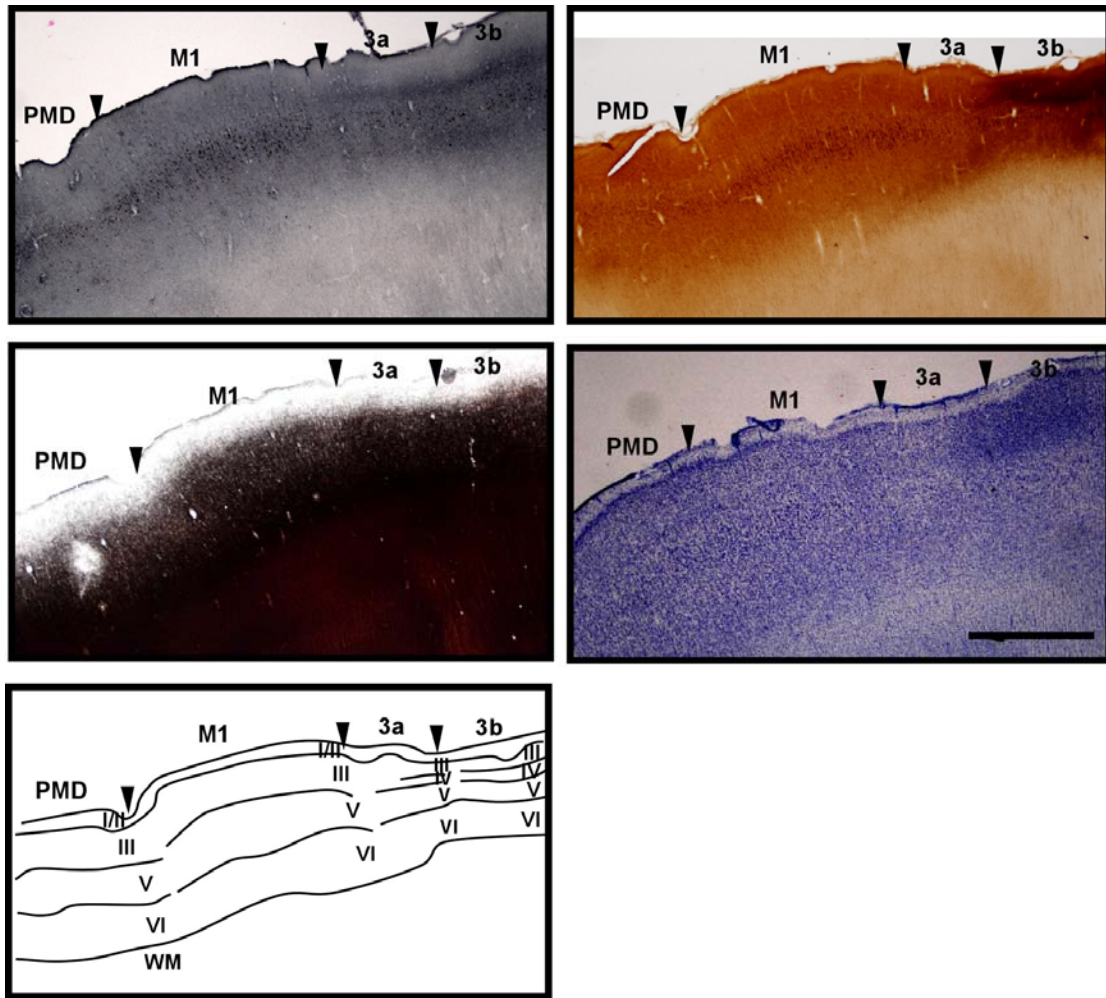
Fig. 4-5. Photomicrographs of the medial sagittal sections from case 01-39 stained with SMI-32 (top-left), CO (top-right), myelin (central-left), and Nissl (central-right), and the drawing of the lamination (bottom). Similar to figure 4 that area 3b was the most darkly stained structure in the medial sections. Area 3b here (perhaps forelimb representation) contained darkly stained layers IV and V in these preparations, and these two layers were well distinguished in SMI-32 and CO. Area 3b had a thinner layer IV, and poorly distinguished layer V compared to area 3b. Thus, area 3a was less darkly stained than area 3b. SMI-32 and CO stainings revealed prominent big pyramidal cells in the layer V of M1, although M1 lacked a layer IV. These four stainings displayed that M1 was more lightly stained than area 3a and 3b. Similar to M1, PMD did not contain layer IV, however, layer V of PMD was less well distinguishable than in M1. Apparently, PMD had less big pyramidal cells than M1. Thus, PMD was much more lightly stained than M1 in SMI-32, CO, and myelin preparations. Nissl staining showed that PMD was more darkly-stained than M1. The arrow marks the architectonic borders. Left, rostral; top, dorsal. Scale bar= 500μm.

four preparations. This also indicated that area 3b layer IV had high density of SMI-32

positive neurons (containing high density of neurofilaments), high density of cytochrome

oxidase metabolic activity of mitochondria, high density of myelinated fibers, and high

density of Nissl substance in granular cells (Fig. 4-4). The rostral adjacent area 3a was

less darkly stained compared to area 3b. Area 3a had thinner or less clear layer IV. The

primary motor area, M1, rostral to area 3a, was lightly stained compared to area 3a. This

lateral portion of M1 lacked of layer IV. Ventral premotor area (PMV), on the other hand,

contained thin layers IV and V, which were moderately stained in these four preparations.

The layer IV in PMV was thinner than the layer IV in area 3b, but thicker than in area 3a.

Thus, compared to lightly-stained lateral M1, PMV had moderate density of SMI-32

positive neurons in layer V, cytochrome oxidase activity in layer IV, and myelinated

fibers in both layers IV and V resulting in more darkly-stained in SMI-32, CO, and

myelin, respectively, preparations.

The medial sections were also processed with these four preparations (SMI-32, CO,

myelin and Nissl). Similar to what had been described before that area 3b was the most

darkly-stained region compared to other motor cortical areas. Area 3b (perhaps forelimb

representation) contained distinctive layers IV and V, which were remarkably darkly

stained under SMI-32, CO, myelin, and Nissl preparations (Fig. 4-5). Layer IV and V of

area 3b were well segregated since layer IV was much more darkly stained than layer V,
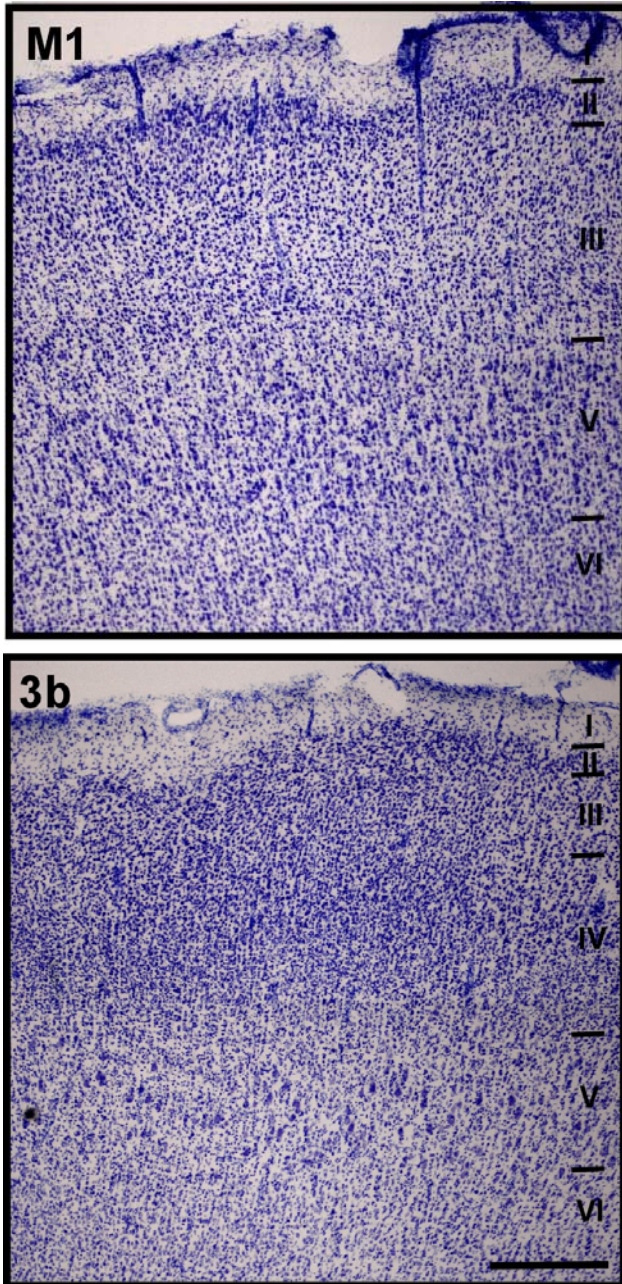
Fig. 4-6. Photomicrographs of the section stained with Nissl preparation. M1 (top) had tick layer III and V, but lacked layer IV. Layer V also contained a high density of big pyramidal cells. Area 3b (bottom) contained a thin layer III and layer V, but a thick layer IV. The granular cells in layer IV were prominent and densely packed. Layer V had less big pyramidal cells than in M1. Horizontal lines mark the architectonic borders among layers. Top, dorsal. Scale bar= 500μm.
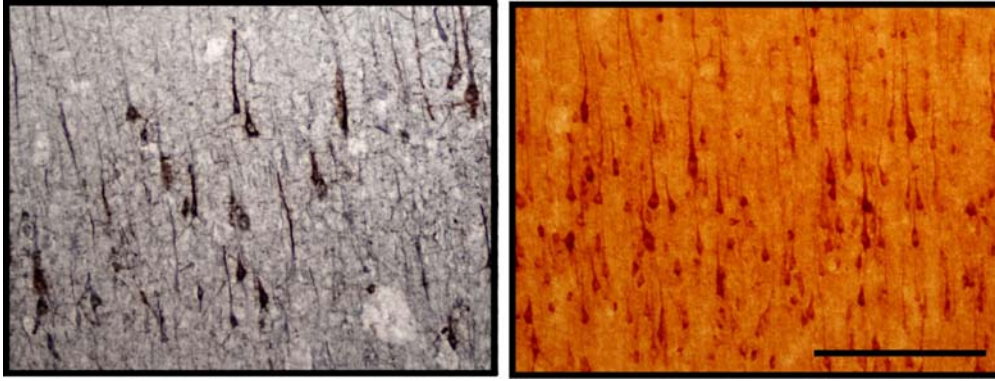
Fig. 4-7. Photomicrographs with high magnification showing the pyramidal cells in M1 stained with SMI-32 (left) and CO (right). These two stainings revealed M1 with a high density of big pyramidal cells. Scale bar= 250μm.

and few big pyramidal cells were also visible in layer V (Fig. 4-6). Area 3a (perhaps forelimb representation) contained thinner layer IV and poorly-defined layer V compared to area 3b. In addition, layer IV of area 3a contained much fewer granular cells and myelinated fibers, and layer V contained much fewer big pyramidal cells than area 3b. Thus, area 3a was less darkly-stained than area 3b. SMI-32, CO (Fig. 4-7), and Nissl (Fig. 4-8) preparations revealed prominent big pyramidal cells in M1 forelimb representation. Moreover, Nissl staining revealed that M1 lacked a layer IV, but had thick layers III and V (Fig. 4-8). The myelin staining displayed moderately-stained M1, which was lighter than area 3a and 3b (Fig. 4-5). The dorsal premotor area (PMD) did not contain layer IV, either, but had a thinner and a poorly-defined layer V compared to M1. The PMD layer V had much fewer pyramidal cells than M1. Thus, PMD was much more lightly-stained in the SMI-32, CO, and myelin stainings than M1 (Fig. 4-5). In the low magnification Nissl preparations, it seemed that PMD contained higher density of Nissl substance resulting in more darkly-stained compared to M1.
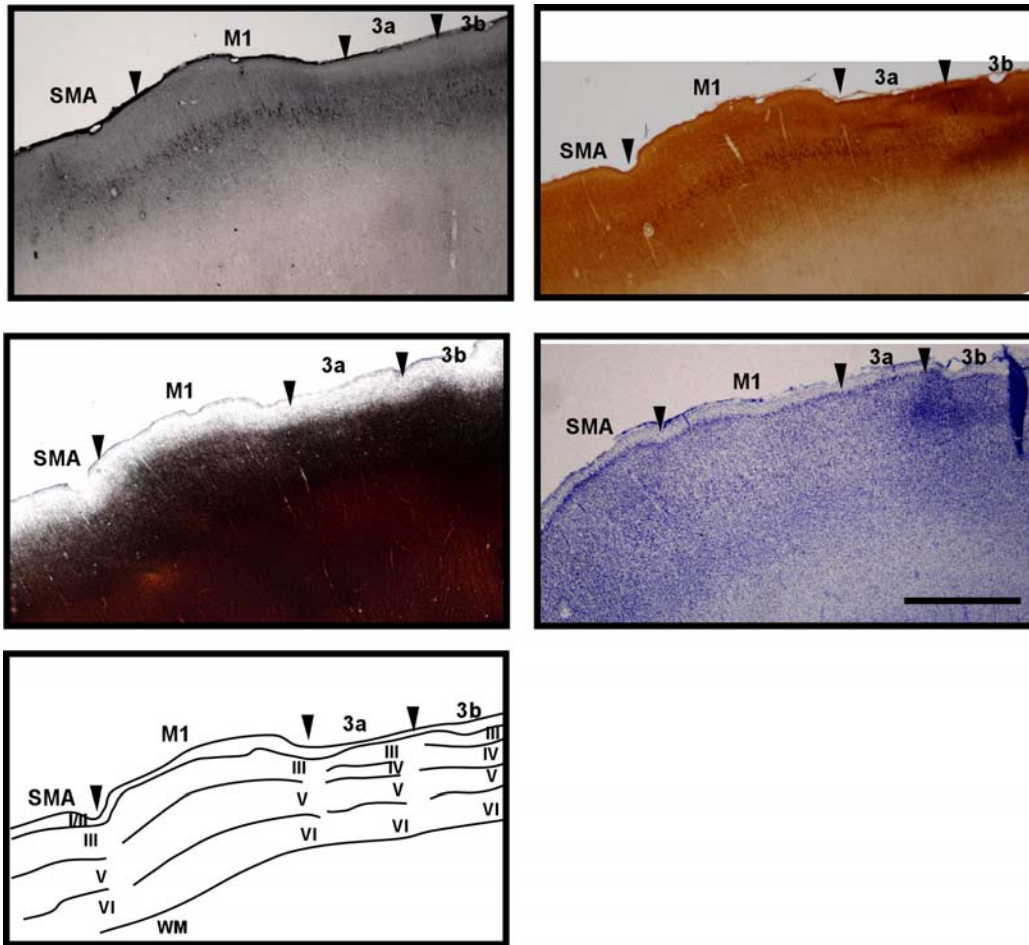
Fig. 4-8. Photomicrographs of the more medial sections from case 01-39 stained with SMI-32 (top-left), CO (top-right), myelin (central-left), and Nissl (central-right), and the drawing of the lamination (bottom). Again, area 3b was the most darkly stained region that contained well distinguishable layers IV and V. Area 3a was less darkly stained than area 3b. Area 3a contained a very thin layer IV, and a poorly-defined layer V. In contrast, M1, contained more big pyramidal cells in layer V than the adjacent cortical areas. M1 was more darkly stained than area 3a in SMI-32 and CO, but more lightly stained than area 3a in myelin and Nissl stainings. The non-primary motor area, SMA, containing poor lamination, was much more lightly stained than M1 in SMI-32 and CO; however, SMA was more darkly stained than M1 in myelin and Nissl preparations. The arrow marks the architectonic borders. Left, rostral; top, dorsal. Scale bar= 500μm.

The more medial sections included the hindlimb/trunk representations of area 3a, 3b and

M1, and SMA. Again, area 3b was the most darkly stained region among these areas.

Similar to the forelimb representation, the hindlimb/trunk representation of area 3b

contained clearly distinguished layers IV and V that were darkly stained in these

preparations (Fig. 4-8). The orofacial representation in area 3b contained a less well distinguished layer V. The Nissl preparation also revealed darkly stained and densely packed granular cells in layer IV of area 3b. As for area 3a, the hindlimb/trunk representation of area 3a contained the similar features of the forelimb representation of area 3a that contained thin, but darkly-stained layer IV, and a poorly distinguished layer V. Overall, area 3a was less darkly-stained than area 3b. The hindlimb/trunk representation of M1 had less big pyramidal cells than those in the forelimb representation, but more than those in the orofacial representation of M1. Although these body movement representations of M1 did not contain layer IV, the layer V of hindlimb/trunk representation contained less pyramidal cells than those in forelimb representation, but much more than those in orofacial representation. Thus, M1, in general, was more lightly-stained than area 3b in Nissl, CO, and myelin preparations, but more darkly-stained than area 3a in SMI-32 staining. The lamination of supplementary motor area (SMA) was not as clear as other motor cortical areas and areas 3a and 3b. The layer V of SMA was very lightly stained in SMI-32 and CO preparations. However, in myelin and Nissl, SMA was more darkly-stained than M1.

Ipsilateral Corticocortical Connections

Distributions of retrograde labeled cells were analyzed after multiple neuroanatomical tracer injections into subdivisions of motor cortex (M1, PMD, PMV, and SMA), areas in the prefrontal cortex, and areas in the posterior parietal cortex following intracortical microstimulation (ICMS). The purpose of prefrontal injections was to verify that these prefrontal regions are not parts of the motor cortex, and the purpose of parietal injections

was to confirm that motor and parietal cortical connections are reciprocal. The use of the

tracers in each cortical area in the frontal cortex and the size of the uptake zone of the

injection sites were described in the thalamocortical connection chapter (Chapter III).

The boundaries of the motor cortical subdivisions were derived from the results of the

ICMS mapping and architectonic stainings. The results support four main conclusions 1)

M1 and PMD received their most dominant cortical projections from the parietal cortex.

M1 had the strongest connections with the anterior parietal cortex, and PMD had the

strongest connections with the posterior parietal cortex; whereas, PMV received

dominant inputs from prefrontal cortex rather than parietal cortex. 2) Dorsal PM (PMD)

had dense connections with the dorsal regions of the cortex, and the ventral PM (PMV)

had dense connections with the ventral regions of the cortex. 3) The cortical areas that

were involved in the same body movements tend to connect with each other. 4) In the

motor cortex, adjacent subdivisions do not necessarily, strongly connect with each other.

Connections of Primary Motor Cortex (M1)

Two animals received tracer injections in the trunk/hindlimb representation of M1. The

uptake zones in these two cases were mainly in M1 with a little bit of overlap with the

caudal part of SMA. The distribution of labeled cells was very similar in these two cases.

The M1 hindlimb area had dominant connections with the dorsal regions of the

hemisphere. The majority of the label was found in the dorsal portions of the cingulate

cortex and these cells were basically clustered in both rostral and caudal, but not the

central, cingulate cortex. There were also lots of labeled cells in SMA in the mesial wall.

Some labeled cells were found in the superior posterior parietal cortex (sPPC) near the tip

of the intraparietal sulcus, and very few labeled cells were seen in the areas near the lateral sulcus (Fig. 4-9). There were some differences in the distribution of the labeled cells between these two cases. The label of case 99-75 in the superior PPC was located more medially than that of case 03-65. Some labeled cells were observed in area 3a and the region caudal to area 3b in case 99-75 (Fig. 4-9a), but no label was found in these somatosensory areas in case 03-65 (Fig. 4-9b). In case 03-65, a lot of labeled cells were seen in the ventral portions of the cingulate cortex, and again, these cells were clustered in the anterior and posterior cingulate cortex. In addition, a lot of labeled cells were seen in PMD and M1 forelimb area, near the FSa and FSp, respectively. Some label was found in the area lateral to the M1 face area, and some was seen in the inferior PPC (Fig. 4-9b). The difference here might be because of the FE tracer used in case 99-75 was not uptaken by the cells very well. Moreover, the injection of CTB in case 03-65 apparently involved the forelimb area of M1, thus, it might result in more extensive connections. The M1 trunk/hindlimb area had dominant connections with the areas in the cingulate cortex, while the M1 forelimb area had dominant connections with the areas in the dorsal regions of the hemisphere. The general connectional patterns of the five animals with tracer injections in M1 forelimb representation were very similar. The strongest inputs to M1 forelimb area were from the parietal cortex, just caudal to area 3b (Fig. 4-10). The inputs from this cortex presumably were related to the forelimb movement. Other cortical areas also projected to M1 forelimb, but in a much weaker degree. These areas were somatosensory areas 3a, 3b, and areas near the lateral sulcus (possibly S2 and PV),
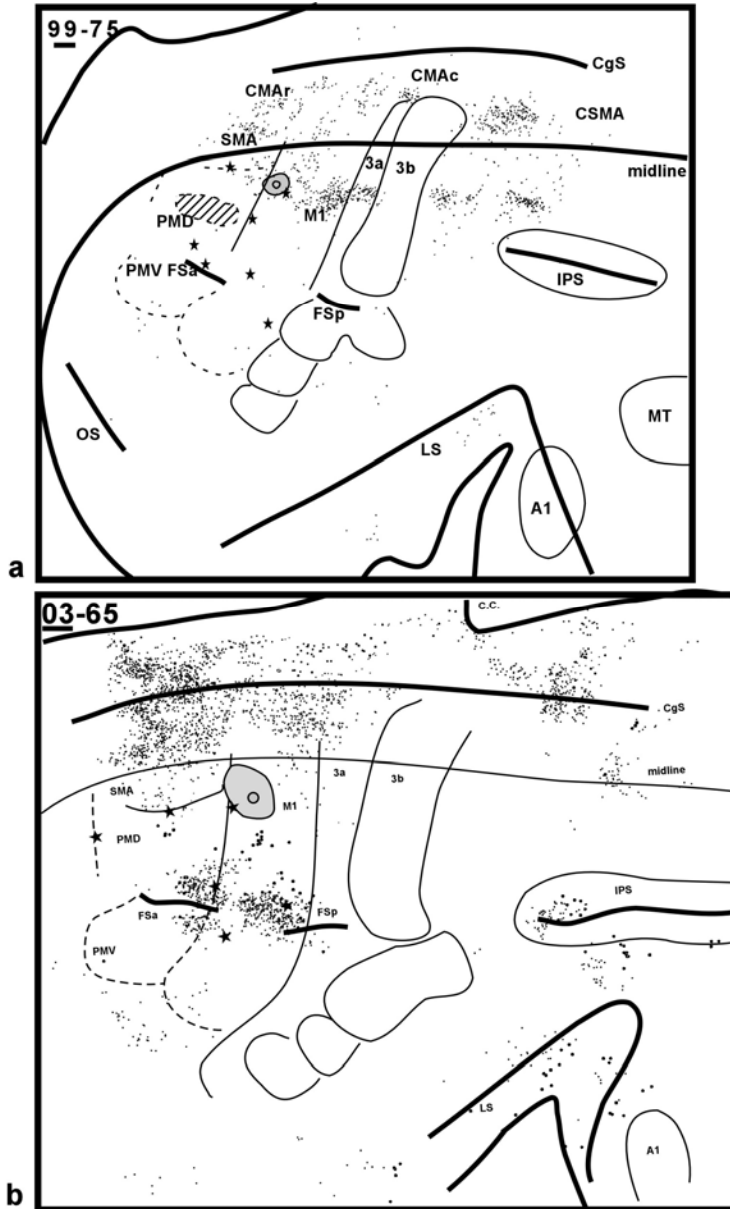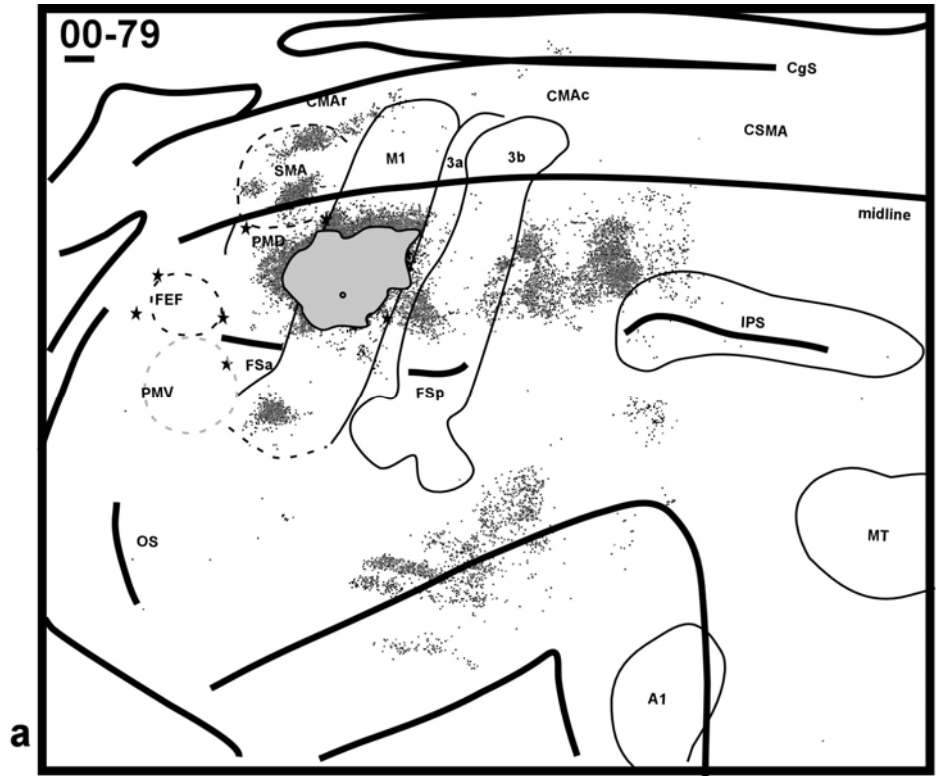
Fig. 4-9. Distribution of retrograde labeled cells shown in the flattened cortex following tracer injections in the hindlimb/trunk representation of M1 in case 99-75 (a) and 03-65 (b). A FE injection was placed in case 99-75 and a CTB injection was placed in case 03-65. Both uptake zones of the tracers were involved with a small portion of SMA, but the CTB injection was also involved with the forelimb representation of M1. Most of the labeled cells were clustered in the very medial regions of the hemisphere including the cingulate cortex. Each dot represents a single retrograde labeled cell, and the solid thin lines represent the match of electrophysiological and architectonic borders. The dash lines are the estimated borders from the study by Wu et al. (2000). See abbreviation list for the abbreviations. Left, rostral; top, medial. Scale bar= 1mm.
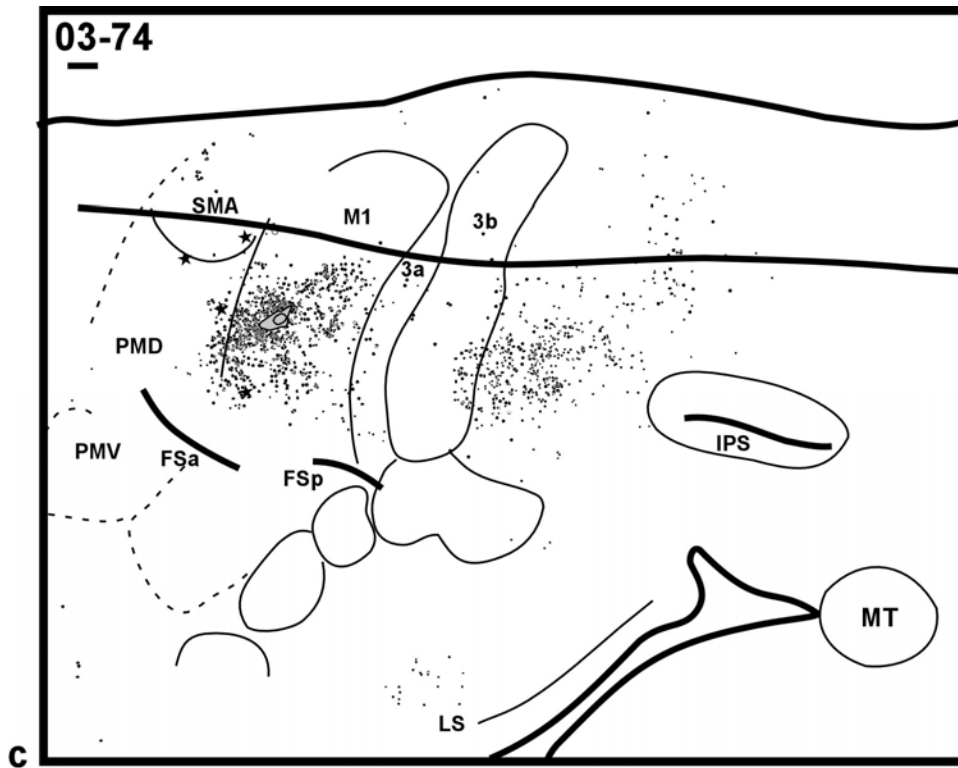
Fig. 4-10. Distribution of retrograde labeled cells shown in the flattened cortex following tracer injection in the forelimb representation of M1 in case 00-79 (a), 03-11 (b) and 03-74 (c). A DY injection was placed in case 00-79 and its uptake zone overlapped with both adjacent PMD and area 3a. A FR injection was made into case 03-11 and its uptake zone overlapped with PMD and also perhaps area 6Ds. On the other hand, the FE injection in case 03-74 was confined to M1 forelimb representation. Most of the labeled cells were seen in the forelimb representations of the somatosensory-related areas in the parietal cortex. See figure 9 for the conventional references. Scale bar= 1mm.

motor areas PMD and SMA, and areas in the posterior parietal cortex such as superior

posterior parietal cortex and caudal portion of cingulate cortex. A DY tracer was placed

in case 00-79 resulted in a large uptake zone (Fig. 4-10a) and a FR tracer was placed in

case 03-11 resulted in a medium-sized uptake zone (Fig. 4-10b). The uptake zones in

both animals extended into PMD and the uptake of case 00-79 also included area 3a.

Additional label was found in some areas in these two cases such as a cluster of labeled

cells in M1 orofacial area, the rostral cingulate cortex, and the inferior PPC. In addition,

more labeled cells were observed in the somatosensory areas near the lateral sulcus in
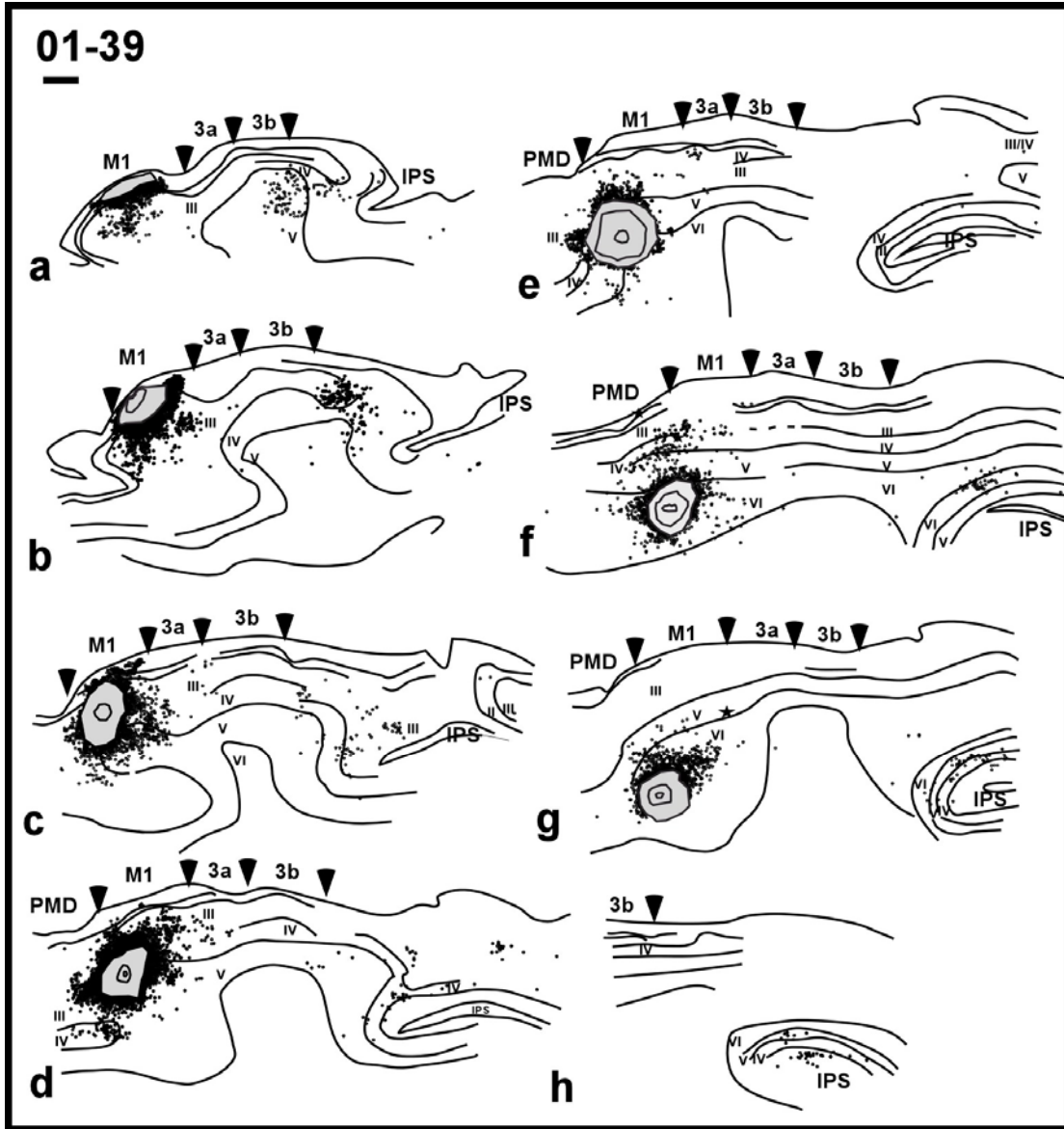
Fig. 4-11. Plot of retrograde labeled cells in series of sagittal section from lateral (a) to medial (h) with DY injection in M1 forelimb area in case 01-39. The injection overlapped slightly with PMD and covered both supragranular and infragranular layers. The distribution of the labeled cells was similar to that shown in the flattened cortex, and the cells were clustered in the supragranular layers in the parietal cortex. Solid lines indicate the architectonic borders among layers. Arrows represent the match of electrophysiological and architectonic borders. Each dot represents single labeled cells. Scale bar= 1mm.

these two cases. More extensive labeling was found in case 03-11, which might be due to the involvement of the injection with 6Ds (defined by Wu et al., 2000), near the caudal tip of FSa. In this case, the label was also found in the prefrontal cortex, very caudal part of the cingulate cortex, PMV, and cortex rostral to MT (Fig. 4-10b). The forelimb sector of M1 received projections from the cells restricted to the supragranular layers of other cortical areas in case 01-39 (Fig. 4-11). As for the intrinsic connections in M1 of case 03-74 received a confined injection within the forelimb representation, similar in the research in macaque monkeys (Huntley and Jones, 1991; Hatanaka et al., 2001), the forelimb representation did not have dense connection with the orofacial representation, but had some intrinsic connections with the trunk/hindlimb representation (Fig. 4-10c). Both injections in the M1 orofacial area were contaminated part of PMV and possibly also 6Ds (Fig 12a,b). The uptake zone of case 03-65 also invaded area 3a (Fig. 4-12b). Nevertheless, the patterns of labeled cells were similar in these two cases. While injections in the trunk/hindlimb sector of M1 had dominant connections with the cingulate cortex, the forelimb representation had strongest connections with cortex caudal to 3b, and the M1 orofacial representation had the strongest connections with the ventral regions of the hemisphere near the lateral sulcus (Fig. 4-12). Dense labeling was also found in PMV. Some cells were also seen in the orofacial representations of area 3a and 3b, and few were seen in the prefrontal cortex and inferior PPC. Overall, the connections of M1 formed a topographic patterns with the most medial M1 (forelimb and trunk representations) having dominant connections with medial cortical areas located in the cingulate cortex (in the medial wall), the forelimb representation located in the dorsal M1 having dominant connections with cortical areas in the dorsal regions of the hemisphere,
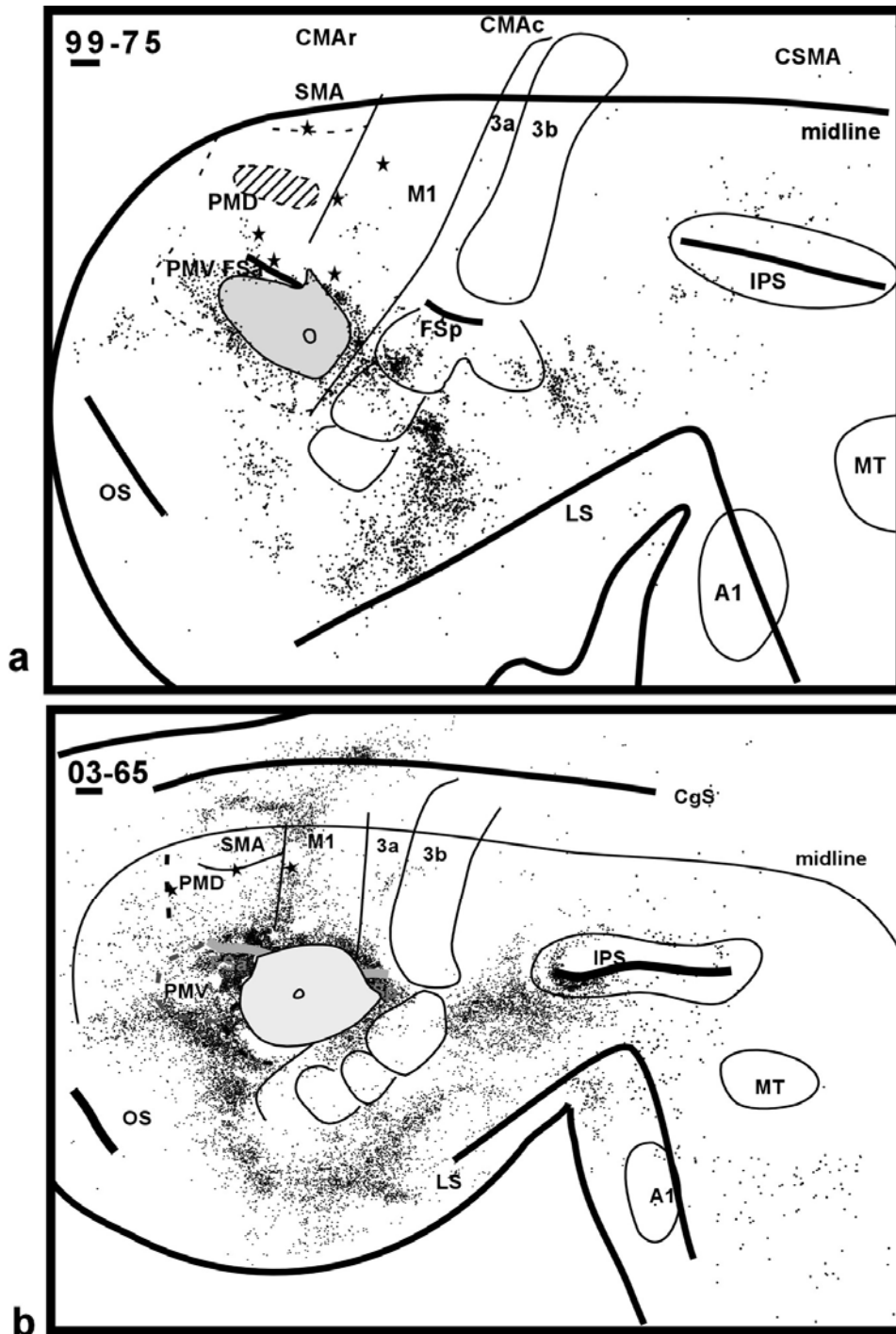
Fig. 4-12. Distribution of retrograde labeled cells shown in the flattened cortex following tracer injection in the orofacial representation of M1 in case 99-75 (a) and 03-65 (b). A FB injection was made into case 99-75 and its uptake zone overlapped with PMV and perhaps area 6Ds. A DY was made into case 03-65 and its uptake zone overlapped with PMV. 6Ds and also area 3a. It was found that most of the labeled cells were located in the somatosensory related areas in the lateral regions of the hemisphere. The striped area in case 99-75 indicates a damaged region. See figure 9 for the conventional references. Scale bar= 1mm.

and the orofacial representation in the ventral M1 having dominant connections with the areas in the ventral regions of the hemisphere. These results are consistent with those of the more limited study of M1 connections of Wu et al (2000).

Connections of Cortex at the Anterior-Posterior Parietal Cortex Junction

Since we found that the anterior parietal cortex (possibly area 1 and 2) and adjoining posterior parietal cortex was heavily labeled following M1 forelimb injections, we wanted to know whether there were also strong projections from M1 to this region. Thus, we placed a FB tracer in the parietal cortex just caudal to area 3b in a part likely to represent the forelimb. Dense labeling was found not only in M1 forelimb representation also in presumptive area 1, somewhat in areas 3b and 3a, other parts of posterior parietal cortex, and in somatosensory areas in the lateral sulcus (Fig. 4-13). These results indicate that M1 sends strong projections to the regions of area 1 and adjoining parietal cortex, and the connections between M1 and this part of parietal cortex are reciprocal.
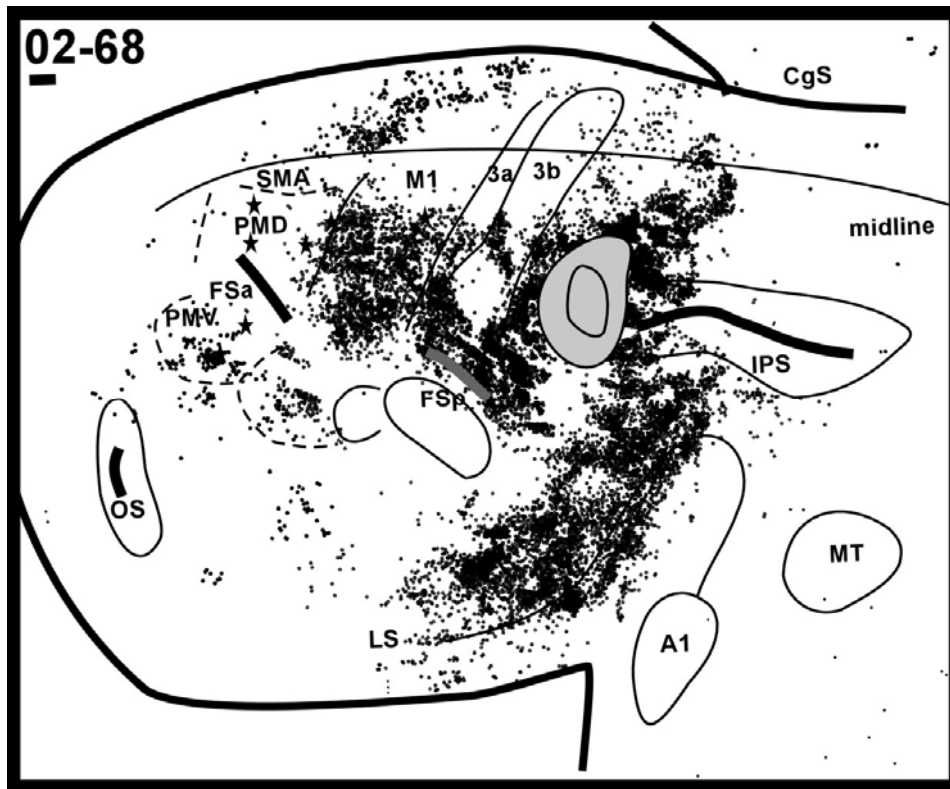
Fig. 4-13. Reconstruction of labeled cells shown in flattened cortex in case 02-68 with a FB injection in the cortex (perhaps forelimb representation) caudal to area 3b in the parietal cortex. Dense label was seen not only in M1 but also in the somatosensory areas in the lateral sulcus, which confirmed that the cortical connections between M1 and area 1 and 2 were reciprocal. See figure 9 for the conventional references. Scale bar= 1mm.

Connections of Dorsal Premotor Area (PMD)

Figure 14 shows the labeled cells in the flattened cortex after the tracers were placed into the dorsal premotor area (PMD). Most of the injections were located in the center of PMD (Fig. 4-14a to d) and confined within PMD that was defined by the ICMS mapping. Some injections were a little bit rostral in PMD (Fig. 4-14e to f), some were a little bit caudal in PMD (Fig. 4-14g) (Table 4-1), and some injections were not confined within PMD, but rather extended into adjacent cortical areas such as M1 or prefrontal cortical areas (Fig. 4-1). All of the injections in PMD resulted in the dense labeling in the

129

posterior parietal cortex. The majority of the labeling was found in the superior parietal

cortex in all cases and in the caudal region of the cingulate cortex (maybe the cingulate

sensory motor area) in most of the cases (Fig. 4-14). Dense label was also found in the

inferior parietal cortex. The upper and lower banks of the intraparietal sulcus had dense

distributions of labeled cells. A few scattered labeled cells were seen in the occipital-

temporal cortex that near MT and A1. In the frontal lobe, some label was seen in the

region that was lateral to PMV and rostral to M1 orofacial area. Some labeled cells were

also seen in the mesial wall (probably pre-SMA). A few label was seen in SMA, PMV

and area rostral to PMD (probably SEF), FEF and anterior cingulate cortex. Except for

the injections in caudal PMD (4-14g), there were very few labeled cells found in M1.

When the injections were placed in the rostral rather than central PMD, the labeled cells

in the parietal cortex were a little bit more caudal. Injections in the caudal part of PMD

resulted in labeling the rostral part of the posterior parietal cortex (Fig. 4-14g). Other

than these differences mentioned above, there was no significant difference whether the

injection was placed in the rostral, central and caudal PMD. Moreover, based on our

ICMS data, which guided the locations for tracer injections, we were not able to

demarcate whether there were rostro-caudal differentiations within PMD. Case 01-123

(Fig. 4-14f) was injected with FE in PMD, the distribution of the labeled cells in the

posterior parietal cortex was similar to that mentioned above, but due to the

characteristics of the tracer, the transport was not as impressive as other injections in

PMD. Moreover, a FR was applied in case 99-75 (Fig. 4-14d) and a WGA-HRP was

applied in case 01-123, the uptake zone of the former case was believed to be confined

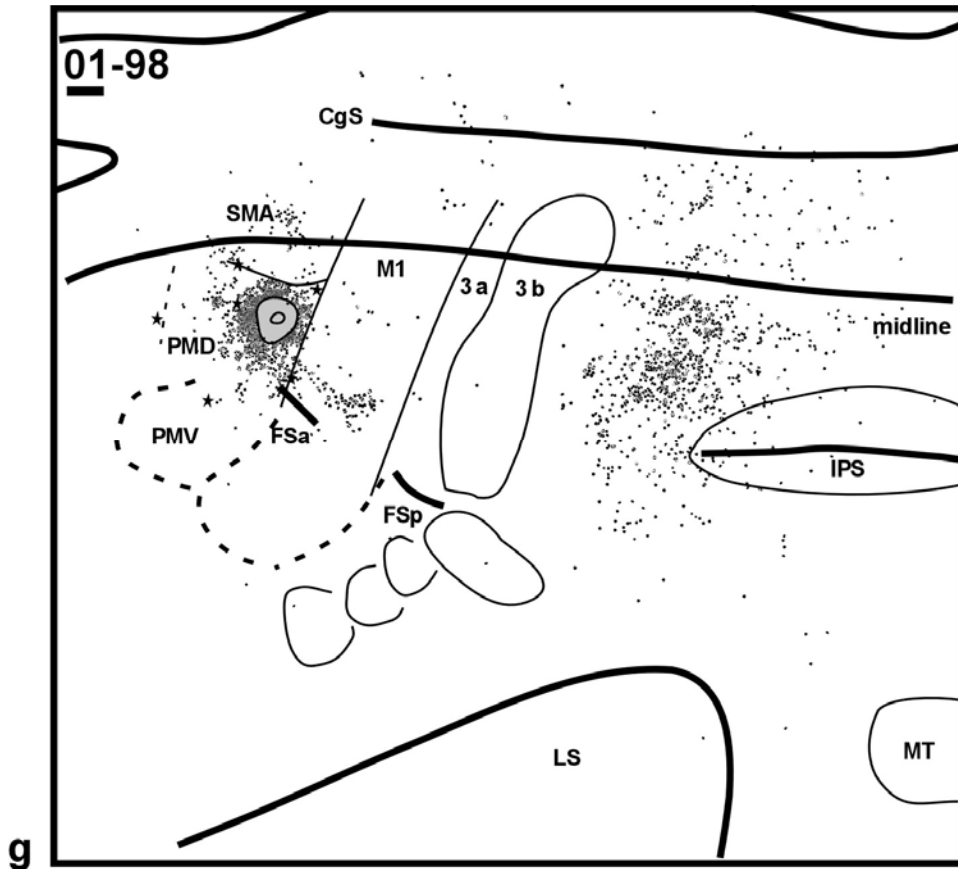within PMD, but the uptake zone of the latter included also SMA and M1. Both

a

b

c

d
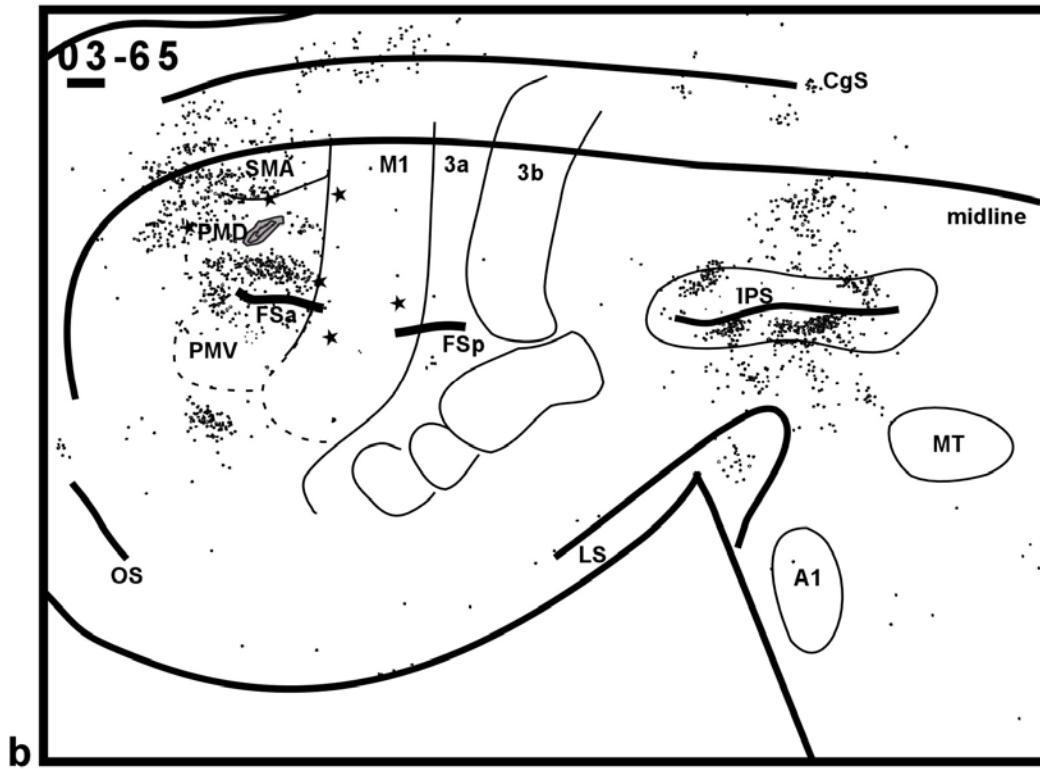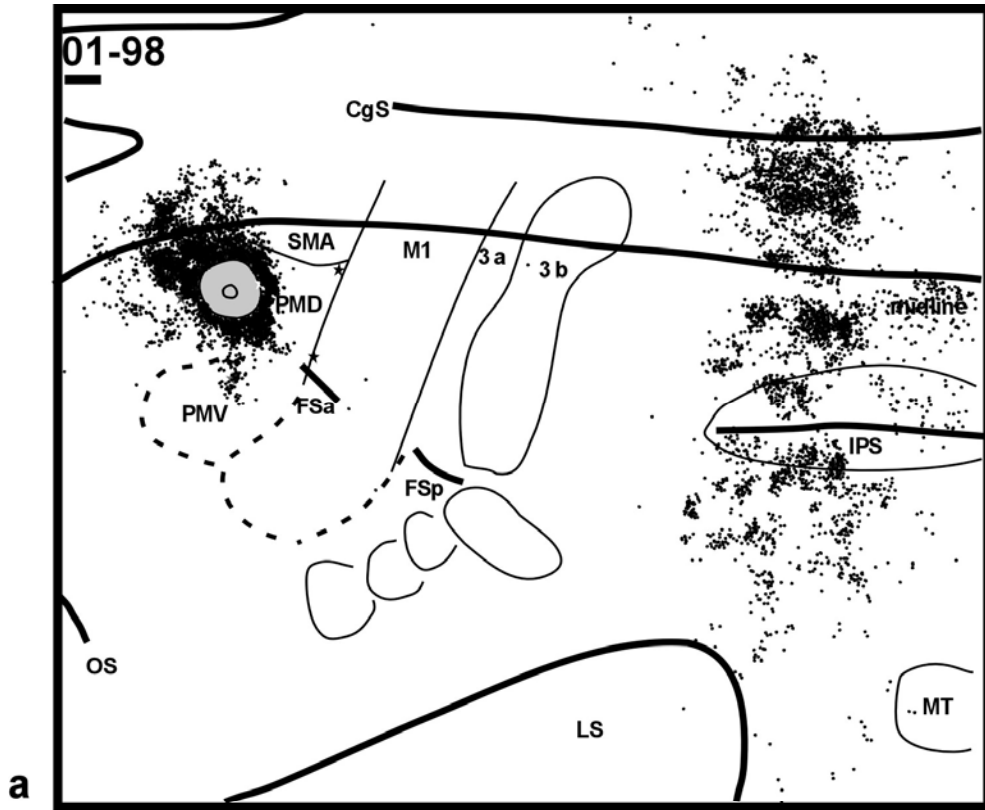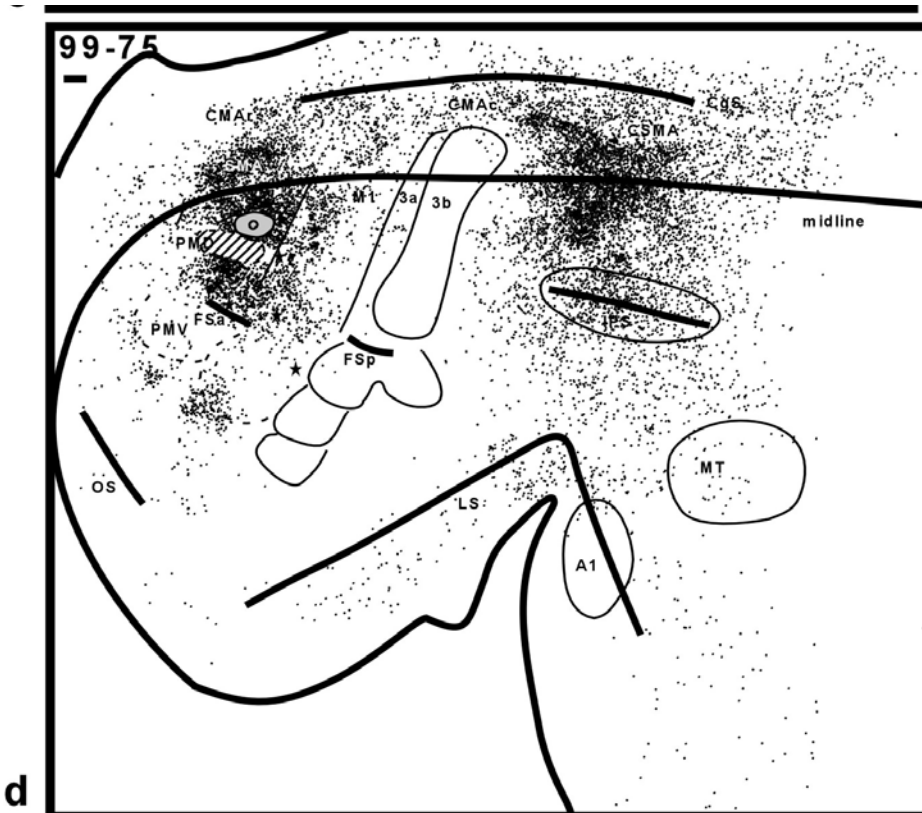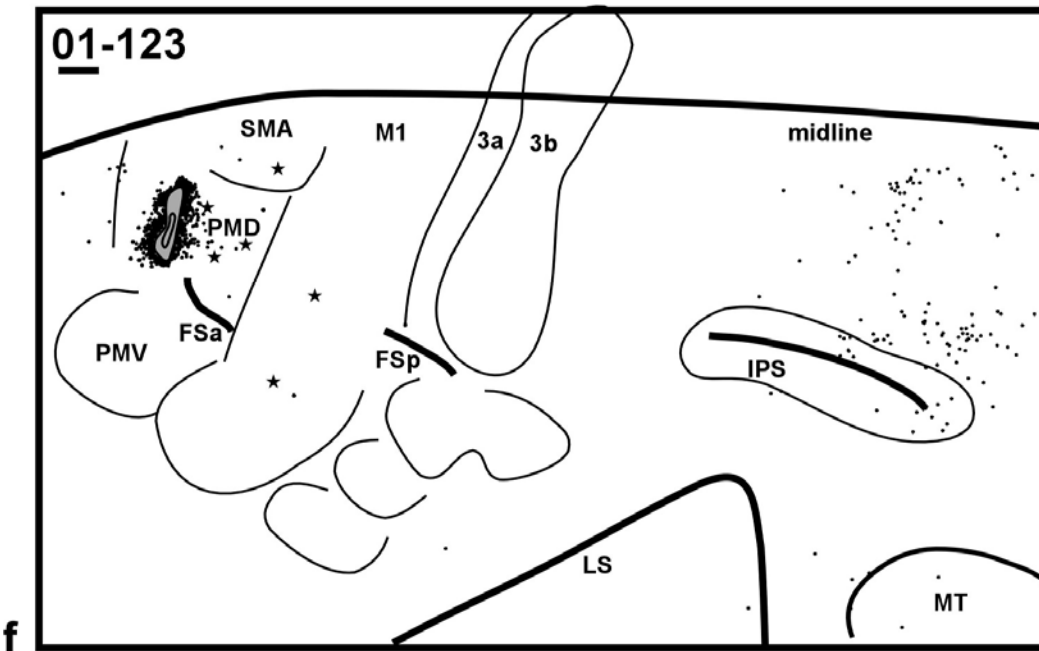
Fig. 4-14. Plot of retrograde labeled cells following tracer injections in PMD. The tracers were placed into the central PMD (a-d), rostral PMD (e-f), and caudal PMD (g). Most of the injections were confined to PMD except for case 01-98 with DY injection that overlapped with the prefrontal cortex. Overall, the majority of the labeled cells were found in the posterior parietal cortex including the caudal cingulate cortex , and especially the superior portion regardless of where the injections were placed in either central, rostral or caudal PMD. See Table 1 for detailed tracer used, and see figure 9 for the conventional references. Scale bar= 1mm.

injections resulted in the labeled cells in M1 and anterior cingulate cortex. Labeling was

also found in area 3a and 3b of case 01-123. Other than this, the distribution of the

labeled cells was similar to that described above.

The sagittal sections showed that the labeled cells were mostly located in the

supragranular layers following an injection in PMD (Fig. 4-15). The distribution of the

labeling in the sagittal sections was similar to that in the flatten cortex showing that

posterior parietal cortex, upper bank of intraparietal sulcus, SMA, and FEF were labeled.

It is difficult to tell whether there are intrinsic connections between forelimb and

trunk/hindlimb representations of PMD. In our ICMS results, we could only find few

sites that initiated trunk/hindlimb movements located in the medial PMD, and the border

between these two body movement representations was not so segregated and clear. We

placed all the tracers in the forelimb area and we believe that the uptake zones or even the

injection sites had included trunk/hindlimb area since the trunk/hindlimb movements

were often mixed with the forelimb movements; thus, it was hard to mark the exact

boundaries. Therefore, we were not able to conclude whether there were intrinsic

connections between different body movement representations in PMD.

To confirm whether PMD also sends strong inputs to superior posterior parietal cortex

(sPPC), due to the fact that sPPC sends strong inputs to PMD following injections in

PMD, two tracers were placed into sPPC. Animal 02-25 received a WGA-HRP injection

in the sPPC, and animal 02-68 received a BDA injection in the lateral sPPC that also

involved the upper bank of the intraparietal sulcus. There were dense distributions of

WGA-HRP labeled cells and some BDA-labeled cells in PMD (Fig. 4-16). A few

patches of WGA-HRP labeled cells were found in the banks of intraparietal sulcus, which

suggested that there might be some functional subdivisions in the banks of intraparietal

sulcus (Fig. 4-16a). In another project, we used long half-second trains of electrical

pulses to microstimulate the intraparietal sulcus in galagos, and we found functional
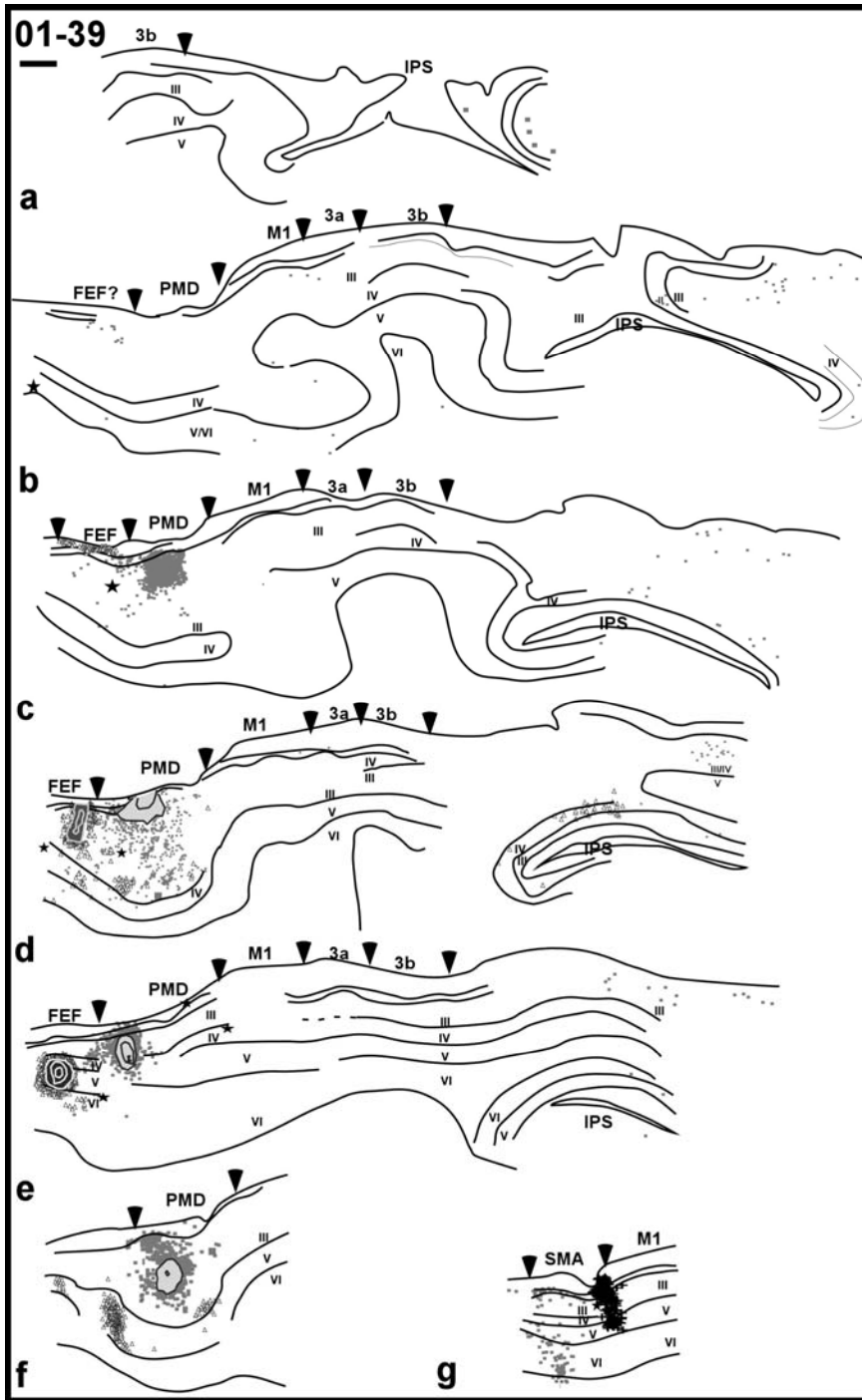
Fig. 4-15. Analysis of retrograde labeled cells in a series of sagittal sections from lateral (a) to medial (g) with FE injection in PMD forelimb area and FB injection in FEF in case 01-39. The injections of both tracers were mainly localized within the supragranular layers. The distribution of the FE labeled cells was similar to that shown in the flattened cortex. Most of the FE cells (light dots) clustered in the supragranular layers in the parietal cortex, and most of the FB cells (dark triangles) were located in the prefrontal cortex with some in the upper bank of intraparietal sulcus. See figure 11 for the conventional references. Scale bar= 1mm.
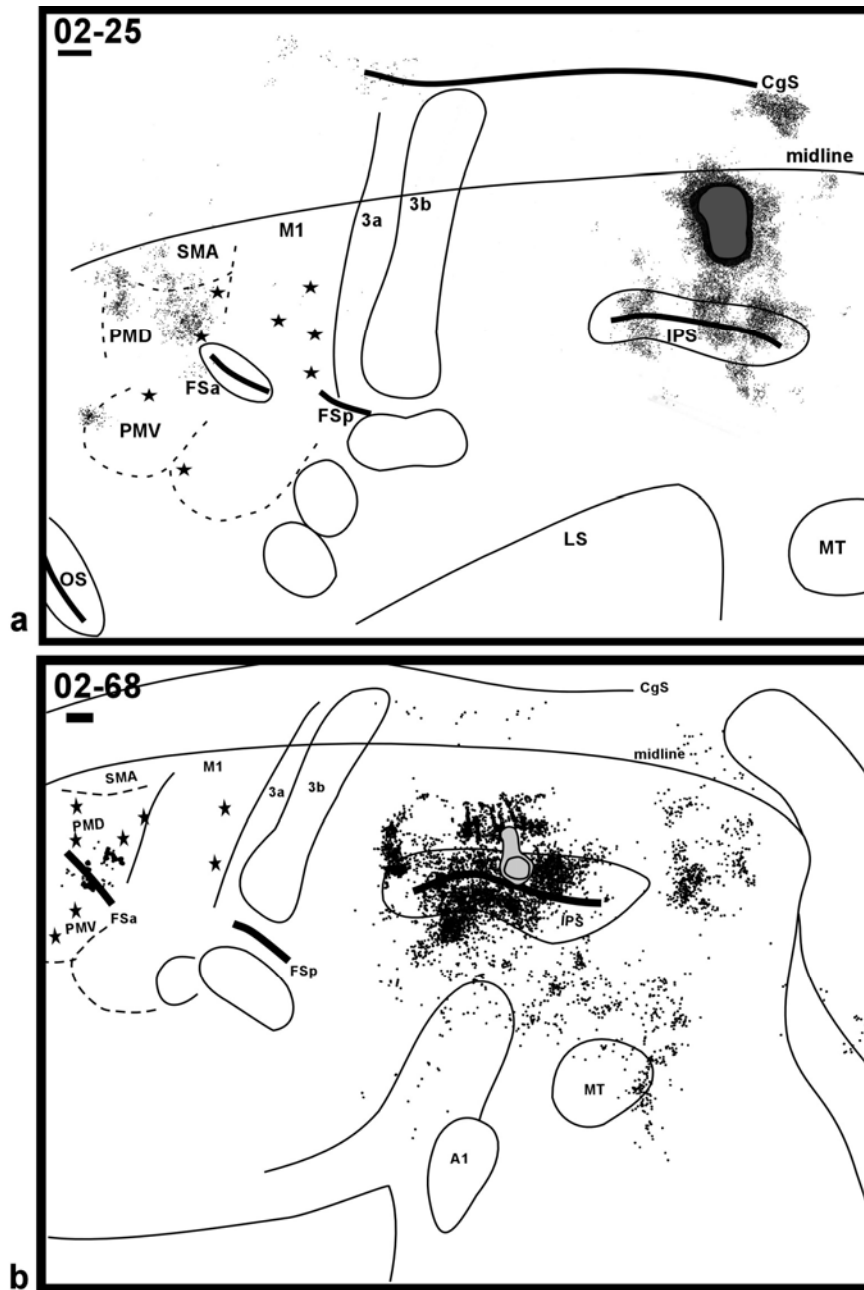
Fig. 4-16. Reconstruction of labeled cells shown in the flattened cortex with a WGA-HRP injection into the superior posterior parietal cortex in case 02-25 (a), and with a BDA injection into the upper bank of the intraparietal sulcus including the superior posterior parietal cortex in case 02-68 (b). Dense WGA-HRP label was seen in the banks of intraparietal sulcus and PMD in case 02-25. Dense BDA-labeled cells were found in the occipital-parietal cortex, and some labeled cells in PMD in case 02-68. We could confirm that PMD and superior posterior parietal cortex were reciprocally connected. See figure 9 for the conventional references. Scale bar= 1mm.

subdivisions (not published). There were also dense foci of BDA labeled cells in the visual cortex of the occipital lobe, which might be because of the involvement of the injection with the upper bank of intraparietal sulcus (Fig. 4-16b). In both cases, labeled cells were found in PMD following injections in the superior posterior parietal cortex, which indicates that PMD sends projections to sPPC, and that PMD and sPPC are interconnected.

Connections of Ventral Premotor Area (PMV)

Injections in PMV strongly labeled prefrontal and parietal cortex. Since we only mapped the medial and caudal borders of PMV with PMD and the caudal borders of PMV with M1 face representation, the full extent of PMV was estimated from the depictions of Wu et al. (2000). The size of PMV is about 3mm wide (medio-laterally) and 4mm long (rostro-caudally), and the injections we made in four cases were likely to be restricted within PMV although part of M1 orofacial representation could have been involved. Following injections in PMV, dense labeling was mostly in the ventral regions of the hemisphere, which was unlike injections in PMD where labeling was mainly restricted in the dorsal regions of the hemisphere. PMV had the strongest connections with prefrontal cortex rostral to PMV. Dense labeling was also found in the parietal cortex around the tip of intraparietal sulcus. Some labeled cells were seen in PMD, M1, prefrontal cortical cortex rostral to PMD and cortex near the orbital sulcus. Few labeled cells were seen in area 3a, cortex caudal to area 3b, and cortex rostral to M1 face representation. Very
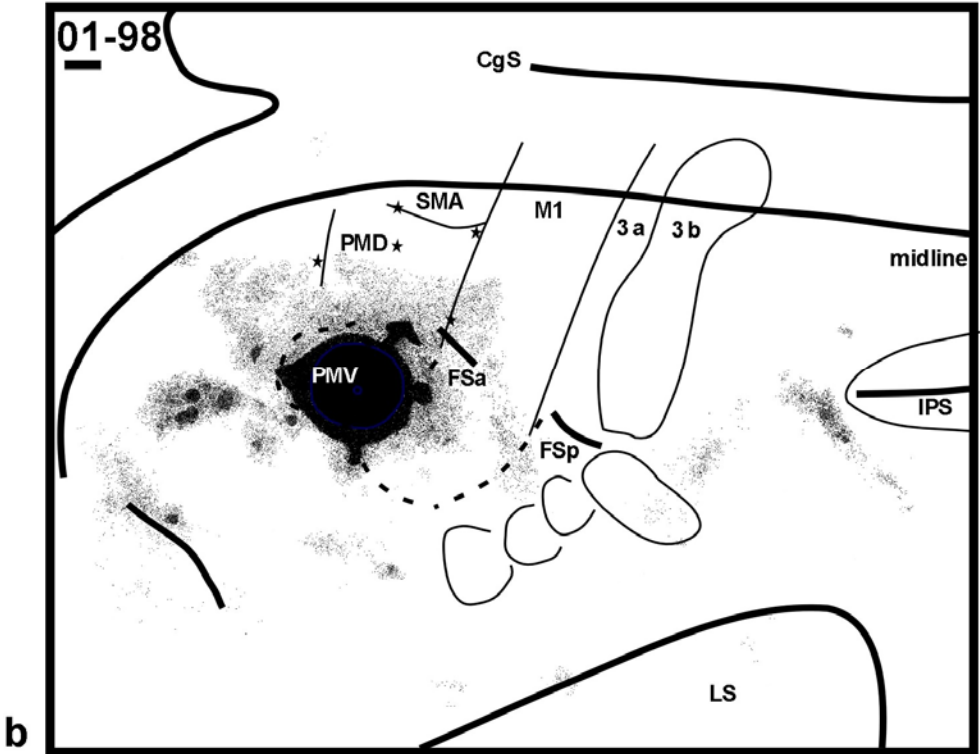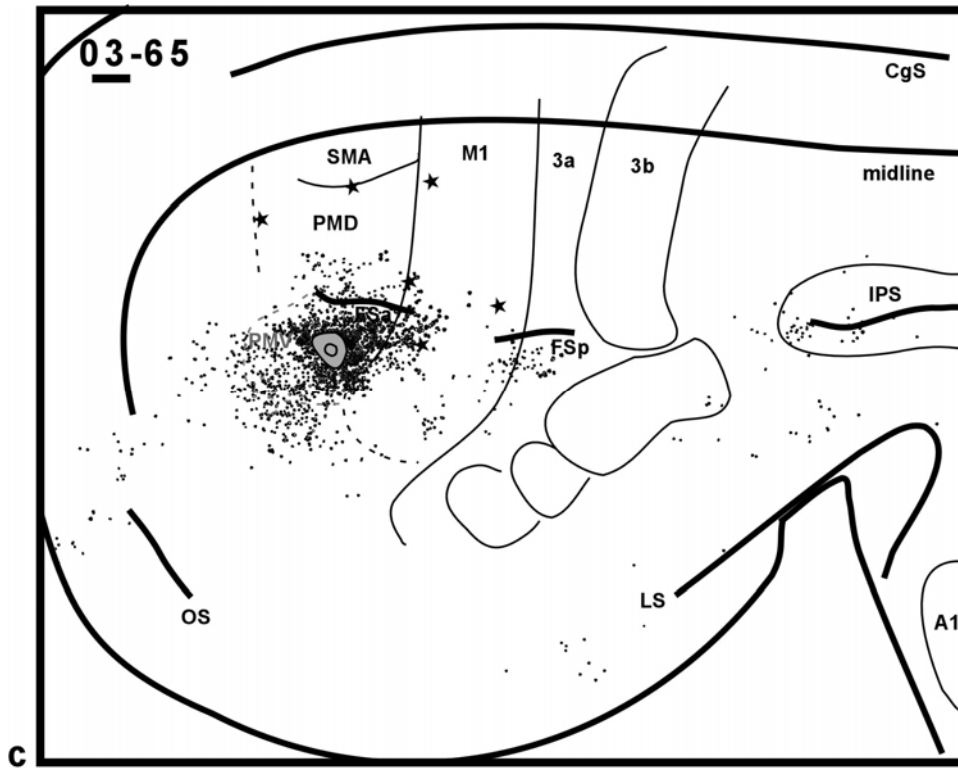
Fig. 4-17. Plot of retrograde labeled cells following tracer injections in the orofacial representation in PMV. A FB injection was made in case 00-79, a WGA-HRP injection was made in case 01-98, and a BDA injection was made in case 03-65. These injections were believed to be restricted to PMV. Unlike the injections in M1 and PMD, most of the labeled cells appeared in the prefrontal cortex, especially the lateral portion of the hemisphere rather than the parietal cortex following PMV injection. See figure 9 for the conventional references. Scale bar= 1mm.

sparse foci of labeled cells were seen in the somatosensory areas in the lateral sulcus (Fig. 4-17). In case 00-79 with a FB injection, the injection site was a little bit more medial than the other PMV injections. This injection resulted in more extensive labeling including the areas mentioned above. Additional labeling was also found in pre-SMA, rostral frontal cortical areas in the cingulate cortex, superior parietal cortex and occipito-temporal cortex (Fig. 4-17a). This injection might have included FEF and area 6Ds near the FSa. Intrinsic connections were prominent within PMV following PMV orofacial injections.
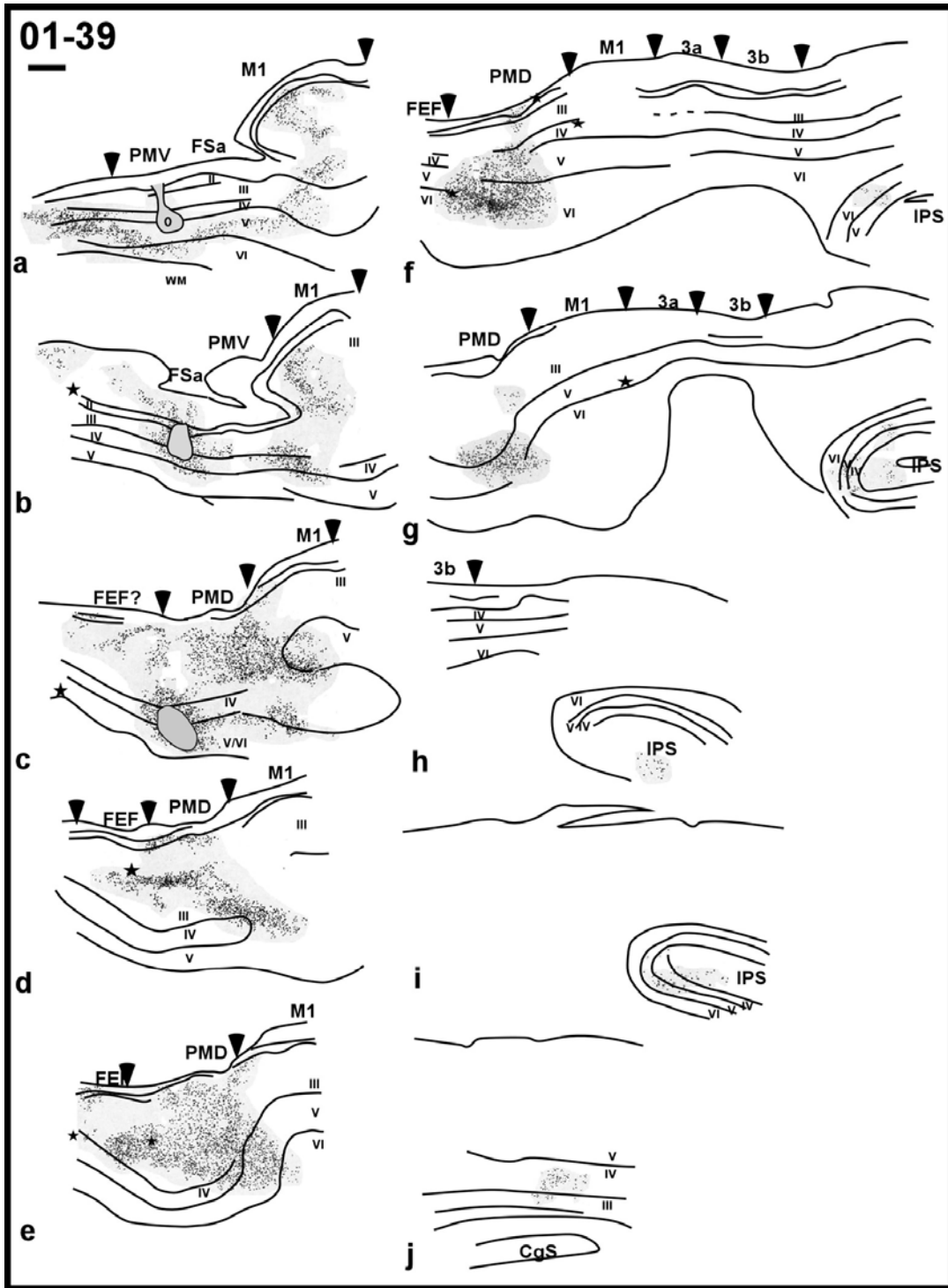
Fig. 4-18. Analysis of retrograde labeled cells in series of sagittal sections from lateral (a) to medial (j) with a WGA-HRP injection in PMV orofacial area in case 01-39. The injection covered both the supragranular and infragranular layers of PMV. The distribution of the labeled cells was similar to that shown in the flattened cortex. Most of the labeled cells clustered in both supragranular and infragranular layers in the prefrontal and frontal cortex. See figure 11 for the conventional references. Scale bar= 1mm.

Sagittal sections from case 01-39 showed similar distribution of labeled cells of cases with flattened cortex. WGA-HRP was injected in PMV and the injection included supragranular and infragranular layers. WGA-HRP labeled cells were found mostly in the prefrontal cortex including FEF, the frontal cortex including PMD and M1, and some labeled cells were seen in the anterior intraparietal sulcus. The labeled cells were seen in both supragranular and infragranular layers (Fig. 4-18).

Two additional tracer injections were applied in the inferior posterior parietal cortex (iPPC) to examine the projections from PMV to iPPC. A FE tracer was placed in iPPC, but mostly was involved with the lower bank of intraparietal sulcus in case 02-68 (Fig. 4-19a), and a DY tracer was placed into iPPC in case 02-25 (Fig. 4-19b). Both injections in iPPC resulted in dense labeling in the sPPC, iPPC, cingulate cortex, and somatosensory areas in the lateral sulcus. PMV was heavily labeled by FE, but only weakly labeled by DY (Fig. 4-19). In addition, there were also densely FE labeled cells in area 6Ds (or PMD) and M1. Thus, the connections between PMV and iPPC are reciprocal, and PMV is more densely connected to dorsal iPPC along the IPS than ventral iPPC.
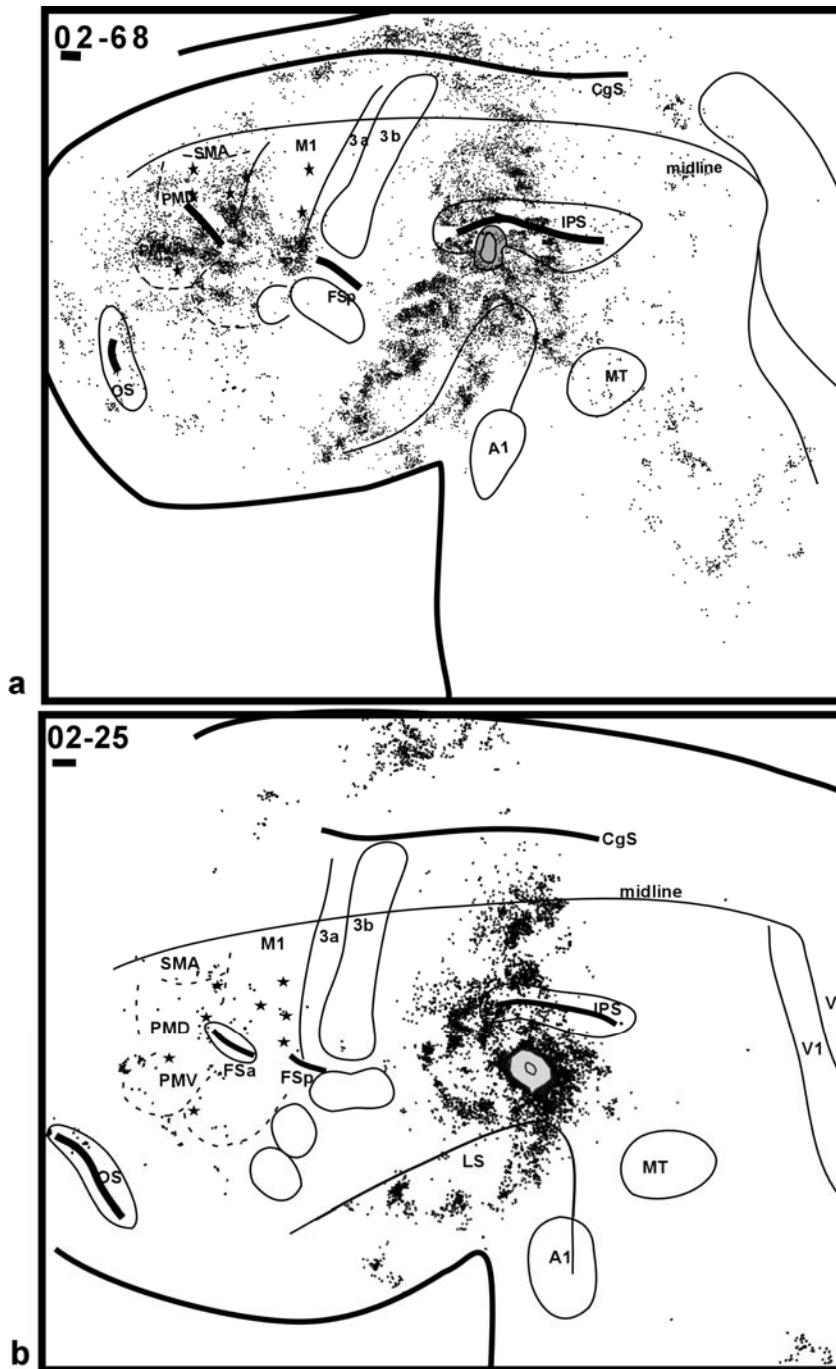
Fig. 4-19. Reconstruction of labeled cells shown in the flattened cortex with a FE injection into the lower bank of the intraparietal sulcus plus the inferior posterior parietal cortex in case 02-68 (a), and a DY injection into the inferior posterior parietal cortex in case 02-25 (b). Dense labeling was seen in both superior and inferior posterior cortex, cingulate cortex and somatosensory areas in the lateral sulcus. Additional FE dense labeling was seen in the frontal motor cortical areas including PMV, PMD, 6Ds and M1; however, very few DY labeled cells were found in the frontal motor areas including PMV. We could confirm that PMV and inferior posterior parietal cortex (including lower bank of intraparietal sulcus) were reciprocally connected. See figure 9 for the conventional references. Scale bar= 1mm.

Connections of Supplementary Motor Area (SMA)

An injection in SMA resulted in a distribution of labeled cells that was similar to that of

M1 and PMD injections. A FR tracer was placed into SMA forelimb representation and

most of the labeled cells were located in the dorsal regions of the hemisphere including

the mesial wall. Very dense labeling appeared in PMD and within SMA, and less dense

labeling appeared in parietal cortex where anterior parietal cortex meets the rostral half of

posterior parietal cortex (Fig. 4-20). There were lots of cells in the mesial wall of

cingulate cortex (maybe the cingulate sensory motor area). There were also labeled cells

in M1, the rostral cingulate motor area, and the region lateral to PMV and rostral to M1

orofacial representation. Very few labeled cells were in the prefrontal cortex, maybe pre-

SMA and SEF, and in the somatosensory areas near the lateral sulcus. We did not map

the whole SMA region, so, we were not able to identify the boundaries between different

body movement representations. However, labeled cells within SMA were densely

packed and spread all over the area. Thus, it is likely that strong intrinsic connections

exist between the different body movement representations of SMA.
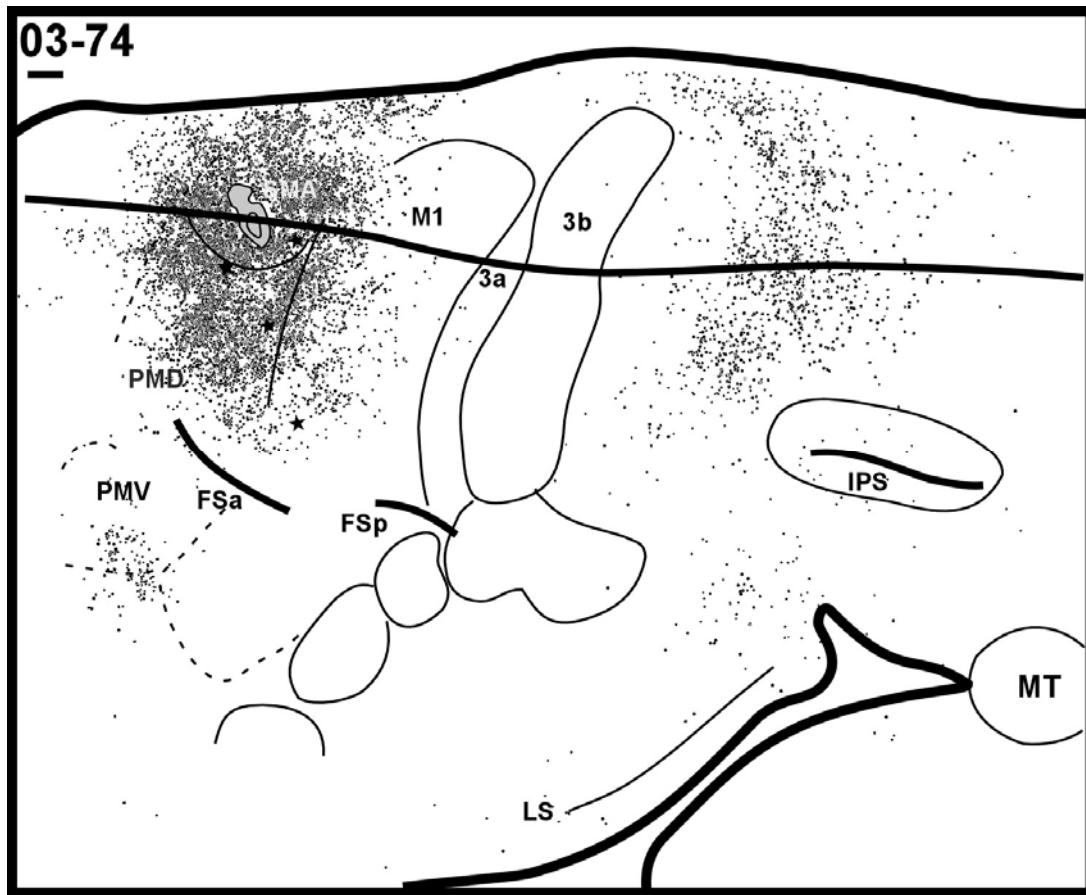
Fig. 4-20. Distribution of retrograde labeled cells following FR tracer injection in the forelimb representation of SMA. The injection was confined to SMA. Majority of the labeled cells were located in the medial regions of the hemisphere especially PMD, SMA, cingulate cortex and posterior parietal cortex. See figure 9 for the conventional references. Scale bar= 1mm.

Connections of Frontal Eye Field (FEF) and Prefrontal Cortex (PFC)

Two tracers were placed into FEF in two animals. FR was used in case 00-79 (Fig. 4-21a) and FB was used in case 01-39 (Fig. 4-15). One tracer, FE, was injected into the cortex rostral to PMD, but overlapped with FEF in case 00-79 (Fig. 4-21b). The distributions of the labeled cells in these cases were very similar although the FB tracer did not label as many cells as the FR and FE. Very dense labeling was found in the prefrontal cortex rostral to PMV, and dense labeling was also in PMD, but mainly in the rostral part of

145

PMD. Some labeled cells were in the banks of posterior tip of IPS, and some labeled

cells were in the posterior parietal cortex in the mesial wall. A few labeled cells were in

the cortex rostral to MT. The FR uptake zone in case 00-79 overlapped with rostral part

of PMD, which might have produced the densely-packed labeled cells in the lateral part

of rostral PMD (Fig. 4-21a). Dense labeling was found throughout the FEF. Thus, it is

likely that there are strong intrinsic connections within FEF.

Sagittal sections from case 01-39 showed that most of the labeled cells were located in

the supragranular layers, including areas in the prefrontal cortex and upper bank of

intraparietal sulcus following injection in FEF (Fig. 4-15).

In order to confirm the evidence from FEF injection that the posterior tip of the IPS has

connections with FEF, a FB tracer was placed into the posterior tip of the IPS in the

posterior parietal cortex in case 02-25 and this resulted in dense labeling in the visual

cortex in the mesial wall, MT, and parieto-occipital cortex and occipital cortex. The

labeled cells in the visual cortical areas formed an elongated strip from medial to lateral.

A few labeled cells were seen in FEF (Fig. 4-21c). This further indicates that this sector

of the posterior tip of IPS is connected with FEF. Although the connections were weak

in this case, but they are reciprocal.
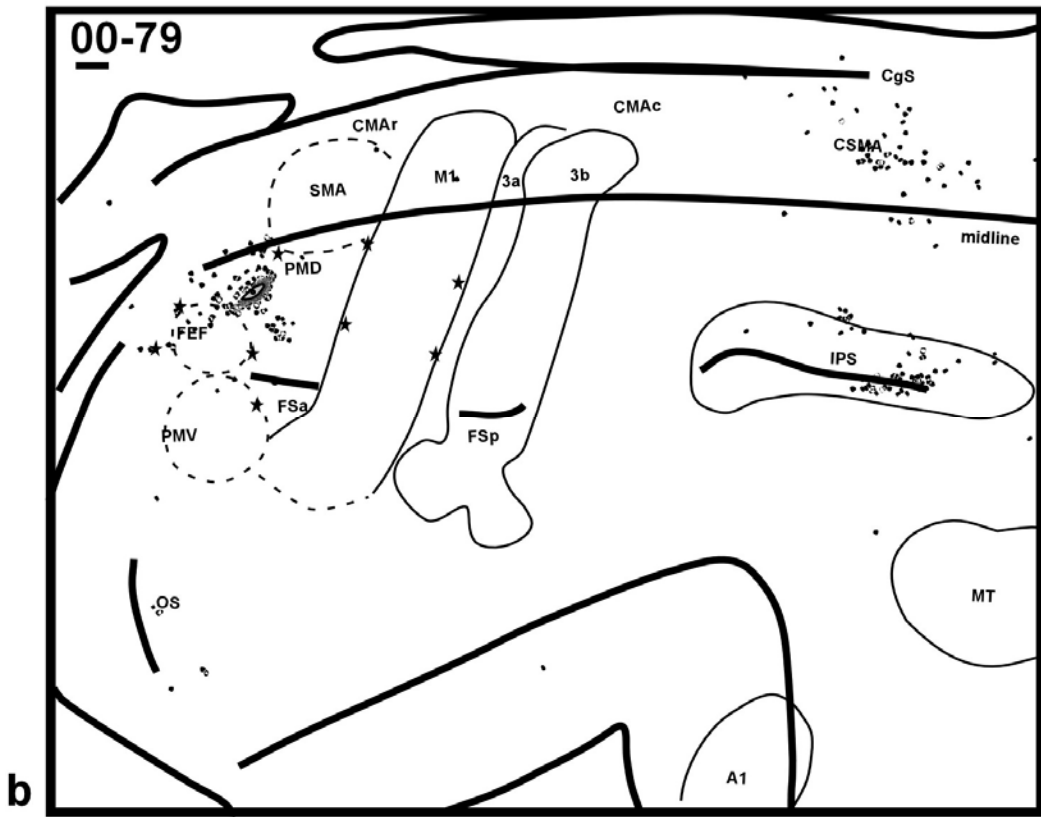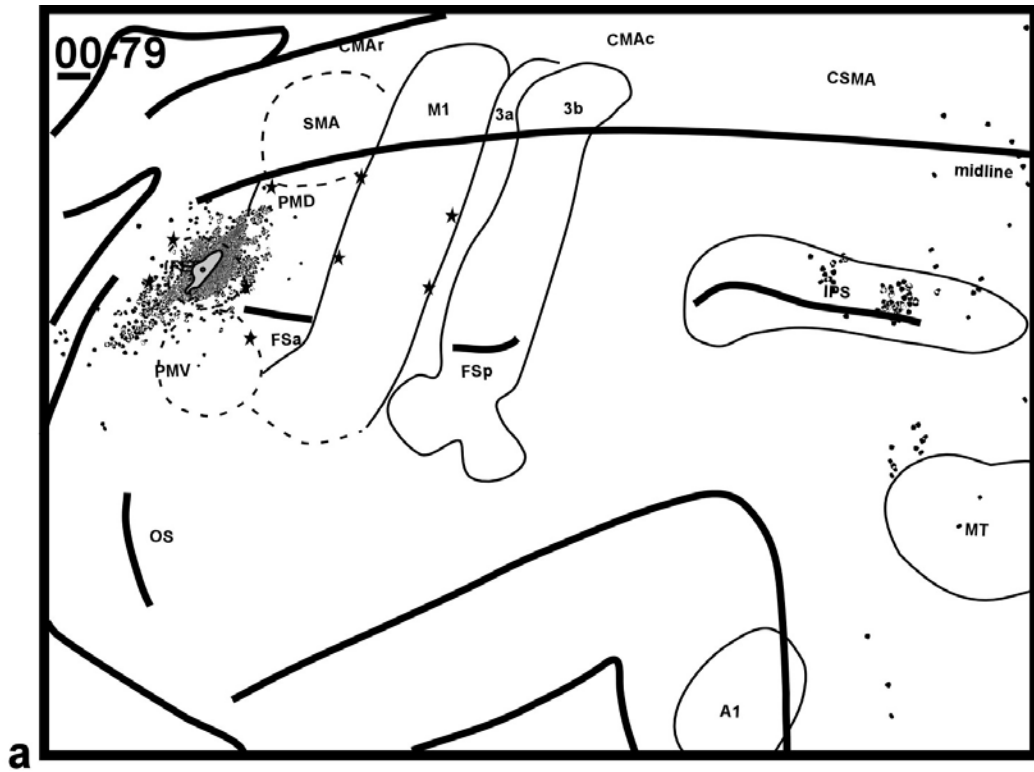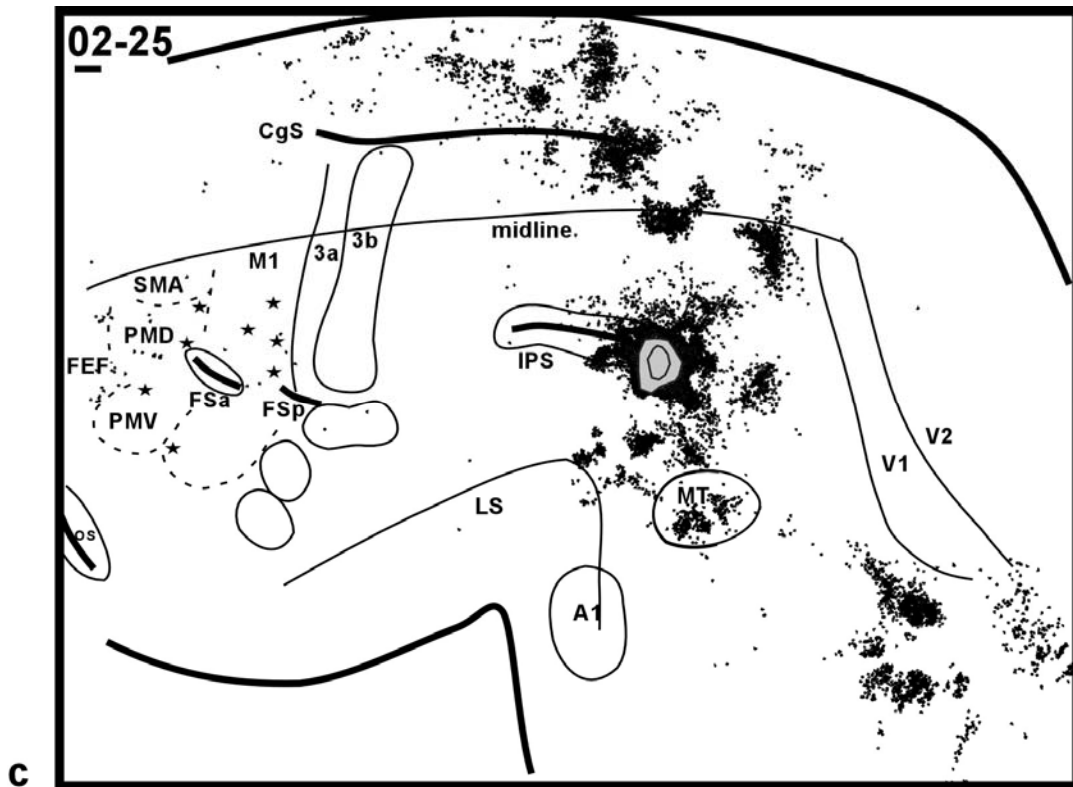
Fig. 4-21. Distribution of retrograde labeled cells following FR tracer injection in FEF (a), and FE in the cortex rostral to FEF (b). A FB injection in the posterior tip of intraparietal sulcus in the posterior parietal cortex (c). The FR injection overlapped with partial rostral portion of PMD. Majority of the FR labeled cells were located in the prefrontal cortex and FEF, and some labeled cells were in the upper bank of posterior intraparietal sulcus (IPS). Thus, in order to confirm whether the connections of FEF and posterior IPS were reciprocal, a FB tracer was placed into the posterior tip of IPS. FB injection resulted in really dense labeled cells in the visual cortex including the mesial wall and occipital lobe, but only very few labeled cells in the frontal lobe including FEF. The connections between FEF and posterior tip of IPS were weakly connected. See figure 9 for the conventional references. Scale bar= 1mm.

In order to determine the connections of prefrontal cortex, a CTB tracer was placed into cortex rostral to PMD, and a BDA tracer was placed into cortex rostral to PMV in the prefrontal cortex (PFC). The uptake zones of both injections were large (CTB: 2.5 wide × 3.0 long, BDA: 2 wide × 2.5 long), and they might include more than one cortical subdivisions. The majority of both CTB and BDA labeled cells were in the frontal cortex

148
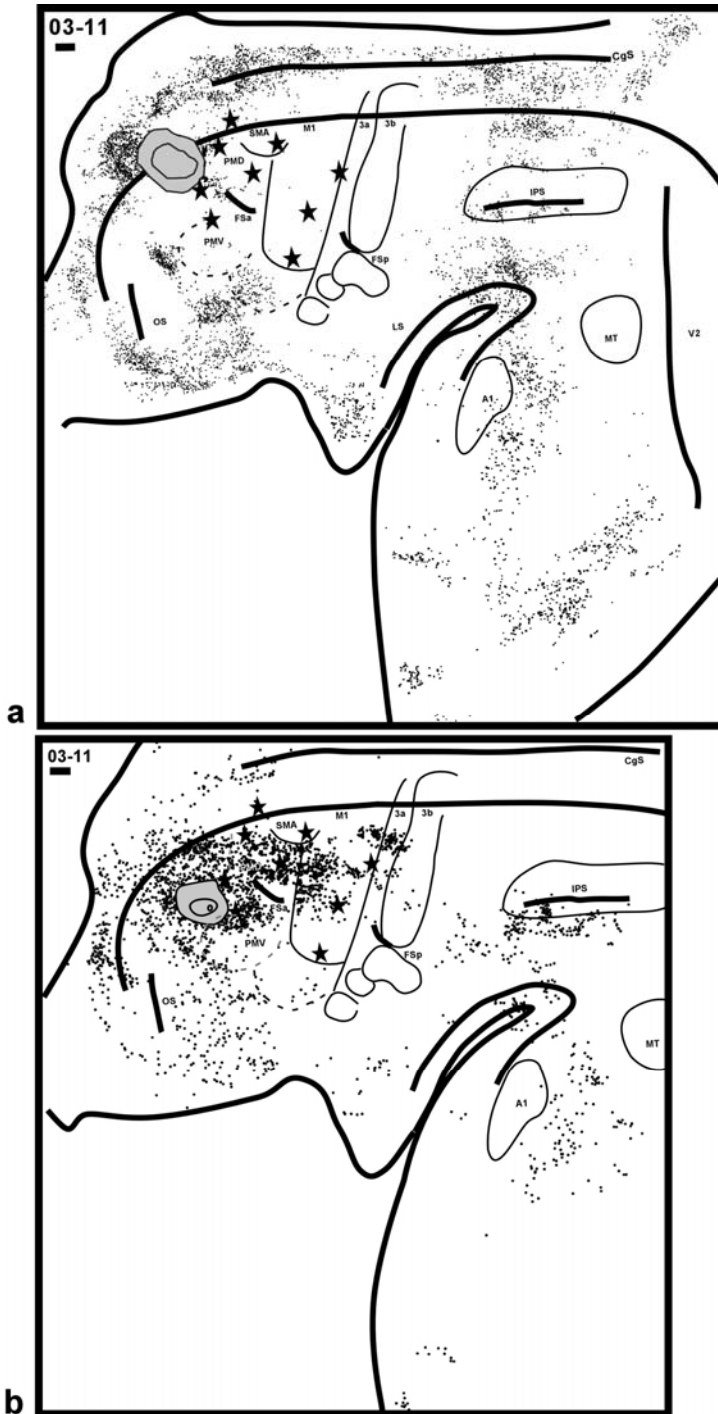
Fig. 4-22. Distribution of the labeled cells following a CTB tracer placed into the area rostral to PMD (a), and a BDA tracer placed into the area rostral to PMV (b) in the prefrontal cortex (PFC). The patterns of these two injections were different from those injected in the motor cortex in that both injections resulted in dense labeling in the prefrontal cortex especially the cingulate cortex and mesial wall. Labeled cells were also found in the temporal and parietal lobes. See figure 9 for the conventional references. Scale bar= 1mm.

including the cingulate cortex, rather than the parietal cortex (Fig. 4-22). There were also

dense labeled cells in the posterior parietal cortex. Almost no CTB labeled cells were

found in the motor cortex, there were only few labeled cells in PMD (Fig. 4-22a);

however, there was dense BDA labeling in PMD, and some labeled cells were in M1 and

PMV (Fig. 4-22b). These two prefrontal injections resulted in extremely dense labeling

in the PFC and dense labeling in the occipito-temporal cortex, which were very different

from the connection patterns following motor cortical injections. In addition, the

thalamocortical connections of these two prefrontal injections were different from the

thalamocortical connections of motor cortex (see Chapter III). Moreover, the

microstimulation we used in this study did not evoke any movements from these

prefrontal regions. Therefore, these prefrontal regions are likely not part of motor cortex.

<u>Discussion</u>

Architecture of Motor Cortex

The present descriptions of the cytoarchitecture of the motor cortex (including M1, PM,

and SMA) and somatosensory cortex (including area 3a and 3b) of galagos in our study,

in general, is very similar to that described by Wu et al. (2000) and earlier by Preuss and

Goldman-Rakic (1991) in galagos, and in studies by other researchers in macaque

monkeys (Barbas and Pandya, 1987; Matelli et al, 1991). In general, M1, PMD and SMA

are characterized as agranular, PMV is dysgranular, and areas 3a and 3b are granular,

although there are some differences. M1 contains more giant pyramidal cells than other

motor cortical areas similar to the results from other studies in macaques and galagos

(Brodmann, 1909; Von Bonin and Bailey, 1947; Barbas and Pandya, 1987; Matelli et al, 1991; Preuss and Goldman-Rakic, 1991; Wu et al., 2000). In addition, the layer V in both M1 and caudal PMD is separated into two distinct sublayers in macaques (Matelli et al., 1991). However, separate layer V in M1 and PMD into sublayers was not apparent in the present study or that of Wu et al. (2000).

Matelli et al. sectioned the macaque brains coronally and processed the sections with CO preparation, and found the areal differentiations in the motor cortex. M1 as well as PMV display high level of CO activity, whereas caudal part of PMD displays low CO activity (Matelli et al., 1991). What we found in galagos is similar to that in macaques. In the lateral regions of the hemisphere, PMV displays high level of CO activity, but the M1 orofacial representation shows low level of CO activity. In the medial regions, PMD shows low a level of CO activity, but M1 forelimb representation shows high level of CO activity. In addition, it was also found that in macaques, there are more SMI-32 positive cells in the layers III and V of M1 than in the PM areas (Gabernet et al., 1999). In galagos, we also found the similar results in general although there are some differences. The results from SMI-32 and CO preparations in galagos are very similar that in the lateral regions of the hemisphere, the layer V/VI of PMV seems to contain slightly higher density of SMA-32 positive cells than in the M1 orofacial representation, which results PMV a little bit more darkly-stained than M1. In the medial sections, the density of SMI-32 positive cells in PMD is apparently lower than in the M1 forelimb representation.

The myelination of motor cortex in the macaque brains was described by Barbas and Pandya (1987). They found that caudal PMD has higher density of myelination than the rostral PMD (Barbas and Pandya, 1987). In our study, we found that M1, in general, has

higher density of myelination than the PM areas, and the myelination in the PM areas is uniformly distributed. Therefore, we were not able to find the differentiations within PM using myelin stains. The results of myelin staining in the sagittal sections corresponds to that in the flattened sections. However, we distinguished the PM subdivisions via CO staining from the sagittal sections, but not from the flatten sections. CO preparations did not reveal clear differentiation in the flattened sections.

Intracortical Microstimulation Mapping

As with macaques, the motor cortex of galago can be delineated into three major subdivisions, M1, PMD and PMV, based on intracortical microstimulation mapping. In these two primates, the threshold in PM is higher than in M1, and the distal movements are more dominant in M1, but the proximal movements are more dominant in PM. Moreover, there are complete and segregated body movement representations including hindlimb/trunk, forelimb, and orofacial from medial to lateral in M1 in both primates (Woolsey et al., 1951; Rizzolatti et al., 1981b and c; Wu et al., 2000).

In macaque monkeys, digit movements can be elicited from a large portion of cortex in M1, and from a small portion of cortex in PM (Woolsey et al., 1951; Rizzolatti et al., 1981b and c); whereas, in galagos, the digit movements can be found only from a small portion of M1, and not from PM. In macaques, from medial to lateral, caudal PMD consists of hindlimb/trunk and forelimb representations. The borders between the adjacent body movement representations are not as clear as those in M1. The adjacent
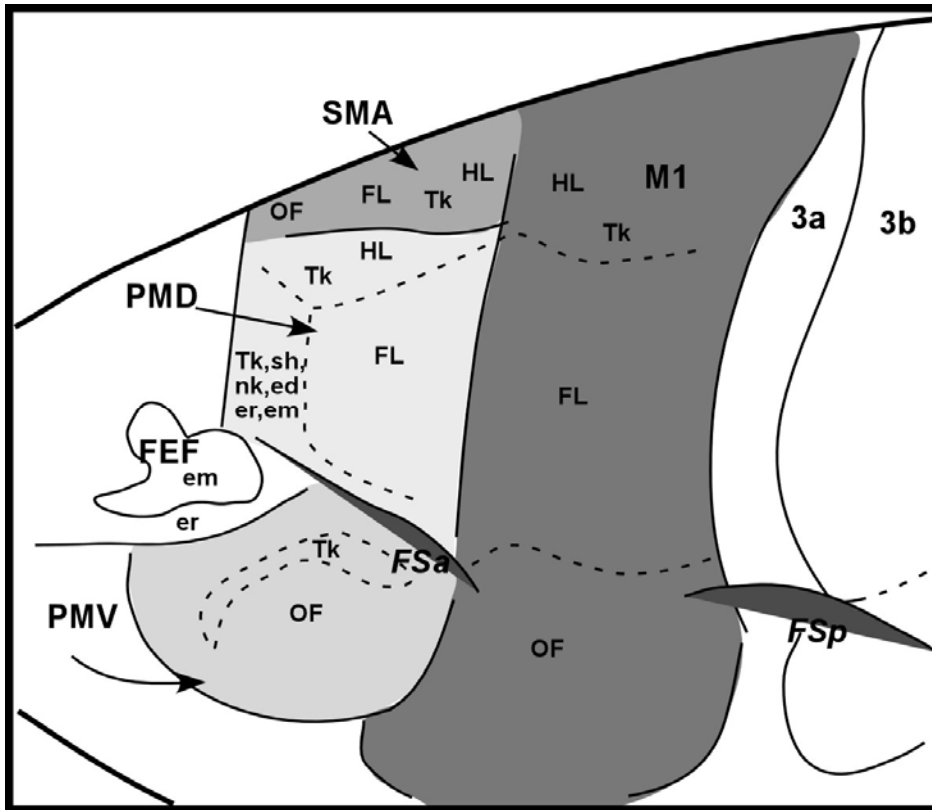
Fig. 4-23. Summary drawing showing the subdivisions of the motor cortical areas with body movement representations. Body movement could be evoked via intracortical microstimulation (see method section). M1 as well as SMA contained complete body movement representations including hindlimb/trunk, forelimb and orofacial. PMD contained mostly forelimb representation and small portion of hindlimb/trunk representation, and the rostral and lateral PMD contained mix of trunk, shoulder, neck, eye lid, and ear movements. PMV contained mostly orofacial movements with a few sites of trunk movements. The body movement representations in PM were not as well segregated as in M1. Solid thin lines represent the electrophysiological borders among different cortical areas, and dash lines represent electrophysiological borders among different body movement representations. See abbreviation list for body movement abbreviations. Left, rostral; top, medial.

representations overlap a little bit,. PMV consists of forelimb and orofacial

representations, and these two representations are largely overlapped (Woolsey et al.,

1951; Godschalk et al., 1995; Tanne-Gariepy et al., 2002). In galagos, we found that

lateral PMD (especially the caudo-medial part) evokes mostly forelimb movements,

while a mix of some hindlimb/trunk movements occur in the medial PMD, and the border

between these two body movement representations is not so clear. PMV consists of

mostly orofacial movements mix with very few upper trunk movements in galagos (Fig. 4-23). PMV in macaques can be divided into two parts, rostral and caudal, based on mapping. The rostral PMV contains mostly distal forelimb movements; whereas the caudal PMV contains mostly proximal forelimb movements (Gentilucci et al., 1988). Our mapping results of PMD in galagos are more similar to PMD in owl monkeys than in macaque monkeys. In galagos, the very small rostral portion of PMD contains mix of trunk, shoulder, neck, ear, eye, and eye blink movements and this area extends from medial to lateral next to FSa that separates PMD and PMV. In owl monkeys, PMD consists of hindlimb/trunk and forelimb representations, and a face movement representation in lateral PMD (Preuss et al, 1996). Microstimulating rostral PMD in macaques and owl monkeys initiates eye, facial and proximal body movements (Fujii et al., 2000; Tanne-Gariepy et al., 2002; Preuss et al., 1996), which is very similar to what we found in galagos.

Our mapping results are very similar to those of Wu et al. (2000), although there are some differences. In Wu et al. (2000) study, it was found that PMD contains complete body movement representations including hindlimb/trunk, forelimb and face from medial to lateral and also some digit movements. We not only found hindlimb/trunk and forelimb movements, but also found mix of trunk, shoulder, neck, ear, eye, and eye blink movements in rostal and lateral PMD. We did not see digit movement in PMD. Wu et al (2000) found not only orofacial and upper trunk movements but also forelimb movements (including shoulder and hand movements) in PMV (Wu et al., 2000). However, we found only orofacial movements with very few upper trunk movements in PMV. The discrepancy here might result from the level of electric currents and types of anesthetic

drugs. The maximal currents we used, very often, were no higher than 250 µA and we used Ketamine as the anesthetic drug. On the other hand, Wu et al. (2000) applied up to 700 µA electric currents and used Telazol as the anesthetic drug.

Corticocortical Connections

The overall corticocortical connection patterns of PM in galagos are very similar to those in macaque monkeys (Fig. 4-24). The PM areas form connections with both the prefrontal and posterior cortex and the connections are mostly located in the supragranular layer (layer III) (Arikuni et al., 1980; Godschalk et al., 1984). However, the corticocortical connections of PM in macaques were also found in layer V (Arikuni et al., 1980; Godschalk et al., 1984). In both galagos and macaques, the dorsal PM (PMD) has strong connections with the cortical regions in the dorsal hemisphere, and the ventral PM (PMV) with the ventral regions (Arikuni et al., 1980; Godschalk et al., 1984; Matelli et al., 1986; Kurata, 1991; Lu et al., 1994; Ghosh and Gattera, 1995; Tanne-Gariepy et al., 2002). In addition, the connections of the motor cortex with the parietal cortex, M1 has strong connections with the rostral portion of the posterior parietal cortex (area 1 and 2), and PMD with the caudal portion of the posterior parietal cortex (Petrides and Pandya, 1984; Cavada and Goldman-Rakic, 1989; Marconi et al., 2001).   PMD of both galagos and macaques does not receive projections from the somatosensory areas in the anterior parietal cortex (areas 3a and 3b) and the lateral sulcus (S2, PV) (Petrides and Pandya, 1984; Cavada and Goldman-Rakic, 1989; Marconi et al., 2001). On the contrary, PMV receives some inputs form area 3a and the somatosensory areas in the lateral sulcus

(Muakkassa and Strick, 1979; Godschalk et al., 1984; Matelli et al., 1986; Barbas and Pandya, 1987; Lu et al., 1994; Ghosh and Gattera, 1995).

It was found that in both galagos and macaques, the adjacent areas in the motor cortex are connected with each other. The adjacent motor cortical areas, most of them, are strongly connected in macaques, but weakly connected in galagos. In macaques, caudal PMD has strong connections with M1 and SMA, and, similarly, PMV has strong connections with M1 and SMA, but caudal PMD has weak connections with PMV (Arikuni et al., 1980; Godschalk et al., 1984; Matelli et al., 1986; Kurata, 1991; Lu et al., 1994; Ghosh and Gattera, 1995; Tanne-Gariepy et al., 2002). In galagos, PMD has weak connections with SMA, M1, and PMV, while PMV has weak connections with PMD and M1. In addition, our results from galagos are similar to those from macaques that the connections of the motor areas with other cortical regions are topographically organized. The forelimb representation of PMD connects with the forelimb representations of M1 and posterior parietal cortex, and the orofacial representation of PMV connects with the orofacial representations of M1. The corticocortical connections of PMD almost do not share with the corticocortical connections of PMV (Arikuni et al., 1980; Godschalk et al., 1984; Matelli et al., 1986; Kurata, 1991; Lu et al., 1994; Ghosh and Gattera, 1995; Tanne-Gariepy et al., 2002).
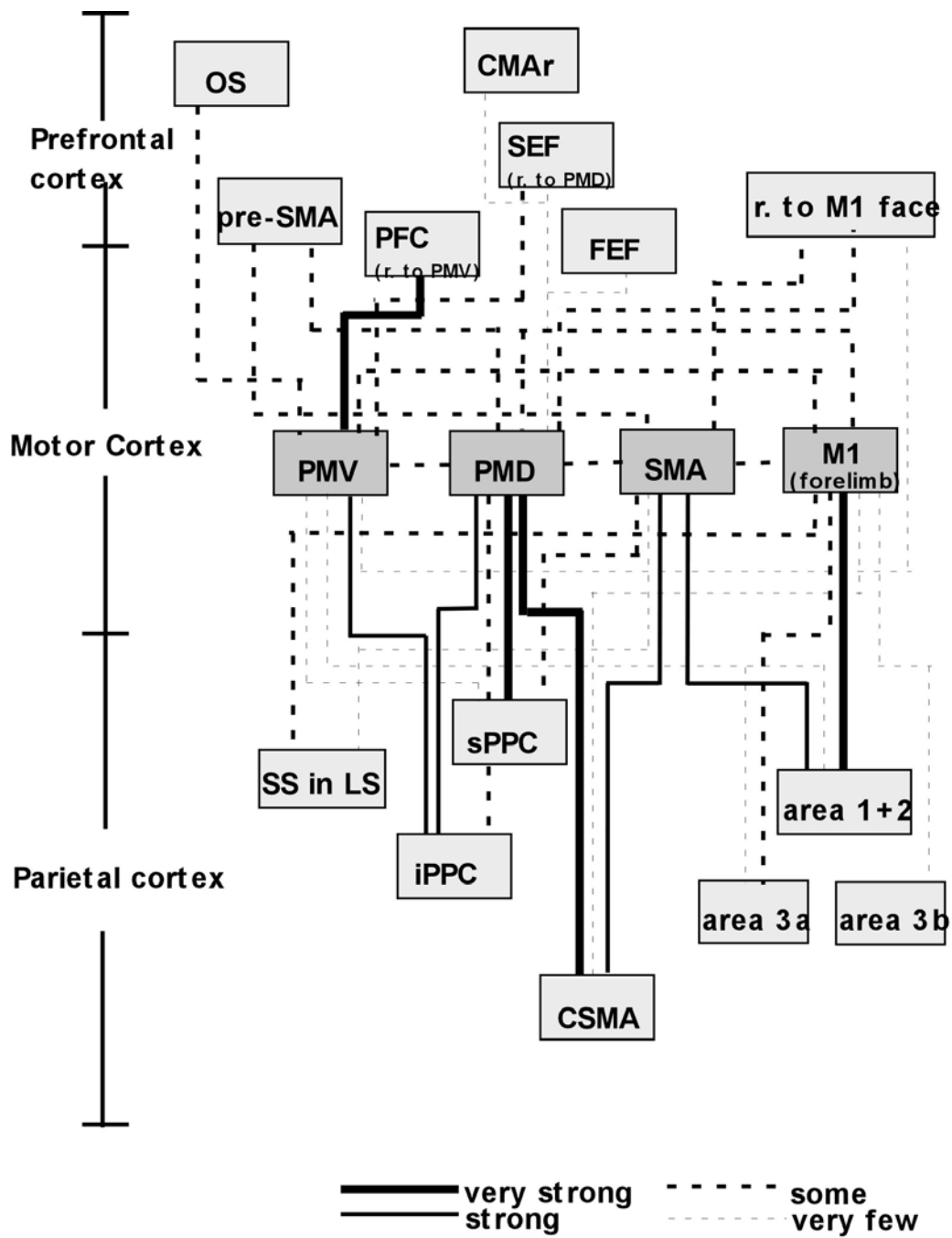
Fig. 4-24. Summary of corticocortical connections of motor cortical areas. Both M1 and PMD had very strong connections with the parietal cortex, and PMV with the prefrontal cortex. Varying thickness of lines indicates different strength of the connections.

Our results of M1 injections, in general, are similar to the study by Wu et al. (2000) with injections in M1 in galagos having more connections with area 3a than with 3b, and the connections of M1 with 3a and SMA being somatotopically organized such as forelimb representation of M1 connects with the forelimb representation of SMA (Wu et al., 2000). We also placed some injections in the prefrontal cortex and posterior parietal cortex, and our results are similar to those reported by Preuss et al. (1991) in galagos. The prefrontal cortex tends to have dense connections with the cortical areas in the prefrontal cortex, posterior parietal cortex, cingulate cortex and temporal lobe, and the posterior parietal cortex receives inputs from the motor cortex (Preuss et al., 1991). As supported by the patterns of thalamocortical connections of the prefrontal cortex in our study (Chapter III), this suggests that the prefrontal cortex is not part of the motor system and does not have much involvement with the motor movements.

There are some differences in the corticocortical connections of PM in galagos and macaques, although the majority of the connections are similar. In macaques, PMV seems to connect with more cortical areas than PMD, besides, PMV receives strong inputs from prefrontal cortex as well as from posterior parietal cortex. Moreover, PMD receives strong inputs from M1, SMA, and the dorsal region of the dorsal lateral prefrontal cortex (DLPFd) (Arikuni et al., 1980; Godschalk et al., 1984; Matelli et al., 1986; Kurata, 1991; Lu et al., 1994; Ghosh and Gattera, 1995; Tanne-Gariepy et al., 2002). However, in galagos, although PMD only has some connections with M1 and SMA, and almost has no connections with the prefrontal cortex, PMD seems to have stronger connections with other cortical areas than PMV, and PMV receives the inputs mostly from the prefrontal cortex rather posterior parietal cortex. The intrinsic

connections of PM in macaques are unlike those of M1 where the adjacent body

movement representations are not connected with each other. Within PMD, the forelimb

and hindlimb representations are connected with each other, and within PMV, the

forelimb and orofacial representations are connected within each other (Arikuni et al.,

1980; Godschalk et al., 1984; Leichnetz, 1986; Matelli et al., 1986; Ghosh et al., 1987;

Kurata, 1991; Hatanaka et al., 2001). In galagos, we also found that the adjacent body

movement representations in M1 do not connected with each other, but we were not sure

about the intrinsic connections of PM. The hindlimb representation of PMD is very

narrow and there is a mix with the forelimb representation. After forelimb injections in

PMD, we did not see many labeled cells in the lateral part of PMD, which is supposed to

contain the hindlimb representation. The borders of upper trunk representation in PMV

are not well marked in galagos. The upper trunk movements are mixed with the orofacial

movements, which occupy the majority of PMV territory.

Motor Cortex Organization in Galagos

There are three important questions we want to clarify about galagos: 1) Does PMD

include a face representation? 2) Does PMV contain a forelimb representation? 3) Is there

PMDr? In order to answer these questions, we would like to compare our study with Wu

et al. (2000) because both studies used similar investigating methods studying the motor

cortex of galagos. In Wu et al. study, they separated PMD into two subdivisions, like in

macaques, caudal (PMDc) and rostral (PMDr) according to the intracortical

microstimulation mapping results and injections in M1 (Wu et al., 2000). They found

that PMDr requires much higher currents to evoke the movements than PMDc, and

stimulating PMDr could evoke trunk, shoulder and face movements. In addition, they

found that M1 receives inputs from PMDc, but not PMDr. They also found the

cytoarchitectonic structure of PMDr is different from PMDc due to that PMDr had layer

IV, and PMDr does not have connections with the spinal cord.

In our stimulation mapping, we did find that the rostral part of PMD needs higher

currents to initiate movements and very often, we could not evoke movements even we

went up to 250 or 300 μA. The movements we found in the rostral PMD included trunk,

shoulder, neck, eye-lid, ear and eye movements, and these movements mixed with each

other in a small region in the rostral PMD extending medially to border SMA and to

latero-caudally to border FSa. We did not separate this rostral region as a distinctive

subdivision of PMD. We rather treated it as a different body movement representation of

PMD due to the following reasons. 1) We used several staining preparations and could

not identify the area differentiation of rostral and caudal PMD if there is any. The whole

PMD region is uniformly-looking. 2) Based on our corticocortical and thalamocortical

connection results, there is no huge difference of the connections whether the tracers

were placed in the rostral or caudal PMD. The connection patterns are very similar.

Moreover, Wu et al. (2000) found that PMDc contains face representation and this

representation sends inputs to M1 face representation (Wu et al., 2000). However, we

were not able to find facial movements and we did not see labeled cells in PMD

following injections in M1 face representation. In addition, the thalamic label in the

motor thalamus was clustered in the central part of the motor thalamus, not the medial

part of the motor thalamus that is normally related to the face movements.

PMV in galagos was found to contain forelimb movements in the Wu et al. (2000) study.

They also found the connections between PMV and M1 following M1 forelimb injection,

and labeling in PMV following the injection in C5 and C6 of the spinal cord (Wu et al.,

2000). C5 and C6 are the spinal segments innervating the muscles of shoulders and arms.

In our study, we were not able to find any forelimb movement in PMV and we did not

see labeled cells in PMV following clean M1 forelimb injections. Besides, following the

PMV injections, the thalamic labeled cells clustered in the medial part of the motor

thalamus, not the central motor thalamus, where is related to orofacial movements. There

are some possibilities that could explain the differences between out study and Wu et al.

(2000), as mentioned above, they used much higher currents during the stimulation

mapping and used Telazol as an anesthetic drug.

Technical Considerations: tracer and Ketamin use, and flattening the cortex

Due to the nature of tracers used in the study, some tracers such as WGA-HRP, DY, and

FB induce large injection sites and zones of uptake that sometimes spread into the

neighboring areas, resulting in the spread of transport. Moreover, some injections may

go too deep into white matter, which may result in spreading of transport to cortical

regions via fibers of passage (Conde, 1987). Even more, some tracers result in poor

transport. In order to overcome these technical problems, various tracers were used in

different cortical areas, and each tracer was placed in the center of the area away from the

electrophysiological borders. Conclusions were based on robust transport data seen

across at least two to four animals for each injected cortical area. The most obvious

example is from animal 01-123. WGA-HRP was injected in PMD of this animal. Both

of the core and zone of uptake of this injection was big enough that spread into M1. Due to this large injection, the labeled cells were found in the areas that normally connect with not only PMD but also with M1. In other animals (99-75 and 01-98) with confined injections in PMD, there was no labeling found in area 3a and 3b, as was seen in case 01-123. Thus, only robust transport resulting from the injection confined within the area of interest was taken into consideration.

One important issue about the ICMS might be that the threshold (minimum electric current to initiate body movements) might fluctuate during mapping procedures while animals were under anesthesia. We used intramuscular injection of ketamine hydrochloride and xylazine to anesthetize the first couple animals, and we found that once the animals were in deep anesthesia, we could not get any response unless we used really high electric currents. This might result in an unstable or inconsistently high threshold, and these high threshold might not be the "real" threshold. One way to solve this problem was to wait for a period of time while the heart rate of the animal came back to a certain range (between 225 and 300, depending on animal). The other way was to use intravenous injection via infusion pump. The most recent cases were anesthetized in this way while mapping. The infusion method kept the animal in a more stable condition with the heart rates in the expected range. The animal was always maintained in the anesthetic condition that resulted in lower and consistent thresholds, which then resulted in more accurate electrophysiology borders and results.

In our study, we usually flattened the cortex instead of cutting it in "traditional" coronal, sagittal and horizontal planes because the flattened sections provide the most accurate view of the general pattern of connections. In flattened sections, we could see all of the

cortical areas and sulci at once, and it is easier to reconstruct the brain compared to the

traditional cutting planes. There are not many sulci in a galago brain compared to

macaque monkeys, thus, flattening a galago brain is not difficult. Besides, we are not

really interested in the distribution of the labeled cells in different cortical layers.

Studying the cytoarchitecture of the cortical layers is not our goal either, since Wu and

her colleagues had investigated the cytoarchitecture of the cortical motor areas in galagos

(Wu et al, 2000).

Conclusions

The organization of the motor cortex in prosimian galagos is very similar to that in

macaques. Thus, the motor cortex of galagos preserves the basic components of

subdivisions of the motor cortex in macaques. The motor cortex of both galagos and

macaques can be divided into three main blocks: the primary motor cortex (M1),

supplementary motor area (SMA), and premotor areas (PM). The PM can be further

divided into dorsal (PMD) and ventral (PMV) subdivisions. However, the PMD as well

as PMV, unlike those in macaques, can not be clearly divided into subareas. In macaques,

PMD is often divided into rostral (PMDr) and caudal (PMDc) subareas, and PMV into

rostral (PMVr) and caudal (PMVc) subareas. Apparently, like the motor thalamus of

galagos, the PMD and PMV are less well differentiated in galagos compared to that in

macaques. Thus, the basic pattern of the motor system organization appeared early in the

course of primate evolution. One difference concerns lack of evoked, precise digit

movements from motor cortex of prosimians. Although in both simians and prosimians,

the premotor-posterior parietal cortical circuits might be involved in hand reaching and

grasping movements, prosimians tend to use whole hands instead of individual fingers.

References

Arikuni T, Sakai M, Hamada I, Kubota K. 1980. Topographical projections from the prefrontal cortex to the post-arcuate area in the rhesus monkey, studied by retrograde axonal transport of horseradish peroxidase. Neuroscience Letters 19: 155-160.

Barbas H, Pandya DN. 1987. Architecture and frontal cortical connections of the premotor cortex (area 6) in the rhesus monkey. Journal of Comparative Neurology 256: 211-228.

Brodmann K. 1909. Vergleichende Lokalisationslehre der Groshirnride, In: Brodmann, K. Leipzig: Barth (reprinted 1925). p 324.

Bruce K, Grofova I. 1992. Notes on a light and electron microscopic double-labeling method combining anterograde tracing with Phaseolus vulgaris leucoagglutinin and retrograde tracing with cholera toxin subunit B. Journal of Neuroscience Methods 45: 23-33.

Campbell MJ, Morrison JH. 1989. Monoclonal antibody to neurofilament protein (SMI-32) labels a subpopulation of pyramidal neurons in the human and monkey neocortex. J Comp Neurol 282: 191-205.

Cavada C, Goldman-Rakic PS. 1989. Posterior parietal cortex in rhesus monkey: I. Parcellation of areas based on distinctive limbic and sensory corticocortical connections. Journal of Comparative Neurology 287: 393-421.

Conde F. 1987. Further studies on the use of the fluorescent tracers Fast blue and Diamidino yellow: effective uptake area and cellular storage sites. Journal of Neuroscience Methods 21: 31-43.

Fujii N, Mushiake H, Tanji J. 2000. Rostrocaudal distinction of the dorsal premotor area based on oculomotor involvement. Journal of Neurophysiology 83: 1764-1769.

Gallyas F. 1979. Silver staining of myelin by means of physical development. Neurol Res 1: 203-209.

Gentilucci M, Fogassi L, Luppino G, Matelli M, Camarda R, Rizzolatti G. 1988. Functional organization of inferior area 6 in the macaque monkey. I. Somatotopy and the control of proximal movements. Experimental Brain Research 71: 475-490.

Ghosh S, Gattera R. 1995. A comparison of the ipsilateral cortical projections to the dorsal and ventral subdivisions of the macaque premotor cortex. Somatosensory and Motor Research 12: 359-378.

Gibson AR, Hansma DI, Houk JC, Robinson FR. 1984. A sensitive low artifact TMB procedure for the demonstration of WGA-HRP in the CNS. Brain Res 298: 235-241.

Godschalk M, Lemon RN, Nijs HG, Kuypers HG. 1981. Behaviour of neurons in monkey peri-arcuate and precentral cortex before and during visually guided arm and hand movements. Experimental Brain Research 44: 113-116.

Godschalk M, Lemon RN, Kuypers HG, Ronday HK. 1984. Cortical afferents and efferents of monkey postarcuate area: an anatomical and electrophysiological study. Experimental Brain Research 56: 410-424.

Hatanaka N, Nambu A, Yamashita A, Takada M, Tokuno H. 2001. Somatotopic arrangement and corticocortical inputs of the hindlimb region of the primary motor cortex in the macaque monkey. Neuroscience Research - Supplement 40: 9-22.

Huntley GW, Jones EG. 1991. Relationship of intrinsic connections to forelimb movement representations in monkey motor cortex: a correlative anatomic and physiological study. Journal of Neurophysiology 66: 390-413.

Kurata K. 1991. Corticocortical inputs to the dorsal and ventral aspects of the premotor cortex of macaque monkeys. Neuroscience Research - Supplement 12: 263-280.

Leichnetz GR. 1986. Afferent and efferent connections of the dorsolateral precentral gyrus (area 4, hand/arm region) in the macaque monkey, with comparisons to area 8. Journal of Comparative Neurology 254: 460-492.

Lu MT, Preston JB, Strick PL, Strickland D. 1994. Interconnections between the prefrontal cortex and the premotor areas in the frontal lobe

Association of antihypertensive agents and blood lipids in a population-based survey. Journal of Comparative Neurology 341: 375-392.

Marconi B, Genovesio A, Battaglia-Mayer A, Ferraina S, Squatrito S, Molinari M, Lacquaniti F, Caminiti R. 2001. Eye-hand coordination during reaching. I. Anatomical relationships between parietal and frontal cortex. Cerebral Cortex 11: 513-527.

Matelli M, Luppino G, Rizzolatti G. 1985. Patterns of cytochrome oxidase activity in the frontal agranular cortex of the macaque monkey. Behavioural Brain Research 18: 125-136.

Matelli M, Camarda R, Glickstein M, Rizzolatti G. 1986. Afferent and efferent projections of the inferior area 6 in the macaque monkey. Journal of Comparative Neurology 254: 460-492.

Matelli M, Luppino G, Rizzolatti G. 1991. Architecture of superior and mesial area 6 and the adjacent cingulate cortex in the macaque monkey. Journal of Comparative Neurology 311: 445-462.

Muakkassa KF, Strick PL. 1979. Frontal lobe inputs to primate motor cortex: evidence for four somatotopically organized 'premotor' areas. Brain Research 177: 176-182.

Preuss TM, Stepniewska I, Kaas JH. 1996. Movement representation in the dorsal and ventral premotor areas of owl monkeys: a microstimulation study. [erratum appears in J Comp Neurol 1997 Jan 27;377(4):611.]

Parvalbumin-like immunoreactivity of layer V pyramidal cells in the motor and somatosensory cortex of adult primates. Journal of Comparative Neurology 371: 649-676.

Rizzolatti G, Scandolara C, Matelli M, Gentilucci M. 1981. Afferent properties of periarcuate neurons in macaque monkeys. II. Visual responses. Behavioural Brain Research 2: 147-163.

Rizzolatti G, Scandolara C, Gentilucci M, Camarda R. 1981. Response properties and behavioral modulation of "mouth" neurons of the postarcuate cortex (area 6) in macaque monkeys. Brain Research 225: 421-424.

Sakai ST, Stepniewska I, Qi HX, Kaas JH. 2000. Pallidal and cerebellar afferents to pre-supplementary motor area thalamocortical neurons in the owl monkey: a multiple labeling study. Journal of Comparative Neurology 417: 164-180.

Tanji J, Kurata K. 1982. Recent studies in the supplementary motor area with a technique of single unit recording from behaving primates. Electroencephalogr Clin Neurophysiol Suppl 36: 378-384.

Tanne-Gariepy J, Bello A, Fadiga L, Rizzolatti G. 2002. Parietal inputs to dorsal versus ventral premotor areas in the macaque monkey: evidence for largely segregated visuomotor pathways. Neuropsychologia 40: 492-502.

Veenman CL, Reiner A, Honig MG. 1992. Biotinylated dextran amine as an anterograde tracer for single- and double-labeling studies. Journal of Neuroscience Methods 41: 239-254.

Vogt O, Vogts C. 1919. Ergebnisse unserer Hirnforschung. J Psychol Neurol (Leipzig) 25: 277-462.

von Bonin G, P. B. 1947. The Neucortex of Macaca Mulatta, In: von Bonin, G,P., B. Urbana: University of Illinois. p 136.

Watanabe-Sawaguchi K, Kubota K, Arikuni T. 1991. Cytoarchitecture and intrafrontal connections of the frontal cortex of the brain of the hamadryas baboon (Papio hamadryas). Journal of Comparative Neurology 311: 108-133.

Weinrich M, Wise SP. 1982. The premotor cortex of the monkey. Journal of
      Neuroscience 2: 1329-1345.

Wise SP, Weinrich M, Mauritz KH. 1983. Motor aspects of cue-related neuronal activity
      in premotor cortex of the rhesus monkey. Brain Research 260: 301-305.

Wong-Riley M. 1979. Changes in the visual system of monocularly sutured or enucleated
      cats demonstrable with cytochrome oxidase histochemistry. Brain Res 171: 11-28.

Woolsy CN, Settlage PH, Meyer DR, Sencer W, Pinto Hamuy T, Travis AM. 1952.
      Patterns of localization in precentral and "supplementary" motor areas and their
      relation to the concept of a premotor area. Res Publ Assoc Res Nerv Ment Dis 30:
      238-264.

Wu CW, Bichot NP, Kaas JH. 2000. Converging evidence from microstimulation,
      architecture, and connections for multiple motor areas in the frontal and cingulate
      cortex of prosimian primates. Journal of Comparative Neurology 423: 140-177.

CHPTER V

GENERAL CONCLUSIONS

The organization of the motor cortex including the premotor cortex in prosimian galagos is very similar to that in simian primate macaque monkeys. In both primates, the motor cortex can be divided into three main regions, the primary motor cortex (M1), supplementary motor area (SMA), and premotor areas (PM). The PM can be further divided into dorsal (PMD) and ventral (PMV) subdivisions. As well in both primates, the motor thalamus can be divided into three main regions, the ventral anterior (VA), ventral lateral (VL) and ventral medial (VM). VA is further divided into medial (or magnocellular in macaques) and lateral (parvocellular in macaques) subdivisions, and VL is further divided into anterior (VLa) (or VLo in macaques) and posterior (VLp) subdivisions. The general corticocortical connection and thalamocortical connection patterns in both species are very similar, too. That is, PMD has predominant connections with the dorsal regions of the hemisphere, and PMV with the ventral regions of the hemisphere. Both M1 and PMD receive significant inputs from the parietal cortex that M1 receives from the rostral portion of the posterior parietal cortex, and PMD from the caudal portion of the posterior parietal cortex. However, PMV receives inputs from both prefrontal and posterior parietal cortex, but it seems that it receives stronger inputs from the prefrontal cortex. As for the thalamocortical connections, PM receives strong inputs from the anterior parts of the motor thalamus including VLa and anterior VLp; whereas M1 receives strong inputs from the posterior VLp. In addition, PMD has predominant

169

connections with the dorsal portion of the motor thalamus; whereas, PMV with the ventral portion.

Despite these similarities of the motor system organization in galagos and macaques, there are also differences existing in these two species. One of the most obvious differences is that the PMD and PMV, as well as VLp of the motor thalamus, in galagos are less differentiated compared to those in macaques. In macaques, the PMD can be further divided into rostral and caudal subareas, and the caudal PMD is further divided into dimple (PMDc-d) and rostro-ventral (PMDc-rv) sub-subareas. Besides, the PMV in macaques is further divided into rostral and caudal subareas, and the rostral PMV can be divided into posterior bank of the arcuate sulcus (PMVr-ab) and convexity of the arcuate sulcus (PMVr-c). The VLp of the motor thalamus in macaques is further divided into three subareas, VLc, VPLo and area X. Although differences in galagos and macaques do exist, the basic pattern of the motor system of galagos is organized in the way that is similar to that in macaques. Thus, we could assume that this kind of motor system organization has appeared early (over 50 million years ago) in the course of primate evolution. The prosimian galagos preserve the basic components of the motor cortex and motor thalamus, which has already been found in macaques. Therefore, it is possible that the organization of the motor system was not greatly modified after the split of strepsirhines and haplorhines. A substantial change did occur after the split of primates from tree shrews (Kaas, 2004).

Reference

Kaas, J. H. (2004). Evolution of somatosensory and motor cortex in primates. The Anatomical Record Part A, 281A: 11-48-1156.